Wildlife and Conflict: The Cost of Protecting Biodiversity

Guy Pincus*
London Business School

This version: December 27, 2025
Click here for most recent version

Abstract

Our planet is experiencing the first human-induced mass extinction of species. In response, policymakers have implemented international trade bans to preserve rare animals and forest species such as rhinos, elephants, and rosewood. Yet little research examines their consequences. Combining georeferenced habitat maps of wild animals and trees with armed conflict data, I uncover sizeable adverse effects of international trade ban treaties. First, event-study estimates reveal that bans raise the likelihood of conflict in habitat areas by about 40%. Two findings support a windfall-related conflict mechanism. For elephant ivory, a natural experiment shows that, in response to supply-side policies, prices change, which in turn changes the likelihood of conflict events in their habitat. Given the elephant's broad habitat, the implied magnitude exceeds that of well-studied conflict minerals. For wild trees, satellite data show that harvesting shifts from high- to low-capacity states once bans are imposed, generating rents that spark violence. An analysis of battles' locations before and after the policy reveals that militias and rebels expand into new, distant areas and are more likely to gain territorial control, consistent with a feasibility mechanism in which windfalls relax budget constraints. A quantitative model suggests that a targeted policy restricting trade in states with strong institutions and smaller wildlife stocks can conserve resources while limiting conflict. Given these spillovers, international trade bans, if maintained, should be accompanied by state-building support for low-income countries, which often lack enforcement capacity.

Keywords: Environmental Policy, Trade Restrictions, Trade Bans, Biodiversity, Armed Conflict, Wildlife, Development, State Capacity, CITES

*I am deeply grateful and indebted to my advisor, Elias Papaioannou, for his guidance throughout this project. I am also grateful to Pello Aspuru, Jean-Pierre Benoît, Nethanel Ben Porath, Chris Blattman, Jesse Bruhn, Pedro Dal Bó, Oeindrila Dube, Eyal Frank, Andrew Foster, Andrea Galeotti, Oded Galor, Gabriel Simões Gaspar, Giorgio Chiovelli, Mayur Choudhary, Julian Marenz, Joseba Martinez, Luis Martinez, Stelios Michalopoulos, David Myatt, Eduardo Montero, Ameet Morjaria, Lakshmi Naaraayanan, Emre Özdenören, Hélène Rey, Natalie Rickard, James Robinson, Raul Sanchez de la Sierra, Andrew Scott, Tommaso Sonno, Paolo Surico, Ahmed Tahoun, Felipe Valencia Caicedo, Stephane Wolton, Shoda Wang, David Weil, and Étienne Le Rossignol. Address for correspondence: London Business School, Regent's Park, London, NW1 4SA, United Kingdom. Email: `gpincus@london.edu`. Website: www.guypincus.com.

JEL classifications: Q56, Q58, O13, F14, D74, Q34, C23

1 Introduction

Scientific evidence indicates that we are undergoing the first human-induced mass extinction of species (Ceballos et al., 2015). Combined with the prevailing view that the private consumption value of wildlife is lower than its social value from conservation (Brondízio et al., 2019; UNODC, 2024), this has motivated the international community to restrict or ban trade in wildlife products to protect biodiversity. The Convention on International Trade in Endangered Species of Wild Fauna and Flora (CITES), the main global mechanism for protecting wildlife (UNODC, 2024), banned international trade in rhino and elephant parts in 1976 and 1990, respectively, due to declining populations. Since then, CITES has regulated or banned the international trade in commodities derived from 38,710 endangered species. However, trade bans could raise prices and alter incentives, thereby empowering illegal actors and potentially fuelling violence (Miron, 1998; Angrist and Kugler, 2008; Becker et al., 2006; Dell, 2015; Castillo et al., 2020). This raises questions about the costs and benefits of conservation-motivated trade bans.

Illegal wildlife trade has been recognised as the third-largest transnational illicit activity, with markets for wild animals and timber estimated at $23 billion and $157 billion annually, respectively, surpassed only by counterfeiting ($923 billion) and the illicit drug trade ($426 billion) (UNODC, 2024). Suggestive evidence links this trade to the activities of armed groups. An INTERPOL (2014) investigation describes the ivory trade as a major source of funding for the Lord's Resistance Army—a rebel group active in Central Africa—while EIA (2020) highlights how the rosewood trade in Senegal finances local armed groups. BBC (2024) refers to the conflict that began in northern Mozambique in 2017 as being driven by "conflict timber", describing how the rosewood trade provided substantial financial resources to local armed groups. This occurred shortly after CITES banned international trade in rosewood in 2016. Despite its importance, both as a conflict-linked commodity and as a public good (Frank and Sudarshan, 2024), wildlife trade and biodiversity protection policies have been largely overlooked in economic research, likely due to challenges of data availability and measurement.

This paper examines the causal impact of global bans on international trade in wildlife-derived products, enacted under the CITES treaty, on armed conflict. In the empirical part of the analysis I document two windfall-related channels linking trade bans to conflict: higher wildlife prices and the relocation of harvesting to states with limited enforcement capacity. The estimates suggest that, because wildlife resources are spatially widespread, their conflict effect is quantitatively important, exceeding the magnitude of industrial conflict minerals such as gold, copper, and silver studied in the literature (Berman et al., 2017). Motivated by these findings, I construct a quantitative social planner model to evaluate how alternative policies can balance the conflict externality and conservation goals. The model shows that targeted bans restricting trade only in a subset of countries can mitigate the conflict externality while conserving wildlife.

CITES's institutional features allow for a causal identification of the effect of its trade bans on conflict. Its mandate is to protect wildlife from risks associated with international trade (UNODC, 2016), and it has the authority to ban international trade in wildlife-derived products. These bans should be enforced by the Convention's 184 signatories at their border crossings, without sanctions on consumers. Parties follow a predetermined schedule and meet every three years to vote on which species to restrict from international trade.

Before estimating the causal effect of the policy on conflict, I first use wholesale price data from China, a major demand market for wildlife products, to document the price response. CITES trade restrictions, which act as supply-side constraints, are associated with an average increase in wildlife prices of about one standard deviation. This pattern suggests that the policy affects the supply of wildlife. Second, to estimate the conflict effect of the policy, I construct a panel dataset, based on a global georeferenced grid ($0.5° \times 0.5°$), with data on habitat of seven genera of endangered wild animals and 24 genera of endangered wild trees, policy dates, and conflict indicators from three different conflict datasets (ACLED, UCDP, GTD). Because no single source provides habitat-suitability data for wild trees, I construct predictive habitat maps using a machine-learning algorithm trained on survey observations of wild tree locations together with bioclimatic and geographic features (Senula et al., 2019). Event-study specifications show that CITES policies increase the likelihood of armed conflicts in the habitat of the affected wildlife by about 2.6 percentage points for wild animals (35% of the baseline risk) and about 3.5 percentage points for wild trees (46% of the baseline risk). This finding is robust to alternative specifications, disaggregation levels, coding options, conflict definitions, exclusion of specific resources and regions from the sample, and inclusion of various potential confounders.

Inspection of the mechanism suggests that the policy generates windfall gains that fuel conflict through two distinct channels: a price channel and a harvest-relocation channel. I first study the African elephant ivory market using policy-driven supply shocks that left ivory's legal status in source countries unchanged. In 1998 and 2007, CITES authorised one-off sales of stockpiled ivory from South Africa, Botswana, Zimbabwe, and Namibia to China and Japan. I use these shocks as instruments in a two-stage least squares (2SLS) framework and show that policies affect conflict via prices: a one-standard-deviation increase in ivory prices raises the likelihood of conflict in elephant habitats by 22%. The reduced-form estimates indicate that the supply-expanding ivory sales in 1998 and 2007 decrease conflict likelihood by 23%. These findings are consistent with Kremer and Morcom (2000)'s theoretical work, where stock releases depress prices and help coordinate on a survival equilibrium. The estimated effect is comparable to the industrial minerals shock estimated by Berman et al. (2017), where a one-standard-deviation price increase raises conflict likelihood by 42%. When accounting for the spatial distribution of elephants and mineral resources, or for the number of people exposed to each shock, the ivory effect exceeds that of minerals. The analysis also shows that the ivory shock primarily drives one-sided attacks against civilians or local militias, and triggers both small- and large-scale conflict events.

Second, a major criticism of CITES policies is that states with low institutional capacity strug-

gle to enforce them (UNODC, 2016). Thus, I examine whether differences in state capacity are associated with the harvesting of wild trees, which creates local windfalls and, consequently, fuels conflict. I test this by introducing a methodological improvement that allows me to proxy tree harvesting at the taxa level.[1] Focusing on wild trees in Africa, I estimate harvest relocation by overlaying satellite-based deforestation data (Hansen et al., 2013) with genus-level habitat distributions (Senula et al., 2019) to construct a proxy for local tree harvesting. Using this proxy, I estimate a synthetic control event study specification (Ben-Michael et al., 2021; Funke et al., 2023) showing that the policy reduces tree harvesting in states with high institutional capacity, while harvesting in low-capacity states increases following the policy. These weak states are also where most of the policy-induced conflict originates. Overall, despite the relocation of harvesting, the CITES policy is effective in reducing total deforestation of wild trees.

Next, I test whether the windfall-related rise in conflict reflects stronger incentives to seize resource-rich territory (predation) or greater feasibility of attacks due to enhanced fighting capacity (Blattman and Miguel, 2010; Berman et al., 2017). I examine the spatial distribution of battles before and after the 2016 rosewood ban. The estimates suggest that, following the ban, armed groups operating in areas likely to benefit from the windfall tend to fight farther from prior locations and are more likely to gain territory. Together, these findings indicate that the ban generates windfalls that strengthen armed groups' fighting capacity and make attacks financially feasible.

Finally, to simulate alternative policies that account for the conservation–conflict trade-off, I construct a quantitative social planner model. The model features a policymaker analogous to CITES, who aims to protect wildlife while considering the conflict externalities of trade bans. Firms harvest and sell rare wild trees, and a local armed group loots these firms and uses the proceeds for territorial expansion to fight against an outside faction. The core mechanisms of the model are heterogeneity in state capacity to enforce the policymaker's global bans and differences in harvesting costs arising from initial stock. It rationalises the relocation of wild tree harvesting from strong to weak states following the ban, as observed in the data, links this relocation to conflict, and suggests a potential mitigation strategy.

Given the empirical evidence that the ban fuels conflict primarily in weak states, the model suggests replacing the uniform ban with a targeted ban applied only to strong states with relatively smaller resource stocks. This more moderate approach—restricting trade in fewer countries—reduces the contraction in wild tree supply due to the ban and, through a dampened price response, limits the relocation of harvesting from strong to weak states. As a result, it mitigates the conflict externality while still protecting wildlife from complete extinction.

The model's comparative statics highlight two additional policy-relevant dimensions. First, and consistent with Becker et al. (2006)'s theoretical work on the cocaine trade, the model shows that

[1] Throughout the paper, I use "taxa" to refer to taxonomic units listed under CITES, which may be defined at the genus or species level. I use "genera" when aggregating species-level data and "species" when referring explicitly to that level. I use "wildlife" to denote both animals and trees, and refer to "wild animals" and "wild trees" as shorthand for these subsets. Unless otherwise noted, these terms refer to CITES-listed taxa. I avoid the labels "endangered", "protected", or "precious" unless they are directly relevant to the discussion or analysis.

the policy-induced conflict externality is amplified for wildlife products with more inelastic demand. For such products, a given supply contraction leads to a larger price increase, which raises the value of loot and thereby fuels more conflict, making a partial ban preferable. Second, the model's counterfactual analysis indicates that for wildlife with higher reproduction rates, and thus faster natural recovery, a full trade ban is less likely to be optimal. In these cases, ecological damage is more easily reversible and consequently carries lower weight in the planner problem.

This paper is related to four strands of the literature. First, it contributes to the environmental policy literature by documenting the conflict cost of conservation-motivated trade bans. Existing work has largely focused on the effectiveness of conservation policies (Assunção and Gandour, 2019; Assunção et al., 2020; Hsiao, 2021; Da Mata and Dotta, 2021; Assunção et al., 2023; Frank and Oremus, 2023), the drivers of environmental degradation (Burgess et al., 2012; Greenstone and Jack, 2015; Burgess et al., 2015, 2017; Couttenier et al., 2022), and the implementation challenges of conservation efforts, particularly in low-capacity states (Balboni et al., 2021b; Glennerster and Jayachandran, 2023; Harstad, 2023).

Second, while most evidence on the violent effects of supply restrictions comes from illicit drug markets (Becker et al., 2006; Angrist and Kugler, 2008; Dell, 2015; Castillo et al., 2020; Castillo and Kronick, 2020), this paper provides evidence of this link in a setting with external validity across geographies and resources. It also identifies a novel windfall mechanism, showing that trade bans shift harvesting into lawless regions and, in doing so, fuel violence. Relatedly, Chimeli and Soares (2017) find that the mahogany export ban in Brazil increased violence, but their analysis is domestic in scope and does not provide evidence on the underlying mechanism.

Third, the paper provides the first causal evidence on the effect wildlife trade has on armed conflict, on a large geographic scale, by identifying a novel source of variation: policy-driven income shocks related to wildlife. Related work has examined commodity shocks (Dube and Vargas, 2013; Bazzi and Blattman, 2014; Berman and Couttenier, 2015; Berman et al., 2017; Ciccone, 2018), the financing of armed groups and militias (Shapiro and Siegel, 2009; Bueno de Mesquita, 2013; Limodio, 2019; Battiston et al., 2022), and climate shocks (Harari and La Ferrara, 2018; McGuirk and Nunn, 2020; Eberle et al., 2020) as drivers of conflict.

Fourth, with the exception of Dal Bó and Dal Bó (2011), Couttenier et al. (2024), and Bonadio et al. (2024), the academic literature has largely overlooked general-equilibrium interactions between conflict and economic activity. The theoretical model links wildlife harvesting, trade policy, and conflict through a supply-side feedback mechanism. It also builds on theoretical papers emphasising funding (Collier et al., 2009; Fearon, 2004) and state capacity (Besley and Persson, 2011b; Acemoglu et al., 2015) as key determinants of conflict.

The remainder of the paper is organised as follows. Section 2 reviews CITES policies, wildlife trade, and their links to armed group activity. Section 3 presents the data. Section 4 discusses the identification strategy, reports the baseline results for the global sample, and provides robustness checks. Section 5 focuses on Africa and examines the mechanism. Section 6 outlines the theoretical model and proposes mitigation strategies based on policy simulations. Section 7 concludes with a

discussion of policy implications.

2 Background

This section first describes the CITES convention—its mandate, policies, and legal scope. It then discusses the market for wildlife and its industrial organisation, providing anecdotal evidence linking wildlife trade to armed group activity.

2.1 CITES

The Convention on International Trade in Endangered Species of Wild Fauna and Flora (CITES) is an international agreement aimed at conserving wildlife by regulating international trade, ensuring that the trade does not cause species extinction. Established in 1973 and entering into force in 1975, with the leadership of the United States, CITES was created in response to growing concerns about the threat global trade poses to endangered species. Today, it has 184 signatories. Appendix Figures A.1 and A.2 show, respectively, the evolution of CITES membership over time and its current global coverage.

CITES is part of a broader international agenda to strengthen cooperation on environmental protection, developed in response to three key challenges: (i) the global interconnectedness of ecosystems, where environmental degradation in one country can have cross-border consequences; (ii) the institutional weakness of some of the most ecologically rich countries, limiting their capacity to safeguard biodiversity; and (iii) misaligned incentives between resource-rich countries that may be tempted to exploit natural assets and others that prioritise conservation.

CITES lists wildlife taxa (at the species or genus level) in three Appendices according to conservation status. Appendix I includes taxa at risk of extinction (e.g., rhinos), with trade allowed only in rare cases such as for scientific purposes. Appendix II includes taxa that could become endangered if trade is not regulated (e.g., hippopotamus). Appendix III includes taxa protected within specific countries that have requested international assistance in controlling trade (e.g., South African abalone).

Parties meet approximately every three years based on a pre-determined schedule at the Conference of the Parties to update listings of wildlife taxa and revise policies. Each Party is responsible for implementing and enforcing CITES regulations at all border crossings. At its launch, CITES listed about 500 taxa. By 2023, more than 38,000 taxa were regulated under CITES, most of them insects, small plants, and marine life.

Signatory countries that do not comply with CITES may face trade bans on legal wildlife products, lose access to technical and financial conservation support, and come under diplomatic pressure from other member states. For example, in 2018, China banned domestic trade in antique ivory following CITES threats of suspension from legal wildlife trade. Additionally, in 2023, CITES imposed trade sanctions on Mexico, suspending all commercial trade in CITES-listed species due to non-compliance with obligations to protect the critically endangered vaquita, a small marine

mammal endemic to the Gulf of California, Mexico.[2] The sanctions affected a wide range of wildlife products (e.g., crocodile leather, reptile skins, reptiles and exotic pets, orchids, and cacti).

2.2 The Industrial Organisation of Wildlife Markets

2.2.1 Demand

Contemporary demand for wildlife products largely originates from Asia, particularly China, reflecting a combination of cultural, economic, and medicinal factors (Zhu, 2020). Traditional medicine remains a major source of demand for products such as rhino horn, tiger bones, and pangolin scales (Mainka and Mills, 1995), while luxury markets value elephant ivory, rosewood, ebony, crocodile leather, and exotic furs for their aesthetic and status appeal (Sosnowski and Petrossian, 2020; Zhu, 2022). Rosewood, in particular, has symbolised wealth and distinction since the Qing dynasty and is increasingly treated as an investment asset (Ding and Yin, 2024).

The recent surge in demand is closely tied to the rising economic power of China and other Asian countries, where growing incomes have fuelled consumption of goods perceived as luxury items, status symbols, or components of traditional medicine (UNODC, 2020). This trend is reinforced by a broader state-led revival of traditional Chinese culture and heritage, initiated under Hu Jintao (2002-2012) and intensified under Xi Jinping (2012-present) (Zhu, 2020).

2.2.2 Supply

The supply of wildlife products has long been dominated by armed groups, predating formal trade restrictions (RUSI, 2015; TRAFFIC, 2015; WWF, 2015; EIA, 2017). UNODC (2020) describes how armed groups across Africa and South-East Asia facilitate poaching by providing resources and retaining the majority of profits. Local brokers then collect wildlife products and transport them to urban storage centres, from which intermediaries—often foreign nationals originating from major destination markets—export the goods by bribing officials to evade customs enforcement.[3] For example, EIA (2014) documents how the Shandong cartel used legal agricultural trade as a cover to smuggle ivory, bribing local politicians in the process. Finally, wholesalers and retailers distribute the products within destination markets.

The Rosewood Trade and Northern Mozambique's Conflict. The insurgencies in northern Mozambique's Cabo Delgado and Nampula provinces since 2017 have been linked to the illicit trade in rosewood (*Dalbergia*), listed under CITES Appendix II since 2016. According to BBC News (2023), demand from China has fuelled illegal logging operations, which in turn finance the al-Shabab insurgent group. A Mozambique government report cited by BBC (2024) states that "*al-Shabab insurgents have taken advantage of the illicit timber trade to fuel and finance the reproduction of violence,*" and further notes that "*the insurgents involvement in the smuggling of fauna*

[2]Other recent examples include Thailand (2013), Belize (2013), Guinea (2013), Lao PDR (2016), the Democratic Republic of Congo (2018), and Nigeria (2022).

[3]Exporters are often nationals of the destination country, as this helps mitigate trust issues inherent in cross-border illegal trade.

and flora products, including wood, and the exploitation of forest and wildlife resources is contributing to a very high level of fundraising for the insurgency group." The same report estimates that "*its revenue from these activities amounted to $1.9 million a month.*" Mozambique analyst Joe Hanlon adds that "*it has also gained enough funds to recruit in neighbouring provinces further south.*" There have also been reports of firms paying a "*10% protection fee*" to the armed group in exchange for permission to carry out illegal logging in forest areas. These dynamics underscore the significant role the high-end illegal timber trade plays in financing conflicts across Africa.

Ivory Trade and Armed Groups' Activity in Africa. Several organisations have documented links between the ivory trade and armed groups' activities. According to United Nations Security Council (2013) "*The Lord's Resistance Army (LRA), an armed group originating in Uganda, is known to have poached elephants in Garamba National Park (Democratic Republic of Congo) and trafficked ivory through South Sudan into Sudan, where it is exchanged for arms and supplies.*" Similarly, an investigation by the INTERPOL (2014) reveals that "*Kony–the LRA leader–ordered his fighters to collect ivory, which was used to barter for food, weapons, and cash*" and that "*the LRA's operations in Garamba have decimated local elephant populations and created an illicit supply route from Congo through South Sudan.*" In Chad and the Central African Republic, the Janjaweed group has targeted parks such as Zakouma National Park. According to Enough Project (2015) "*Heavily armed horsemen conducted cross-border poaching raids, massacring hundreds of elephants in a matter of days. The ivory was transported north, reportedly taxed or protected by armed groups.*" According to Global Initiative Against Transnational Organized Crime (2017) "*ivory, along with gold and diamonds, became a resource exploited by the Seleka and Anti-Balaka armed factions in the Central African Republic, who used it to fund military operations.*"

The Supply Chain of Ivory. Poachers typically earn about 10% of the final raw ivory price (UNODC, 2016). For an adult African elephant, whose tusks can weigh up to 100 kg (Milliken et al., 2000), this can make poaching an attractive source of income. As tusks move along the supply chain, their price can increase by 200–300% at multiple stages, and again after being carved into high-value artefacts (UNODC, 2016). Appendix Figure A.3 illustrates the supply chains of elephant ivory and rhino horn.

2.2.3 Further Anecdotal Evidence

Data from the African Elephant Database, a pan-African aerial census conducted every 5 to 10 years, further supports the link between armed groups and poaching. During the Chadian Civil War (2005–2010), major fighting occurred near Am Timan and Mongo. In early 2005, a census in Zakouma Park near Am Timan counted 3,885 elephants. By 2014, only 443 remained—a 90% decline. Similarly, Lake Fitri near Mongo had 200 elephants in 2005 and only 70 in 2015, a 65% drop. In the Democratic Republic of the Congo, the Kivu civil wars (2004–2013) took place near Maiko and Kahuzi-Biega National Parks. In 1992, Maiko and surrounding areas had an estimated 6,500 elephants; by 2015, only 100 remained. In Kahuzi-Biega, the elephant population fell from 1,150 in 2002 to 70 in 2015. These represent declines of 94–98%. Although descriptive, the analysis

suggests armed groups' involvement in poaching.

3 Data

This section discusses the data sources, the different conflict datasets, variable definitions, and measurements. I also provide various statistics describing the data.

3.1 Data Sources

The sample for the main analysis consists of a global grid divided into $0.5^\circ \times 0.5^\circ$ cells (approximately 55×55 kilometres at the equator), with the unit of analysis being the cell–year. The main outcome variable is a conflict indicator, with wildlife habitat and trade restriction dates as the key explanatory variables. I use wildlife prices and deforestation data to explore the mechanism.

3.1.1 Conflict

To maximise spatial and temporal coverage, I use georeferenced conflict data from three main sources: the Uppsala Conflict Data Program (UCDP) (Sundberg and Melander, 2013), the Armed Conflict Location and Event Data (ACLED) (Raleigh et al., 2010), and the Global Terrorism Database (GTD) (LaFree and Dugan, 2007). Each source has its own strengths and limitations. UCDP covers conflicts since 1989 with at least 25 battle-related deaths and requires at least one organised actor, potentially omitting relevant events just below the threshold. ACLED, starting in 1997 (Africa), 2010 (Asia), and 2017 (Latin America), imposes no fatality threshold and captures a broader range of events, though it may include less relevant incidents. The GTD has been available globally since 1970 and focuses solely on terrorism.

All three datasets draw on news, media, NGO, and government reports. Compared to ACLED, UCDP's strict fatality threshold and GTD's narrow event definition help reduce measurement error and media bias. These concerns are mitigated using cell and country-year fixed effects. In ACLED, I follow Berman et al. (2017) in coding "battles", "violence against civilians", and "protests and riots" as conflict events, and I also conduct a separate analysis by subcategory.

3.1.2 Habitats

In constructing habitat measures for wildlife taxa (wild animals and trees), I first select the relevant taxa. I do so by first selecting only taxa that are discussed in Groves and Rutherford (2023) and UNODC (2024) as heavily traded in illicit markets and protected under CITES. Second, due to econometric identification requirements, I focus solely on taxa with well-defined geographic ranges.[4] Given this, the full sample includes seven taxa of endangered wild animals along with 24 taxa of endangered wild trees.

[4]For instance, some birds and snakes are known to be traded in illicit markets, but do not have well-defined habitat.

Wild animals' habitat data are sourced from the International Union for Conservation of Nature (IUCN), the leading scientific conservation organisation specialising in wildlife monitoring, which provides binary species-level range maps. I aggregate these maps to the genus level for consistency with the policy. There is no single source providing habitat suitability measures for wild tree taxa. To overcome this limitation, I gather georeferenced observations of wild tree species from the Global Biodiversity Information Facility (GBIF) and aggregate them to the genus level. Species within each genus are pooled due to limited occurrence records per species, allowing for more reliable habitat suitability estimation. To minimise measurement error, I disregard the time dimension of these surveys and treat the observations as a time-invariant proxy for taxa presence at each location. Following established methods in the quantitative ecology literature (Phillips et al., 2006; Senula et al., 2019), I use these observations as inputs to a Maximum Entropy machine learning model to construct genus-level habitat suitability maps based on bioclimatic and geographical features. Then I convert these genus-level habitat distribution maps into binary habitat measures—to be consistent with the IUCN wild animal maps—which I use as proxies for the spatial distribution of wild tree species. Appendix Section F provides further details on how the wild tree habitat maps were constructed.

3.1.3 Policy

Policy change dates are sourced from the CITES website and summarised in Appendix Table A.2. Most wild animal taxa are listed under Appendix I, with the exception of abalone, hippopotamus, and crocodiles, which are listed under Appendix II. All wild tree taxa—typically listed at the genus level—except *Dalbergia nigra* (Appendix I) are listed under Appendix II, with zero commercial trade quotas, effectively constituting a trade ban. Unless stated otherwise, policies are enforced 90 days after announcement.

3.1.4 Prices

Due to the illicit nature of the wildlife trade, there is no official source of wildlife prices. Of the 31 taxa in the sample, I obtained annual price data for six. Price data for three tree taxa—*Dalbergia* and *Pterocarpus* (2009–2020), and *Diospyros* (1997–2021)—were sourced from China's largest domestic wholesale raw wood market, the Yuzhu International Timber Market (Ding and Yin, 2024). Rhino horn and elephant ivory prices from the 1970s–1980s were obtained from surveys of retail markets in Hong Kong (IUCN, 1990).

For contemporary elephant ivory and Nile crocodile leather, I follow Farah and Boyce (2019) and Hauenstein et al. (2019) in using prices of close substitutes. Nile crocodile leather prices are proxied using American alligator leather prices, and contemporary elephant ivory prices are proxied using mammoth ivory.[5] To validate the reliability of the mammoth ivory price series, I use three

[5]Discovered in Siberia in 1992, mammoth ivory has been legally exported from Russia, primarily to China. Its prices, sourced from Comtrade, reflect wholesale values of uncarved ivory and are less prone to measurement error compared to other ivory price sequences derived from surveys and confiscation data.

alternative sequences as part of the sensitivity checks. First, Do et al. (2021) and Sosnowski et al. (2019) estimate ivory prices from confiscation data, controlling for various fixed effects, but their sequences end in 2013 and 2016, respectively. Second, I scrape and aggregate ivory transaction data from auction-house websites for the period 2012–2021, when antique ivory could still be legally sold in the UK. Both alternative sequences are highly correlated with mammoth ivory prices, with one showing a correlation of 0.82 ($t = 5.68$) and the other 0.85 ($t = 6.64$). The main estimates remain robust when either is used.

To summarise, I use close substitutes for two of the seven price sequences: contemporary elephant ivory and Nile crocodile. For the remaining five (*Dalbergia*, *Diospyros*, *Pterocarpus*, rhino horn, and elephant ivory from the 1970s–1980s), prices are sourced from Chinese markets, the primary destination for these products. All prices refer to uncarved raw materials.

3.1.5 Deforestation of Wild Tree Taxa

Official statistics on traded quantities of wild trees are not available at the taxon level. Moreover, many of these taxa are traded in illicit markets. To estimate changes in harvested quantities of wild tree taxa following the policy, I combine remote-sensing deforestation data (Hansen et al., 2013) with taxa-level habitat maps on a $0.1^\circ \times 0.1^\circ$ grid. This yields a proxy for taxa-level harvesting quantities.

The deforestation measure of Hansen et al. (2013) is based on satellite imagery. Tree cover loss is defined as a stand-replacement disturbance, or the complete removal of tree canopy, at the pixel level. The original dataset provides annual estimates of tree cover loss relative to year-2000 forest cover, at a spatial resolution of 1 arc-second (30×30 metres). A common practice is to aggregate it to the unit of analysis ($0.1^\circ \times 0.1^\circ$ in my case) (Burgess et al., 2012; Berman et al., 2023).

3.1.6 Industrial Minerals

For comparison with the industrial mineral shock estimates, I use data from Berman et al. (2017), covering 14 minerals across Africa. I extend their dataset through 2024 by merging it with updated price series for the respective minerals.

3.1.7 Other Data

To examine heterogeneity by state institutional capacity, I use the Combined Polity Score variable from the Polity IV dataset.

3.2 Descriptive Statistics

The final sample consists of 176 countries, of which 172 experienced at least one conflict or terror event across all datasets. A total of 149 countries have some form of resource presence, 59 with wild animals and 149 with different species of wild trees. The sample includes 96,440 unique cells, covering the periods 1997–2024 (ACLED), 1989–2023 (UCDP), and 1970–2021 (GTD). Overall, 16.5% of cells

(15,916) experienced at least one conflict event during the sample period. Unconditional conflict probabilities are 5.5% (ACLED), 1.2% (UCDP), and 0.82% (GTD). Conflict is more likely in resource cells, with ACLED estimates of 10.4% in wild animal areas, 11.8% in wild tree areas, and 16.1% in mineral areas. This may reflect unobserved characteristics, highlighting the importance of including cell and country-year fixed effects in the analysis.

Figure 1 displays the global distribution of conflict events recorded in ACLED.[6] Most events are clustered in the Great Lakes region of Africa, extending through Middle Africa toward the West Coast. Additional clusters appear along the South-East coast and in the Horn of Africa. Outside Africa, notable clusters are observed along Brazil's East Coast, in Central America, and in Central Asia. Appendix Table A.4 reports pairwise correlations across conflict datasets, indicating that conflict events are spatially correlated across the three sources. ACLED records the highest number of events, and GTD the lowest.

[6] Appendix Figure A.4 shows the distribution of events based on UCDP and GTD.

Figure 1: Spatial Distribution of ACLED Conflict Events

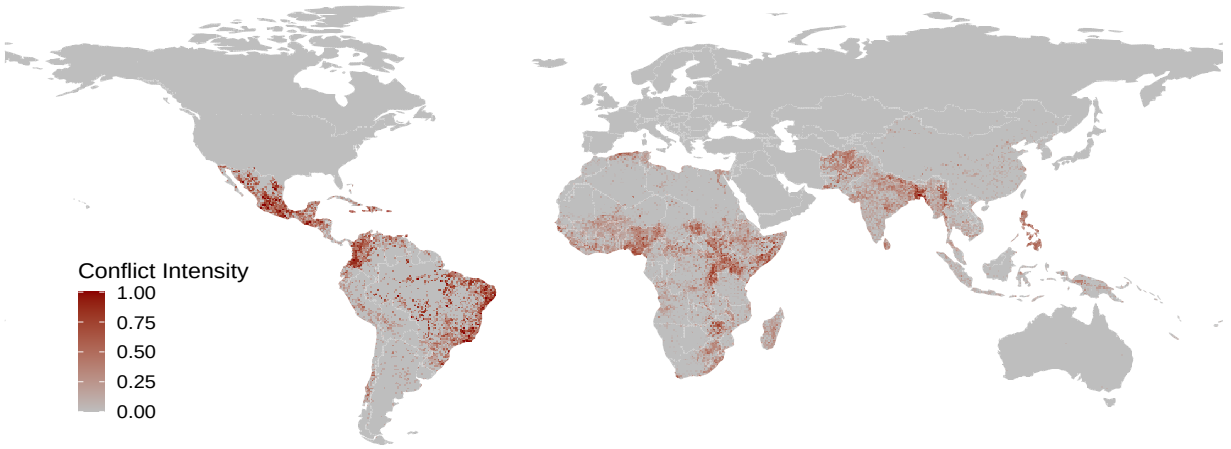

(a) Global

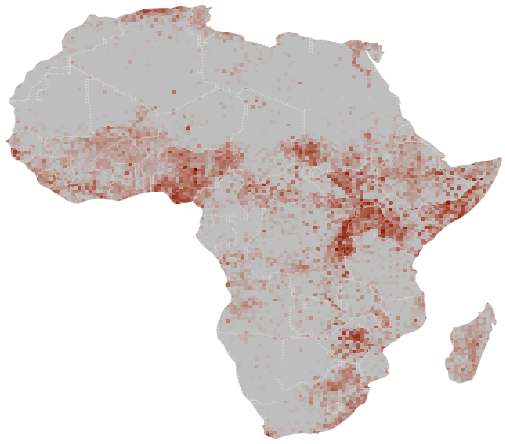

(b) Africa

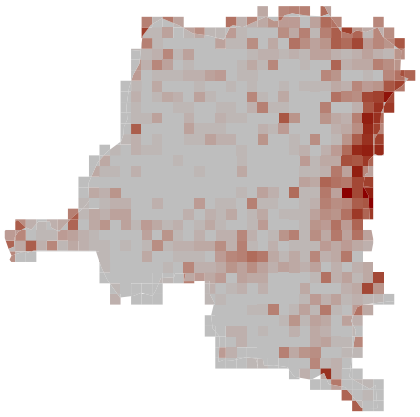

(c) Democratic Republic of Congo

Notes: Panel (a) shows the spatial distribution of ACLED (1997–2024) conflict events, where darker shading indicates a higher proportion of years with at least one recorded incident. Panels (b) and (c) show conflict maps for Africa and the Democratic Republic of Congo (DRC), respectively.

Overall, 5% of cells are suitable for wild animals and 10% for wild trees. Elephants (African and Asian) have the largest animal habitat, covering 2.8% of cells, while *Dalbergia* is the most widespread tree genus, suitable for 4.5% of cells. Figures 2 and 3 show the spatial distributions of wild animals and trees included in the sample: animals are concentrated primarily in sub-Saharan Africa and South-East Asia, while trees are concentrated in sub-Saharan Africa, South-East Asia, and Latin America. 10.3% of habitat cells are suitable for more than one taxon, which may complicate identification. I address this issue by assigning each cell to the wildlife taxon that was first listed by CITES.[7] Appendix Table A.5 reports descriptive statistics of the main variables of interest.

[7]If two wildlife taxa are suitable for the same cell and were listed at the same time by CITES, I exclude those cells.

Figure 2: Spatial Distribution of Wild Animals Habitat

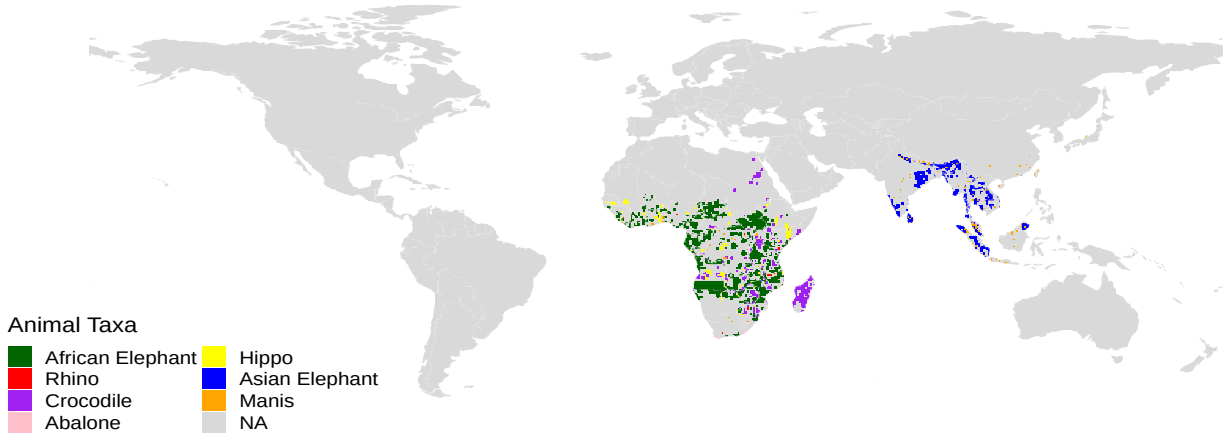

(a) Global

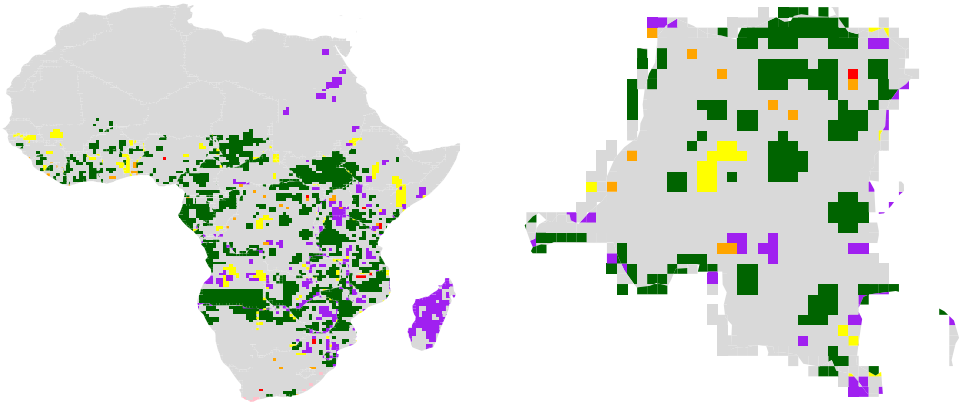

(b) Africa **(c)** Democratic Republic of Congo

Notes: Panel (a) shows the spatial distribution of areas suitable for wild animals. Panels (b) and (c) show habitat distributions for Africa and the Democratic Republic of Congo (DRC), respectively. The colours indicate habitat suitability for different wild animals.

Figure 3: Spatial Distribution of Wild Trees Habitat

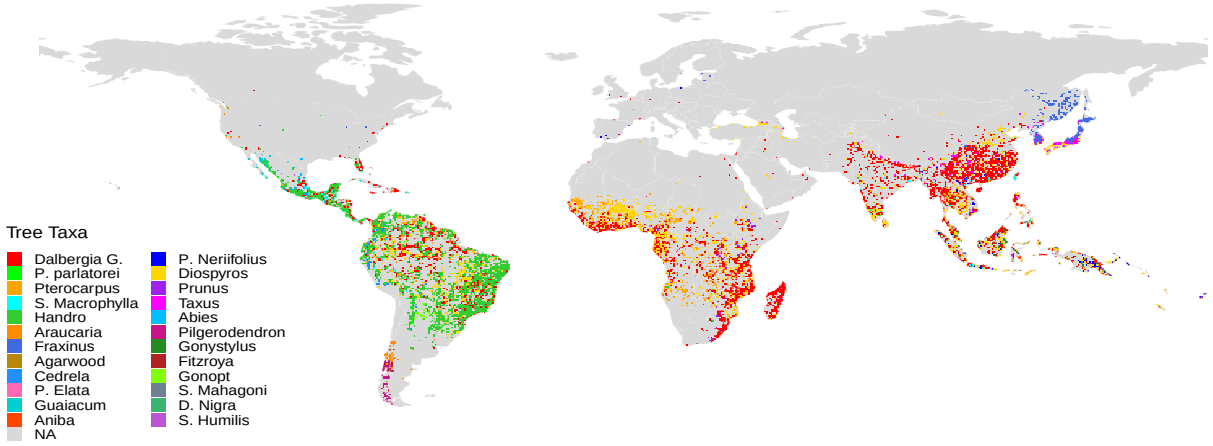

(a) Global

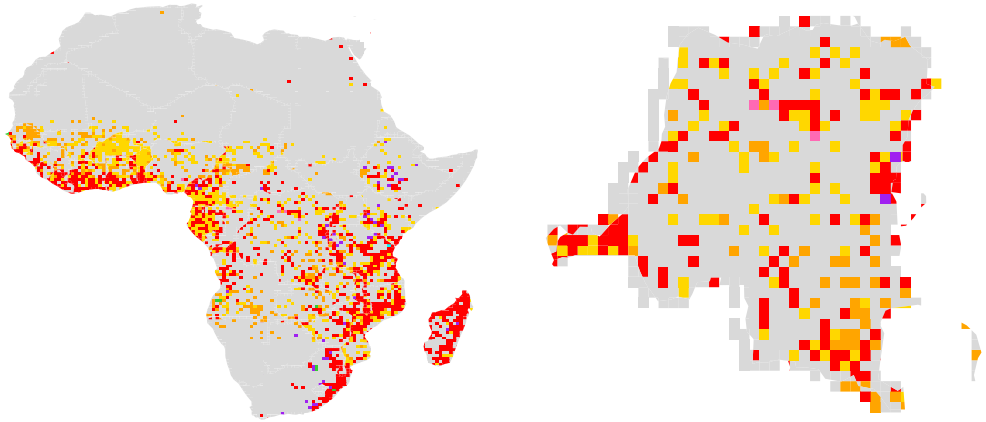

(b) Africa **(c)** Democratic Republic of Congo

Notes: Panel (a) shows the spatial distribution of areas suitable for wild trees. Panels (b) and (c) show habitat distributions for Africa and the Democratic Republic of Congo (DRC), respectively. The colours indicate habitat suitability for different wild trees.

3.2.1 CITES Policies and Wildlife Prices

CITES restricts exports from source countries and imposes no sanctions on consumers. These restrictions are enforced at both exporters' and importers' borders. Therefore, the policy is interpreted as a negative supply shock moving the supply curve inward. Figure 4 presents suggestive evidence showing that CITES restrictions are, as expected, associated with higher wildlife prices. Appendix Figure A.6 shows the corresponding event study estimates, suggesting an average price increase of about one standard deviation following the policy. The estimates also support the parallel trends assumption.

Figure 4: Wildlife Prices and CITES Policies

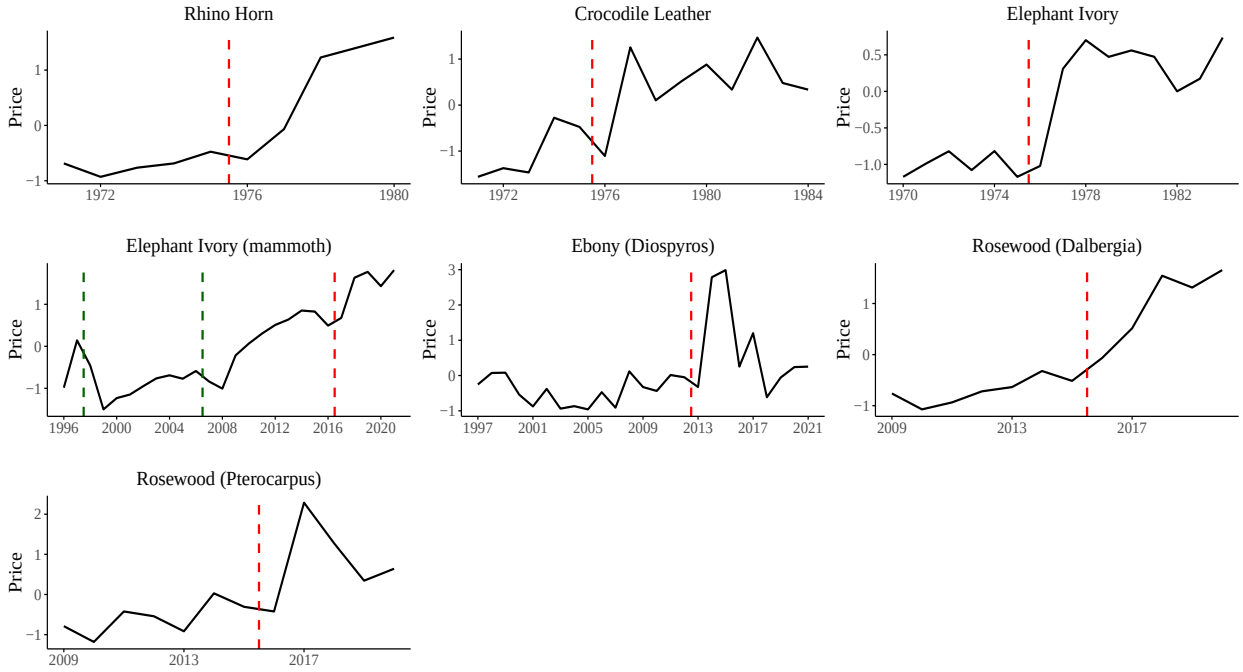

Notes: The figure shows detrended wildlife prices together with policy changes: restrictive policies in red and expansionary policies in green.

Appendix Figure A.7 reports the number of confiscation events of elephant ivory, rosewood, and ebony before and after the corresponding policies, suggesting a tightening of supply following the trade restrictions.

Taken together, the evidence suggests that CITES policy reduces wildlife supply and is associated with higher wildlife prices.

4 Empirical Analysis

This section details the empirical strategy. Then it presents the main estimates and assesses their robustness using a series of alternative specifications.

4.1 Identification Strategy

To assess how CITES restrictions on international wildlife trade affect conflict, I estimate a linear probability model (LPM) using an event study specification. Following the conflict literature (Berman et al., 2017; Ciccone, 2018; Limodio, 2019; McGuirk and Nunn, 2020, 2024), I use a binary indicator for whether at least one conflict event occurs in a given cell-year as the outcome variable. The main explanatory variable is the interaction between policy timing and a habitat suitability indicator.[8] Using binary variables helps mitigate measurement error relative to counts

[8] For each cell, I have one wildlife, and for mixed cells, I assign the wildlife listed first by CITES, so the suitability measure is unique per cell.

or continuous measures. This identification strategy—interacting a global shock with local cell-level characteristics—follows recent advances in the conflict literature (Miguel et al., 2004; Dube and Vargas, 2013; Berman et al., 2017). Concerns about potential confounders and omitted variables (e.g., geographic variation or domestic policies) are mitigated through cell and country-year fixed effects. An advantage of using wildlife habitat as a proxy for trade is that data on habitat and policy timing are available for all wildlife in my sample.[9] The core logic is to test whether conflict likelihood changes in habitat areas following a global shock to the trade of a specific wildlife. Since CITES meetings occur on a predetermined three-year schedule and policies take effect within 90 days, I code the announcement year as the event start ($t = 0$).

Recent works demonstrate that least squares estimation in staggered event studies, as in my case, can produce biased estimates of the average treatment effect (De Chaisemartin and d'Haultfoeuille, 2020; Callaway and Sant'Anna, 2021). The problem arises because least squares with staggered rollout not only leverages comparisons between treated units and "pure" controls, but also compares treated units to those treated earlier. These so-called "forbidden" comparisons are problematic when dynamic treatment effects are heterogeneous. Therefore, I estimate the static and dynamic association between trade restrictions and conflict using the imputation method of Borusyak et al. (2024), which is well-suited to my setting.

I analyse wild animals and wild trees separately, because the data are constructed independently, and estimate the following equation[10]:

$$Y_{k,t} = \sum_{\substack{r=-7 \\ r\neq -1}}^{7} \beta_r \left(M_{k,w(k)} \times D_{w(k),t+r} \right) + \lambda_k + \delta_{c,t} + \epsilon_{k,t} \tag{1}$$

$Y_{k,t}$ is a binary indicator for conflict in cell k and year t. The term $\beta_r \left(M_{k,w(k)} \, D_{w(k),t+r} \right)$ captures the treatment effect in event time r. The index r represents the relative time to when trade in wildlife taxon $w(k)$ becomes restricted under CITES. The term $w(k)$ denotes the unique wildlife taxon suitable for cell k. $D_{w(k),t+r}$ is an indicator that equals one in years t that are r periods before or after the restriction year for taxon $w(k)$. $M_{k,w(k)}$ is a time-invariant indicator for the suitability of cell k for wildlife taxon $w(k)$. The specification includes cell (λ_k) and country-year ($\delta_{c,t}$) fixed effects, to control for time-invariant factors and time-varying country-level shocks. The coefficients of interest, β_r, are identified from within-cell variation in CITES trade restrictions over time. To mitigate concerns about serial correlation, I cluster standard errors within a 500 kilometre spatial radius, which yields the most conservative estimates.

[9] This is in contrast to data on trade volume, prices or trade routes. An alternative approach would follow Berman et al. (2017) in using variation in international prices as a continuous treatment. However, due to the illegal nature of the trade, consistent price data is difficult to obtain. Nonetheless, Appendix Table B.1 presents analogous estimates for the six species for which I do have price data.

[10] I combine the two in the sensitivity checks.

4.2 Baseline Results

Figure 5 displays event study estimates (equation (1)) using the ACLED conflict outcome. Panel (a) presents estimates for wild animals. The parallel trends assumption holds, and the estimates are positive and statistically significant, showing an average increase of 2.6 percentage points (corresponding to 35% from the baseline risk) in the likelihood of conflict in cells suitable for wild animals following the policy. The effect intensifies up to the fifth post-policy period and then diminishes.

Panel (b) presents estimates for wild trees. The parallel trends assumption holds, and the estimates are positive and statistically significant. On average, the policy leads to a 3.54 percentage points (corresponding to 46% from the baseline risk) increase in the likelihood of conflict in cells suitable for wild trees, with the effect increasing monotonically over time. The lower standard errors for the wild tree estimates may reflect greater accuracy in the spatial data on tree distribution.

Table 1 reports difference-in-differences estimates using ACLED, UCDP, and GTD conflict outcomes, all consistent with the event study findings. Importantly, the UCDP estimates—capturing large conflict events with a death threshold above 25—are also positive and statistically significant (for animals: 1.29 percentage points and a 42% rise from the baseline conflict risk; for trees: 0.8 percentage points and a 27% rise from the baseline conflict risk). The GTD estimates, which also capture events from the 1970s and 1980s, are similarly consistent, showing positive and statistically significant effects (for animals: 1.5 percentage points and an 86% increase from the baseline conflict risk; for trees: 1.4 percentage points and an 80% increase from the baseline conflict risk).

These estimates are consistent with, and fall between, those reported in other papers (Berman et al., 2017; Eberle et al., 2020; McGuirk and Burke, 2020; McGuirk and Nunn, 2025) that use a similar methodology with ACLED data to study changes in conflict likelihood following different shocks.

Figure 5: Wildlife Trade Restrictions and Conflict Likelihood

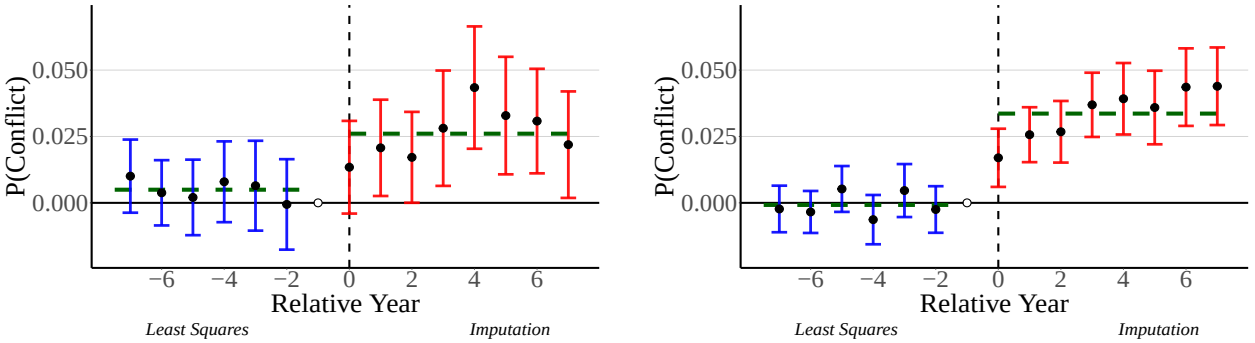

(a) Wild Animals **(b)** Wild Trees

Notes: The figure reports LPM estimates obtained using the staggered event-study imputation estimator proposed by Borusyak et al. (2024). The pre-treatment coefficients are estimated by least squares, while the post-treatment coefficients are estimated using the imputation estimator. Each observation corresponds to a cell–year (1,430,970 for wild animals and 1,435,230 for wild trees). Estimates are based on equation (1). The dependent variable is a binary indicator for conflict incidence, equal to one if at least one conflict event occurs in a given cell and year, based on the ACLED dataset. The main explanatory variable is an indicator for habitat cells of protected wildlife in post-policy periods. The specification includes cell and country–year fixed effects. The omitted period is the year preceding the policy announcement. The first and last coefficients are binned. The green horizontal lines indicate the mean of the pre- and post-treatment coefficients. Error bars represent 95% confidence intervals, with standard errors spatially clustered to allow for spatial and temporal correlation within a 500 km radius of each cell's centroid.

Table 1: Wildlife Trade Restrictions and Conflict Likelihood: Difference-in-Differences

	Dep. Var.: Conflict (0/1)					
	Animals			Trees		
	ACLED	UCDP	GTD	ACLED	UCDP	GTD
	(1)	(2)	(3)	(4)	(5)	(6)
Habitat × *Policy*	0.027***	0.013***	0.015***	0.035***	0.008***	0.014***
	(0.007)	(0.005)	(0.004)	(0.004)	(0.003)	(0.002)
	[0.003]	[0.001]	[0.001]	[0.002]	[0.001]	[0.001]
Cell FE	Y	Y	Y	Y	Y	Y
Country-Year FE	Y	Y	Y	Y	Y	Y
Observations	1,430,970	3,338,930	4,960,696	1,435,230	3,348,870	4,975,464
Dep. Var. Mean	0.076	0.030	0.017	0.076	0.030	0.017
Dep. Var. SD	0.265	0.171	0.131	0.265	0.171	0.131

Notes: The table reports LPM estimates using the Borusyak et al. (2024) imputation difference-in-differences estimator. Each observation corresponds to a cell-year. The variable *Habitat* is an indicator measuring the suitability of cell k for wildlife taxon w, and *Policy* indicates the timing of CITES trade restrictions imposed on wildlife taxon w at time t. The dependent variable is a binary indicator for conflict incidence, equal to one if at least one conflict event occurs in a given cell and year, based on the conflict datasets referenced in the column title. Coefficients are reported with spatially clustered standard errors (in parentheses), which allow for spatial and temporal correlation within a 500 km radius of each cell's centroid. Standard errors reported in square brackets are clustered at the country-year and cell levels, allowing for within-country spatial correlation and infinite serial correlation within a cell. * significant at 10%; ** significant at 5%; *** significant at 1%.

4.3 Sensitivity Analysis

In this subsection, I discuss sensitivity checks.

Exogeneity of Policy. Although the parallel trends assumption is satisfied, there may still be concerns about potential endogeneity, specifically whether CITES responds to poaching crises linked to conflict or targets conflict-affected regions. This is unlikely given how CITES operates. While scientific recommendations inform CITES decisions, the final outcome is political and requires a two-thirds majority vote among member countries. Frank and Wilcove (2019) show that there are often long delays—averaging 10 years—in implementing trade bans on threatened species, reflecting the slow and unpredictable nature of the political process. In addition, I perform a text analysis of CITES protocols, which reveals no explicit mention of armed conflict or armed groups in official meetings. Furthermore, Appendix Figure D.1 shows an anticipation test, where I shift the policy year six periods earlier, yielding insignificant estimates. To further address concerns about policy endogeneity, Appendix Figures D.2 and D.3 confirm that the estimates remain robust when iteratively excluding different continental subregions, or random batches of 10% of the observations, reducing concerns that CITES systematically targets conflict-prone regions.

Measurement Error. A concern with using wildlife habitat classification as a proxy for treatment exposure is measurement error. I implement two exercises to address this. First, Appendix Table D.2 reports country-level, shift-share style estimates, using policy years as shifts and the total number of habitat cells as a proxy for each country's wildlife stock as shares. This aggregation helps reduce the risk of local-level measurement errors. Second, Appendix Tables D.3 and D.4 report estimates using a $0.25° \times 0.25°$ and $1° \times 1°$ grid resolutions to test robustness to cell-size.

Potential Confounders. Due to the large spatial coverage of wildlife habitat, another concern is that its distribution may overlap with other valuable resources—such as gold, minerals, or crops—potentially confounding the estimates. To mitigate this concern, I exclude all cells geologically suitable for gold (Girard et al., 2022), as well as those that overlap with industrial mineral sites (Berman et al., 2017).[11] To further ensure that spatial confounders are not driving the estimates, I divide the sample into above- and below-median groups based on urban areas, crop production, human footprint, and population density, and replicate the ACLED estimates from Table 1 for each subsample. Following Eberle et al. (2020), I also exclude all Sahel countries. Estimates are reported in Appendix Table D.5. Although coefficient magnitudes vary, probably due to substantially reduced sample sizes, the estimates remain robust across all specifications.

Different Control Groups. The global approach—necessary for external validity and to capture a wide range of resources and policy shocks—raises concerns about the adequacy of the control group. To mitigate this concern, I estimate a staggered event study specification using the augmented synthetic control estimator from Ben-Michael et al. (2021), which constructs control groups that perfectly match the pre-trends of treated units. Estimates are reported in Appendix Figure D.4 and Appendix Table D.6. Furthermore, in Appendix Table D.7, I pool wild animals and wild trees, defining treatment as CITES restrictions on either category. The estimates are consistent with the main analysis, showing slightly larger coefficients.

Sensitivity to Spatial Clustering. Appendix Figure D.5 plots the baseline estimates using different levels of spatial clustering, from $1° \times 1°$ to $10° \times 10°$ (110×110 km to $1{,}100 \times 1{,}100$ km at the equator), showing that the statistical inference are insensitive to the choice of spatial cluster size.

Alternative Conflict Outcomes. Conflicts are difficult to measure and are likely measured with error (Berman et al., 2017). Thus, the common approach in the conflict literature is to estimate a linear probability model with a binary conflict outcome (Bazzi and Blattman, 2014; Berman and Couttenier, 2015; Berman et al., 2017; Ciccone, 2018; Eberle et al., 2020; McGuirk and Nunn, 2020). Appendix Table D.8 reports estimates using the total number of conflict events and total number of deaths ($log(x+1)$) in a given cell-year. Appendix Table D.9 reports estimates using conflict onset instead of conflict incident.[12] Appendix Table D.10 presents estimates using a binary indicator for conflicts with above-median fatalities, yielding results consistent with the baseline analysis.

[11] Although the geological suitability map from Girard et al. (2022) is specific to gold, it covers approximately 43% of African cells and likely captures other artisanal mining areas as well.

[12] Following Berman et al. (2017), I define conflict onset as the year of transition from peace to conflict in a given cell.

Alternative Estimators. Appendix Table D.11 shows estimates using the estimators from Callaway and Sant'Anna (2021) and Sun and Abraham (2021), which are consistent with those reported in Table 1.

5 Mechanism

This section examines the mechanism by which restrictions on wildlife trade increase conflict, drawing on the commodity-conflict literature (Becker et al., 2006; Angrist and Kugler, 2008; Fearon, 2008; Dube and Vargas, 2013; Bazzi and Blattman, 2014; Berman et al., 2017; Ciccone, 2018) emphasising the role of windfalls in fuelling violence.

First, focusing on the harvesting of wild trees, I show that harvesting activity shifted from strong, more compliant states to weak states, where most of the conflict effect originates. Second, given evidence that the policy affects wildlife prices (Figure 4 and Appendix Figure A.6), I focus on the ivory market, where I leverage supply shocks that left the legal status of elephant ivory unchanged as a natural experiment to estimate the price effect of CITES policies on conflict. Additionally, I aggregate the estimates by spatial and population exposure and compare them to the effect of the industrial minerals shock studied by Berman et al. (2017). After establishing the conflict-windfall nexus, I explore how armed groups' fighting dynamics and winning likelihood have changed following the policy.

The empirical analysis in this section focuses solely on the African sample, mainly due to better temporal coverage provided by the ACLED dataset and for consistency across subsections.[13]

5.1 Evidence of Windfall Gains

5.1.1 Quantities

While CITES policy is global, countries vary in their capacity to enforce it. For example, Botswana and South Africa have stronger enforcement capacity and are likely more effective at implementing CITES bans on wildlife trade than the Central African Republic or the Democratic Republic of Congo. Given stable demand, such heterogeneous enforcement can shift harvesting from high-capacity to low-capacity states, generating windfalls in weaker ones. This matter is discussed by Heid and Márquez-Ramos (2023). I refer to this as the harvesting-relocation windfall channel and test whether it is associated with conflict. I focus on wild trees in Africa, for which I can estimate

[13]The main reasons for focusing on Africa are as follows. First, the ACLED dataset—the most detailed of the three—provides the longest temporal coverage for Africa (starting in 1997, compared to 2010 for Asia and 2017 for Latin America), which allows me to analyse the spatial dynamics of battles and the type of violence associated with the windfall. Second, ACLED's temporal coverage for Africa also enables me to exploit the natural experiments in the ivory market in 1998 and 2007. Third, the analysis in Berman et al. (2017), which I use as a benchmark, is also restricted to Africa. Fourth, for the wild tree analysis, constructing a global grid at the $0.1^\circ \times 0.1^\circ$ resolution is computationally too demanding (where such a fine grid is necessary to reduce measurement error regarding the dominant species in a given cell). Fifth, splitting the global sample into high- and low-capacity states would place almost all countries with precious trees in the low-capacity category, leaving too little variation for the analysis.

harvested quantities at the taxon level using satellite data combined with habitat suitability.[14] In particular, for the estimation, I construct a finer, $0.1° \times 0.1°$ grid, which is necessary to reduce measurement error regarding the dominant taxon in a given cell, and combine satellite deforestation data from Hansen et al. (2013) with taxon-level habitat suitability.[15] CITES is likely to target taxa experiencing high harvesting pressure and therefore exhibiting different pre-trends. To address this, I use a staggered event-study synthetic control estimator (Ben-Michael et al., 2021; Funke et al., 2023), constructing the control group based on pre-treatment outcomes. Using this approach, I estimate changes in deforestation at locations suitable for CITES-listed wild tree taxa following the imposition of the trade restrictions. I use the Polity IV Combined Polity Score variable as a measure of state capacity to divide the sample into countries with above- and below-median institutional capacity.

I estimate the following synthetic control staggered event-study specification:

$$Y_{k,t} = \sum_{r=-7}^{6} \beta_r \big(M_{k,w(k)} \times D_{w(k),t+r}\big) + \lambda_k + \delta_{c,t} + \epsilon_{k,t} \tag{2}$$

$Y_{k,t}$ denotes the approximated $log(x+1)$ harvested quantity in cell k and year t. The term $\beta_r \big(M_{k,w(k)}\, D_{w(k),t+r}\big)$ captures the treatment effect in event time r. The index r represents the relative time to when trade in wildlife taxon $w(k)$ becomes restricted under CITES. The term $w(k)$ denotes the unique wildlife taxon suitable for cell k. $D_{w(k),t+r}$ is an indicator that equals one in years t that are r periods before or after the restriction year for taxon $w(k)$. $M_{k,w(k)}$ is a time-invariant indicator for the suitability of cell k for wildlife taxon $w(k)$. The specification includes cell (λ_k) and country-year ($\delta_{c,t}$) fixed effects, to control for time-invariant factors and time-varying country-level shocks.

To assess whether the harvesting-relocation windfall is associated with an increase in conflict, I re-estimate the conflict event-study specification for wild trees (akin to equation (1)), but splitting the sample into countries with high and low state capacity.

Figure 6, panel (a), shows a decrease of about 9.7% in harvesting in strong states following the policy, while panel (b) shows an increase of about 5.5% in weak states. On average, in the African sample, the policy reduced harvesting by 0.5% (Appendix Table C.3), suggesting that most conservation benefits were offset by increased harvesting in weak states.

In Figure 7, I replicate the event-study specification in equation (1) for a sample restricted to Africa, splitting it into states with high and low institutional capacity. This shows that the policy–conflict relationship is primarily driven by weak states, with an average increase of 3.3 percentage points in conflict likelihood, compared to only 0.15 percentage points in strong states, which is statistically insignificant (Appendix Table C.4).[16] This suggests that differences in production elasticity, driven by variation in enforcement capacity across states, underlie the windfall heterogeneity

[14] Data on wild animal poaching are limited in spatial coverage and subject to selection and reporting biases.

[15] The finer grid is necessary to reduce measurement error in measuring the harvested taxon.

[16] Appendix Table C.5 reports the difference-in-differences coefficient for the entire African sample, showing an average increase of 5.3 percentage points in conflict likelihood.

and are associated with the policy–conflict relationship.

Figure 6: Trade Restrictions and Harvesting of Wild Trees by State Capacity: Synthetic Control

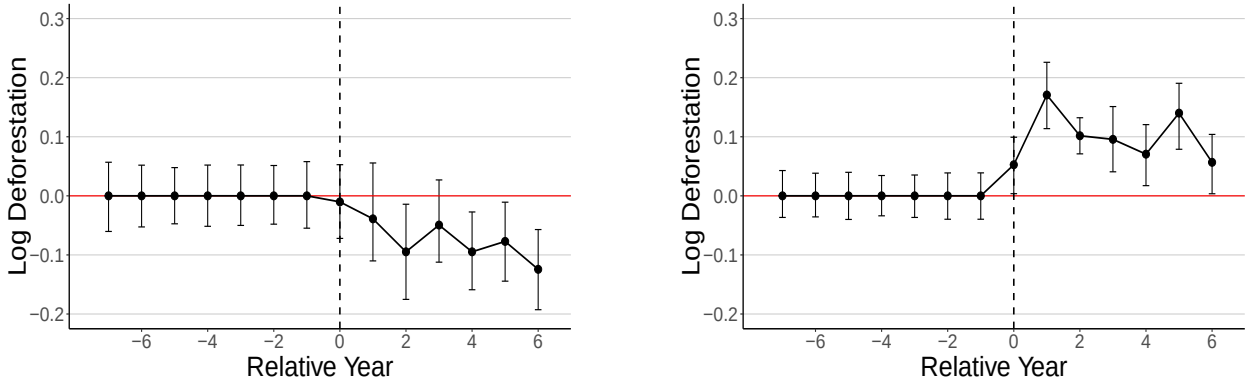

(a) High State Capacity **(b)** Low State Capacity

Notes: The figure displays staggered event-study synthetic control estimates (Ben-Michael et al., 2021) for harvesting of CITES protected wild trees in African countries with above (a) and below (b) median state capacity. Each observation corresponds to a cell-year, where cell size is $0.1° \times 0.1°$. The sample includes 523,016 (781,298) observations for the high- (low-) capacity state sample, defined as above and below the median of the Polity IV Combined Polity Score variable. The dependent variable is the $log(x+1)$ of harvested quantities of trees, based on remote sensing estimates (Hansen et al., 2013). The main explanatory variable is an interaction between post-policy and habitat indicators, capturing the location and timing of taxa protected by CITES. The specification includes cell and country–year fixed effects. Standard errors are computed using the wild bootstrap, following the procedure for synthetic control estimators recommended by Ben-Michael et al. (2021).

Figure 7: Trade Restrictions on Wild Trees and Conflict by State Capacity

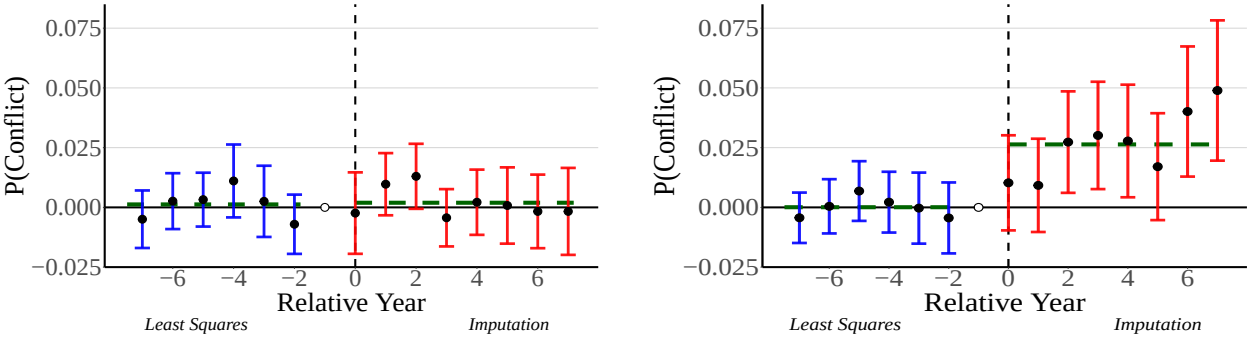

(a) High State Capacity **(b)** Low State Capacity

Notes: The figure reports LPM estimates using the staggered event study imputation estimator suggested by Borusyak et al. (2024). The pre-treatment coefficients are estimated using least squares, whereas the post-treatment coefficients are estimated with the imputation estimator. The left (right) chart reports estimates for African countries with above- (below-) median state capacity, based on the Polity IV Combined Polity Score. Each observation corresponds to a cell-year (131,663 for high-capacity and 191,137 for low-capacity states). The estimates are based on equation (1). The dependent variable is a binary indicator for conflict incidence, equal to one if at least one conflict event occurs in a given cell and year, based on the ACLED dataset. The main explanatory variable is an indicator for habitat cells of protected wildlife in post-policy periods. The specifications include cell and country–year fixed effects. The omitted period is the year preceding the policy announcement. The first and last coefficients are binned. The green horizontal lines indicate the mean of the pre- and post-treatment coefficients. Error bars represent 95% confidence intervals, with standard errors spatially clustered to allow for spatial and temporal correlation within a 500 km radius of each cell's centroid.

5.1.2 Prices

The African elephant ivory market provides a suitable setting to estimate the effect of the policy on conflict via prices. To estimate this effect I use two policy-driven supply shocks, which, importantly, did not change the legal status of ivory. In 1998 and 2007, CITES approved organised sales of ivory from South Africa, Botswana, Namibia, and Zimbabwe to China and Japan. The rationale behind this policy was to suppress prices and reduce poaching incentives (Hsiang and Sekar, 2016; UNODC, 2016). I use the two shocks as instruments for ivory prices. I follow Dube and Vargas (2013) and estimate a 2SLS specification to test whether policies affect conflict through prices.

Importantly, for the exclusion restriction to hold, the policy shocks—ivory sales—must affect local conflicts across Africa only through their impact on prices, and not through any other channel. To mitigate this concern, I exclude the four African countries that participated in the sales from the sample.[17] Given that all policy decisions were made by CITES and were outside the control of the remaining African countries in the sample, the validity of this assumption appears plausible.

I estimate the following 2SLS specification:

$$M_k \times \ln(p_t) = \gamma_1(M_k \times Expan_t) + \gamma_2(M_k + \gamma_3(Minerals_{k,t}) + \lambda_k + \delta_{c,t} + \nu_{k,t} \tag{3}$$

$$Y_{k,t} = \beta_1 \left(\widehat{M_k \times \ln(p_t)} \right) + \beta_2(Minerals_{k,t}) + \lambda_k + \delta_{c,t} + \epsilon_{k,t} \tag{4}$$

$Expan_t$ is an indicator variable for the expansionary policies in the ivory market at time t. I define the announcement year and the subsequent year as a treatment window to capture the policy shock, and interact it with the indicator variable M_k, which equals one if cell k is designated as elephant habitat.[18] $\ln(p_t)$ denotes the price of elephant ivory. To mitigate concerns about other confounders—such as geographic variation, domestic policies, or shocks to other commodities—the specification includes cell and country-year fixed effects, as well as control for the industrial minerals shock (Berman et al., 2017).

Table 2 reports the 2SLS estimates. Columns (1)–(3) of Panel A present aggregated estimates for ACLED, UCDP, and GTD, respectively. The ACLED and UCDP coefficients show increases in conflict likelihood of 1.7 and 1.3 percentage points, respectively, corresponding to 23% and 45% relative to the baseline risk. The GTD coefficient is smaller: 0.5 percentage points, or 33% relative to the baseline risk, and is less precisely estimated, but points in the same direction. Comparing across—standardised—shocks, column (1) suggests that the mineral shock (Berman et al., 2017) has a stronger effect on ACLED conflict events compared to the ivory shock (0.032 compared to 0.017). In contrast, column (2) shows that the mineral shock has a weaker effect on UCDP large-scale conflict events (0.002 compared to 0.014). Panel B reports the first-stage estimates, with associated F-statistics that are above conventional thresholds for instrument strength. Panel C reports the

[17] Moreover, Appendix Table D.14 reports 2SLS estimates obtained by iteratively excluding each of Africa's five continental subregions.

[18] I code the shocks as follows: CITES 1st sale as 1998 and 1999; CITES 2nd sale as 2007 and 2008.

reduced-form estimates, showing that expansionary policy shocks reduce conflict likelihood by 1.8 percentage points, and Panel D reports the corresponding OLS estimates. The 2SLS coefficients are approximately 1.5 to 2.5 times larger than their corresponding OLS coefficients. This could be driven by attenuation bias in OLS due to price endogeneity, for example, if some large producing locations act as price makers. Finally, Panel E reports population-weighted least squares (WLS) estimates, showing the average partial effect with each cell weighted by its population. The coefficients on the ivory and industrial-mineral shocks are larger in magnitude than their OLS counterparts.

Table 2 columns (4)–(6) report estimates based on ACLED sub-categories. Columns (4)–(5) of Panel A show that most of the ivory conflict effect is driven by one-sided violence, defined as events where a recognised armed group attacks civilians or small unrecognised militias. In contrast, most of the mineral shock effect is driven by battles between armed groups. Column (6) reports placebo estimates testing the effect of the ivory shock on protests and riots; the coefficients are statistically insignificant. In summary, Table 2 provides evidence of a direct link between CITES supply-side policies, induced price changes, and the likelihood of local conflict events.

Appendix Tables D.12, D.13, and D.14 present placebo exercises supporting the exogeneity assumption of the policies with regard to ivory-related conflicts. Appendix Table D.15 reports estimates using three alternative ivory price sequences. Appendix Table D.16 presents a sufficient-statistics test in which both the policy vector and the price series are used to explain conflict incidence, showing that the policy vector has no effect on conflicts once I control for prices.

Table 2: Policies, Prices and Conflict in the Elephant Ivory Market: 2SLS

	Dep. Var.: Conflict (0/1)					
	Aggregated			ACLED Sub-Categories		
	ACLED	UCDP	GTD	One-Sided Violence	Battles	Protests/Riots
	(1)	(2)	(3)	(4)	(5)	(6)
Panel A: IV Estimates						
$\widehat{Habitat \times Price}$	0.017***	0.014***	0.006*	0.008***	0.004	0.002
	(0.006)	(0.005)	(0.003)	(0.004)	(0.004)	(0.003)
$Mineral \times Price$	0.032***	0.002	0.002	0.004**	0.007***	0.035***
	(0.007)	(0.003)	(0.002)	(0.002)	(0.002)	(0.006)
Panel B: First Stage						
$Habitat \times Expansionary\ Shock$	−0.829***	−0.770***	−0.770***	−0.829***	−0.829***	−0.829***
	(0.086)	(0.084)	(0.084)	(0.086)	(0.086)	(0.086)
F-Stat	42,369	68,934	68,934	42,369	42,369	42,369
Panel C: Reduced Form						
$Habitat \times Expansionary\ Shock$	−0.018***	−0.011***	−0.004**	−0.004	−0.010***	−0.002
	(0.006)	(0.004)	(0.002)	(0.003)	(0.003)	(0.001)
Panel D: OLS						
$Habitat \times Price$	0.012***	0.006**	0.003	0.005***	0.007***	0.001
	(0.003)	(0.003)	(0.002)	(0.002)	(0.002)	(0.002)
$Mineral \times Price$	0.032***	0.002	0.002	0.004**	0.007***	0.035***
	(0.007)	(0.003)	(0.002)	(0.002)	(0.002)	(0.006)
Panel E: WLS						
$Habitat \times Price$	0.017***	0.011**	0.004	0.011**	0.003	0.003
	(0.006)	(0.005)	(0.002)	(0.004)	(0.004)	(0.004)
$Mineral \times Price$	0.041***	0.001	0.003	0.007**	0.007***	0.041***
	(0.007)	(0.003)	(0.003)	(0.002)	(0.002)	(0.007)
Cell FE	Y	Y	Y	Y	Y	Y
Country-Year FE	Y	Y	Y	Y	Y	Y
Dep. Var. Mean	0.076	0.030	0.017	0.032	0.033	0.023
Dep. Var. SD	0.265	0.171	0.131	0.161	0.173	0.151
Observations	305,312	836,992	836,992	276,256	276,256	276,256

Note: The table reports 2SLS estimates for African elephants. Each observation corresponds to a cell-year, and the sample is restricted to Africa. Columns 1–3 report estimates for aggregated conflict variables, whereas columns 4–6 report disaggregated categories, excluding state-related violence. Panel A reports the main 2SLS estimates, where the variable *Habitat* is an indicator measuring the suitability of cell k for African elephants, and *Price* denotes the log price of ivory at time t. The estimates are based on equations (3) and (4). The dependent variable is a binary indicator for conflict incidence, equal to one if at least one conflict event occurs in a given cell-year, based on the conflict dataset mentioned in the title. Panel B reports the first-stage estimates, in which policies explain the price shocks. *Expansionary Shock* is an indicator for policy-driven increases in ivory supply (1998, 1999, 2007, 2008). Panel C reports reduced-form estimates of the effects of these policies on the conflict indicator. Panel D presents OLS estimates from regressing the conflict indicator on the interaction term *Habitat* × *Price*. Panel E presents population-weighted least squares (WLS) estimates. Coefficients are reported with spatially clustered standard errors (in parentheses), which allow for spatial and temporal correlation within a 500 km radius of each cell's centroid. * significant at 10%; ** significant at 5%; *** significant at 1%.

Aggregation. Although the industrial minerals shock (Berman et al., 2017) has a larger marginal effect on conflict than the ivory shock (0.0322 versus 0.0124 in the OLS specification), the total conflict impact also depends on resource spatial distribution and population exposure. Shocks to scarce, geographically concentrated resources affect fewer people and locations, whereas widely distributed resources can be more devastating. Only 195 grid cells contain industrial minerals, compared to 1,717 cells that are suitable for African elephants. For instance, based on the Berman et al. (2017) industrial mining sample, Uganda has no industrial mining activity, yet approximately 15% of its land area is suitable for elephants. The broad spatial distribution of wildlife habitat and its lower marginal effect on conflict, compared to the concentrated presence and greater marginal impact of industrial minerals, may explain why wildlife-related shocks have been overlooked in the literature.

To account for differences in spatial distribution, I use the OLS estimates reported in Table 2, Panel D, column (1), and multiply them by the number of grid cells that are suitable for or contain each resource.[19] Additionally, to account for population exposure, I use the population-weighted least squares (WLS) estimates reported in Table 2, Panel E, column (1). I then multiply the standardised coefficient estimates by the number of cells containing each resource, and by the average population of the corresponding elephant or mineral grid cells to approximate total population exposure.

Figure 8 displays aggregated conflict estimates for price shocks to ivory, industrial minerals, and industrial gold. In the Affected Area panels, the y-axis represents the expected increase in the number of grid cells with at least one conflict event following a one-standard-deviation increase in the corresponding price index, computed by multiplying the OLS coefficient (Panel D, column (1)) by the number of cells suitable for or containing the resource. In the Affected Population panels, the y-axis represents the expected increase in the number of people, measured in 100,000-person units, living in conflict zones, following a one-standard-deviation increase in the price index, calculated by multiplying the WLS coefficient (Panel E, column (1)) by the total population of the corresponding resource cells. Although the marginal per-cell effects are larger for industrial minerals and industrial gold, ivory is more damaging on an aggregate basis when weighted by affected area or population exposure.

[19] The OLS coefficients in Panel D provide the most conservative estimates of the ivory shock.

Figure 8: Aggregated Price–Conflict Estimates by Geographic and Population Exposure: Elephant Ivory, Industrial Minerals, and Industrial Gold

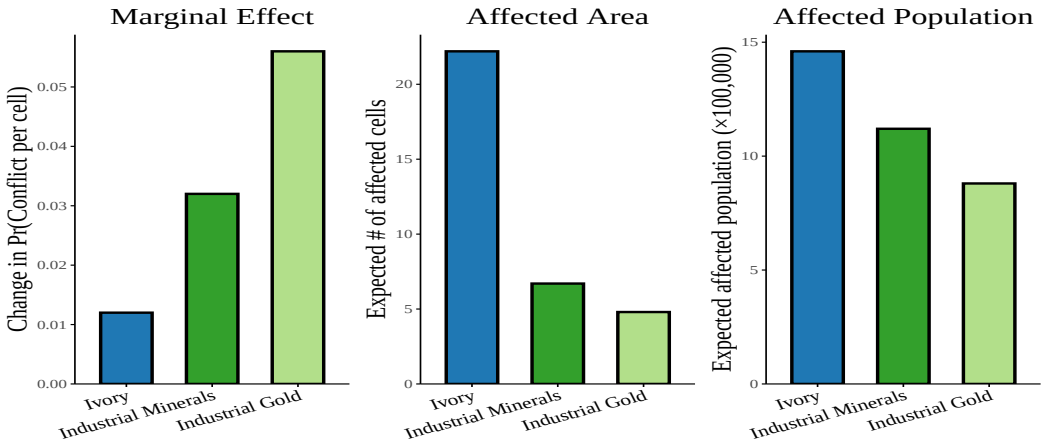

Notes. The figure shows conflict exposure to ivory, industrial minerals, and industrial gold price shocks using three comparisons: marginal effect, total affected area, and affected population. Calculations are based on the standarised coefficients reported in Table 2, Panel D, column (1) (OLS) for the marginal effect and affected area, and on Panel E, column (1) (WLS) for the affected population. The left panel reports the per-cell marginal effect (change in conflict probability), the middle panel shows the expected number of grid cells affected (marginal effect multiplied by the number of resource cells), and the right panel reports the expected affected population, which is scaled in units of 100,000.

5.2 Windfall and Channels of Violence

This subsection examines how armed groups' fighting dynamics have changed following the windfall gains arising from CITES trade restrictions.

The literature (Blattman and Miguel, 2010; Bazzi and Blattman, 2014; Berman et al., 2017; Jaimovich and Toledo, 2021) highlights several mechanisms through which windfall gains can fuel conflict. First, such gains ease financing constraints for armed groups, making rebellion and attacks more feasible (e.g., through mobilisation or arms purchases). Second, the increased returns from capturing resource-rich areas incentivise territorial competition among armed actors. Third, windfalls exacerbate grievances and social instability by leaving certain segments of society relatively disadvantaged. Fourth, by reshaping migration patterns and altering the size and composition of local populations, windfalls can heighten ethnic tensions and trigger conflict.

This subsection presents two empirical tests. The first disentangles the feasibility and competition channels, while the second examines whether groups likely to benefit from the policy-induced windfall capture more or less territory following CITES policies. Given the lack of anecdotal evidence linking grievances or migration to wildlife trade or CITES policies, I focus solely on the feasibility and competition channels.

5.2.1 Spatial Distribution of Battles

To assess whether competition or feasibility is the empirically dominant channel, I examine changes in the spatial distribution of armed clashes. Specifically, I construct a distance measure capturing how far from their pre-policy strongholds groups fight. If the competition channel is empirically

stronger, following the policy, I would expect groups outside wildlife habitat (who likely did not receive windfalls) to move toward resource-rich areas to contest rents; consequently, clashes should concentrate nearer to the territories of windfall-exposed groups. Given that the outcome measures distance to each group's own stronghold, this implies that, relative to their own pre-policy pattern and to rivals, windfall groups would exhibit a smaller post-policy increase—or a relative decrease—in fighting distance, appearing to fight closer to their strongholds. If the feasibility channel is empirically dominant, by contrast, I would expect the windfall-exposed groups (those with pre-policy territory overlapping habitat) to expand outward and fight farther from their previous battlegrounds following the policy.

To implement this test, I proceed as follows. First, I focus on the 2016 rosewood ban. Second, I select well-recognised armed groups that fought in at least three distinct locations between the start of the sample (1997) and 2013—three years before the 2016 trade ban on rosewood—and construct a group–battle–location–year panel.[20] Third, for each armed group, I draw a convex hull around its pre-policy conflict locations and compute the polygon's centroid, which I treat as the group's central location.[21] Fourth, using these pre-policy polygons, I classify groups as "rosewood" according to the share of polygon area overlapping with rosewood habitat (*Dalbergia* and *Pterocarpus*). I label as "rosewood" those in the upper half of the overlap distribution and the remainder as "non-rosewood". Fifth, I restrict the sample to 2014–2018—two years before and after the rosewood ban (2016).[22] Sixth, I define the outcome as the log distance between each conflict event and the group's centroid, computed as the geodesic distance in kilometres, and I estimate the effect of the interaction between a post-policy indicator and the group's rosewood classification indicator. A positive coefficient suggests that rosewood groups, likely to benefit from the windfall expand outward and fight farther away from their strongholds after the policy, implying that the feasibility channel is empirically dominant. A negative coefficient suggests that rivals move toward windfall territories, fighting closer to windfall groups' strongholds, supporting the competition channel.

Figure 9 illustrates the logic of the empirical test by examining the fighting dynamics of the Anti-Balaka group in the Central African Republic. Based on the overlapping-polygon classification, the group is classified as a "rosewood" group likely to benefit from the rosewood windfall. The grey-blue polygon marks the group's territory, derived from battles between 1997 and 2013, and the green dot indicates the centroid of that polygon. Purple dots represent the group's battles locations in 2014–2015—just before the CITES ban on rosewood in 2016—while red dots represent battle locations in 2017–2018—just after the ban. On average, the purple dots (pre-policy battles) were located 249 kilometres from the group's centroid, while the red dots (post-policy battles) averaged 414 kilometres.

[20] At least three locations are required to construct a convex hull, which I use as a proxy for pre-policy territory.

[21] The centroid of a polygon is the area-weighted average position of all points inside it.

[22] This is necessary because I calculate groups' territories using data from the pre-policy period up to three years before each policy shock. This is also important to avoid any contamination from other shocks.

Figure 9: Anti-Balaka Territory and Battles in the Central African Republic

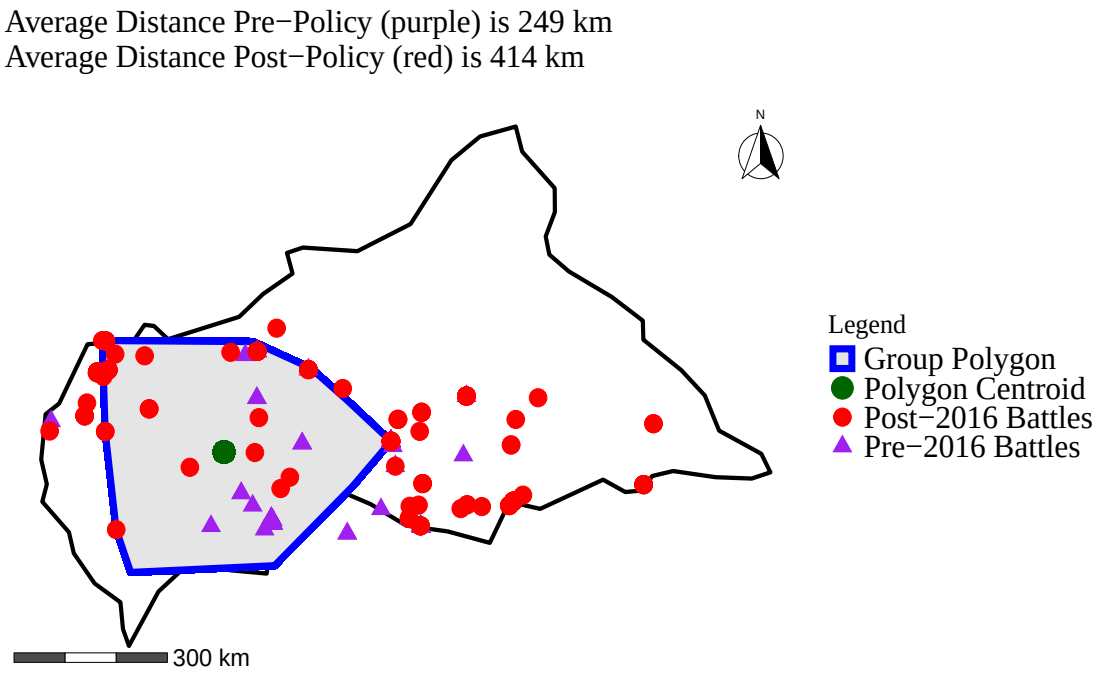

Notes: The figure shows the spatial distribution of battles fought by the Anti-Balaka group, classified as a "rosewood" group, in the Central African Republic, before and after the 2016 CITES ban on rosewood (*Dalbergia* and *Pterocarpus*). The grey-blue polygon delineates the group's fighting territory based on battles from 1997–2013, and the green dot marks its centroid. Purple dots represent battles in 2014–2015, and red dots represent battles in 2016–2018 (after the ban).

To test whether the pattern observed in Figure 9 is anecdotal or systematic, I estimate the following difference-in-differences specification:

$$Distance_{g,b,k,t} = \gamma Policy_t \times RosewoodGroup_g + \eta_g + \lambda_k + \delta_{c,t} + \epsilon_{g,b,k,t} \tag{5}$$

$Distance_{g,b,k,t}$ is the (log) kilometre distance between battle b, fought by group g in location k at time t, and the group's centroid, defined based on its pre-sample conflict locations. $Policy_t$ is a post-policy indicator, and $RosewoodGroup_g$ is an indicator for whether the group's polygon overlaps with rosewood habitat and falls in the upper half of the distribution. The specification includes group, cell, and country-year fixed effects to account for group- and location-specific heterogeneity, as well as national-level shocks occurring in the same year. Standard errors are spatially clustered to allow for spatial and temporal correlation within a radius of 500 kilometres of each battle location.[23]

Table 3 reports the estimates. Rosewood-linked groups fought, on average, approximately 17% farther away from their baseline locations in the post-policy period, relative to non-rosewood groups. These findings suggest that the feasibility channel is empirically stronger: rosewood-heavy armed groups, likely to benefit from the windfall, appear to have used it to expand their territorial reach. Appendix Figure C.1 presents event-study estimates showing parallel pre-trends.

[23] I also experiment with clustering standard errors at the country–year and group level.

Table 3: Rosewood Ban and Armed Groups' Battle Distance

	Dep. Var.: $\log(Distance_{g,b,k,t})$		
	(1)	(2)	(3)
RosewoodGroup × *Policy*	0.168***	0.144***	0.167**
	(0.037)	(0.052)	(0.068)
	[0.033]	[0.050]	[0.066]
Group FE	Y	Y	Y
Location FE	N	Y	Y
Country-Year FE	N	N	Y
Observations	8,429	8,429	8,429
Dep. Var. Mean	5.718	5.718	5.718
Dep. Var. SD	0.756	0.756	0.756

Notes: The table reports OLS estimates. Each observation corresponds to a group–battle–location–year. The sample is restricted to African countries over 2014–2018 and to events in which at least one side is an armed group that had fought three or more battles by 2013. The dependent variable is the log distance between group battles and their pre-sample calculated strongholds. *RosewoodGroup* is an indicator for whether a group's pre-sample territory overlaps (above the sample median) with the rosewood habitat. *Policy* is an indicator for the post-CITES rosewood ban period (2016 and onward). Locations are assigned based on a $0.5^\circ \times 0.5^\circ$ grid. Coefficients are reported with spatially clustered standard errors (in parentheses), allowing for spatial and temporal correlation within a 500 km radius of each cell's centroid. Standard errors in square brackets are two-way clustered by country–year and group, allowing for within-country spatial correlation and serial correlation within groups. * significant at 10%; ** significant at 5%; *** significant at 1%.

5.2.2 Wildlife Windfall and Territorial Change

This subsection focuses on the 2016 rosewood and provides suggestive evidence on whether armed groups trading rosewood are more likely to win battles following the rosewood trade ban. For clashes between armed groups against the government, ACLED records which actor gains territory. I use this information to construct a win-loss indicator for each battle and use this as an outcome variable. I construct a group–battle–location–year panel, using battles of non-rosewood groups as a control group. I interact a "rosewood group" indicator with a "post-policy" indicator, and restrict the sample to the two years before and after the policy (2014–2018). I view this analysis as suggestive, as following the policy, groups or the government might strategically engage in battles, confounding causal inference.

I estimate the following specification:

$$Win_{g,b,k,t} = \gamma Policy_t \times RosewoodGroup_g + \eta_g + \lambda_k + \delta_{c,t} + \epsilon_{g,b,k,t} \tag{6}$$

$Win_{g,b,k,t}$ is an indicator variable for whether group g, fought battle b in location k at time

t, gained territory. $Policy_t$ is a post-policy indicator, and $RosewoodGroup_g$ is an indicator for whether the group's polygon overlaps with the rosewood habitat and falls in the upper half of the distribution. The specification includes group, cell, and country-year fixed effects to absorb group- and location-specific heterogeneity and contemporaneous national-level shocks. Standard errors are two-way clustered at the group and country-year levels or at a spatial radius of 500 kilometres of each battle location.

Table 4 reports the estimates, showing that rosewood-linked armed groups are more likely to gain territory following the rosewood trade ban, with the probability of gaining territory increasing by 41 percentage points.

Table 4: Rosewood Ban and Winning Likelihood

	Dep. Var.: $Win_{g,b,k,t}(0/1)$		
	(1)	(2)	(3)
RosewoodGroup × *Policy*	0.259**	0.459***	0.416***
	(0.132)	(0.087)	(0.074)
	[0.124]	[0.091]	[0.059]
Group FE	Y	Y	Y
Location FE	N	Y	Y
Country-Year FE	N	N	Y
Observations	6,468	6,468	6,468
Dep. Var. Mean	0.4499	0.4499	0.4499
Dep. Var. SD	0.4975	0.4975	0.4975

Notes: The table reports LPM estimates obtained using OLS. Each observation corresponds to a group–battle–location–year. The sample is restricted to African countries over 2014–2018 and includes only clashes between well-recognised armed groups with government forces. The dependent variable is a dummy equal to one if the group gains territory in a given battle, serving as a proxy for victory. *RosewoodGroup* is an indicator for whether a group's pre-sample territory overlaps (above the sample median) with rosewood (*Dalbergia* and *Pterocarpus*) habitat. *Policy* is an indicator for the post-CITES rosewood ban period (2016 and onwards). Locations are assigned based on a $0.5^\circ \times 0.5^\circ$ grid. Coefficients are reported with spatially clustered standard errors (in parentheses), allowing for spatial and temporal correlation within a 500 km radius of each cell's centroid. Standard errors in square brackets are two-way clustered by country–year and group, allowing for within-country spatial correlation and serial correlation within groups. * significant at 10%; ** significant at 5%; *** significant at 1%.

6 Model

In this section, I develop a social planner model motivated by the empirical patterns in the market for wild trees. The model serves two main purposes. First, it provides a theoretical framework

that rationalises the observed empirical findings and clarifies the underlying mechanism. Second, I use the model to evaluate alternative policies and suggest an approach that mitigates the conflict externality while still protecting the environmental resource.

In constructing the model, I am guided by the following empirical findings: the policy intervention raised wildlife prices, increased the likelihood of conflict (an effect driven almost entirely by weak states), reduced overall harvesting of the wild trees, and led to a divergence in outcomes across state capacity—harvesting fell in strong states but rose in weak ones. In addition, following EIA (2017) and BBC News (2023), I assume that the *modus operandi* of armed groups involves issuing logging concessions and levying protection fees proportional to logging revenues. Appendix Section E provide the full derivation of the model.

6.1 Model Setup

Consider an international economy comprising multiple countries engaged in the extraction and trade of a valuable environmental resource (e.g., precious wild trees). Each country hosts a representative profit-maximising harvesting firm that operates under diminishing returns and faces a global price. Countries differ along two key dimensions: their resource endowment and their institutional capacity. There are N countries, of which N_w are weak and N_s are strong. Let F_i denote a pre-determined production factor proportional to the stock of wild trees in country i, and let $s_i \in \{0, 1\}$ indicate whether the state has strong ($s_i = 1$) or weak ($s_i = 0$) institutional capacity.[24] The international price of the resource is denoted p, and firms take this price as given.

In each country, a representative harvesting firm chooses its harvesting level $h_i \geq 0$ to maximise profits, subject to two types of frictions. First, in weak states only, local armed groups loot a fraction $t_i \in [0, 1]$ of firm revenue. Second, an international environmental organisation (the policymaker), which aims to protect biodiversity, can impose a global trade ban ($\tau = 1$) on endangered species. Due to institutional capacity, the ban is enforced solely in strong states and imposes on the harvesting firm a regulatory cost per unit harvested that exceeds the post-ban price ($\theta > p(\tau)$). These frictions generate asymmetric responses to policy across countries. In weak states, looting dilutes revenue but does not prevent harvesting, whereas in strong states, enforcement is effective and binding under a ban.

The demand side is captured by a downward-sloping world inverse demand curve for the resource $p(Q) = a - bQ$, where Q is the total global quantity and $a, b > 0$. Firms are small relative to the global market and internalise only their private costs and local constraints. Hence, total harvested quantity and market price depend on the trade policy regime $\tau \in \{0, 1\}$, where $\tau = 1$ denotes the global trade ban imposed by the international policymaker.

6.1.1 Harvesting Sector

The representative harvesting firm chooses quantity $h_i \geq 0$ to maximise:

[24] F_i can be interpreted as a factor reflecting the stock of wild trees, where a higher stock implies a lower search cost in country i.

$$\Pi_i \;=\; p(\tau)\, h_i(1-t_i) \;-\; \frac{h_i^2}{2F_i} \;-\; \tau\, s_i\, \theta\, h_i. \tag{7}$$

Equilibrium. Under high enforcement in strong states ($\theta > p(\tau)$) and an interior solution in weak states, optimal harvesting follows:

$$h_i^*(s_i,\tau) = \begin{cases} F_i\, p(0)(1-t_i), & \text{if } \tau = 0,\ s_i = 0, \\ F_i\, p(0), & \text{if } \tau = 0,\ s_i = 1 \text{ (since } t_i = 0), \\ F_i\, p(1)(1-t_i), & \text{if } \tau = 1,\ s_i = 0, \\ 0, & \text{if } \tau = 1,\ s_i = 1 \text{ (since } \theta > p(1)). \end{cases} \tag{8}$$

In weak states, the loot decreases harvesting, whereas following the ban, due to enforcement, harvesting in strong states comes to a halt. Accordingly, profits at the optimum follow:

$$\Pi_i^*(s_i,\tau) = \begin{cases} \frac{1}{2}\, F_i\, p(0)^2(1-t_i)^2, & \text{if } \tau = 0,\ s_i = 0, \\ \frac{1}{2}\, F_i\, p(0)^2, & \text{if } \tau = 0,\ s_i = 1, \\ \frac{1}{2}\, F_i\, p(1)^2(1-t_i)^2, & \text{if } \tau = 1,\ s_i = 0, \\ 0, & \text{if } \tau = 1,\ s_i = 1. \end{cases} \tag{9}$$

Aggregation. Let $\bar{F}_w$ and $\bar{F}_s$ denote average production factors proportional to forest stocks in weak and strong states. For weak states, set $t_i = t$, since optimal loot is independent of local stock (as shown later). The effective supply coefficients for before and after the ban are:

$$S_0 \;=\; (1-t)\, N_w\, \bar{F}_w \;+\; N_s\, \bar{F}_s, \qquad S_1 \;=\; (1-t)\, N_w\, \bar{F}_w. \tag{10}$$

With linear inverse demand $p(Q) = a - bQ$ and $Q(\tau) = S_\tau p(\tau)$, market clearing yields regime-specific prices and quantities:

$$p(\tau) \;=\; \frac{a}{1+bS_\tau}, \qquad Q(\tau) \;=\; \frac{a\, S_\tau}{1+bS_\tau}, \qquad S_\tau \in \{S_0, S_1\}. \tag{11}$$

6.1.2 Armed Sector

Armed Groups Revenue. In each weak state ($s_i = 0$) an armed group extracts a share $t_i \in [0,1]$ of the representative harvesting firm's revenue, taking the world price $p(\tau)$ as given. Following the firm's optimal production, armed groups choose the loot rate to maximise:

$$R_{ji}(t_i) \;=\; t_i\, p(\tau)\, h_i^*(t_i) \;=\; F_i\, p(\tau)^2\, t_i(1-t_i). \tag{12}$$

This yields $t^* = \frac{1}{2}$, a global optimum independent of local stocks. Substituting this back provides the following optimal revenue expression:

$$R^*_{ji} \;=\; \frac{F_i\, p(\tau)^2}{4}. \tag{13}$$

Violence. Additionally, in each weak state, there is an outside faction $(-j)$ that does not loot the harvesting firm and is challenged by the group that loots the harvesting firm (j). j group decision to attack is based on subjective winning expectation, which is a function of group j's amount of resources relative to its subjective assessment of group $-j$'s resources.

Specifically, the armed groups competition and hence the conflict probability is modelled as follows: let $\pi_i(\tau) \in [0,1]$ denote the conflict probability in weak state i under policy $\tau \in \{0,1\}$. I model group j competing against a rival group $-j$, whose baseline resources are fixed at R_{-ji} but whose realised resources are subject to a multiplicative lognormal shock, capturing uncertainty about the rival's true strength:

$$\widetilde{R}_{-ji} \;=\; R_{-ji}\, Z_{-ji}, \qquad \ln Z_{-ji} \sim \mathcal{N}(0, \sigma^2),$$

The violence production function with exponent $\delta > 0$, capturing the violence elasticity, is given by:

$$\pi_i(\tau) = \frac{\big(R^*_{ji}(\tau)\big)^{\delta}}{\big(R^*_{ji}(\tau)\big)^{\delta} + \big(R_{-ji} Z_{-ji}\big)^{\delta}}.$$

Under the lognormal distribution, the expectation is $\mathbb{E}[Z^{\delta}_{-ji}] = \exp\left(\frac{1}{2}\delta^2\sigma^2\right)$. Taking expectations with respect to Z_{-ji} and constructing a unit-free violence measure by normalising using the baseline values, I obtain:

$$\pi_i(\tau) = \frac{\pi_i(0)\, \rho(\tau)^{\delta}}{\big(1 - \pi_i(0)\big) + \pi_i(0)\, \rho(\tau)^{\delta}}\;, \qquad \rho(\tau) = \left(\frac{p(\tau)}{p(0)}\right)^2. \tag{14}$$

Aggregation. Let $\bar{V}_i(\tau)$ denote observed intensity (e.g., affected resource cells), with a scaling factor $\Lambda_i > 0$, then:

$$\bar{V}_i(\tau) \;=\; \Lambda_i\, \pi_i(\tau), \qquad \frac{\bar{V}_i(\tau)}{\bar{V}_{i0}} = \frac{\pi_i(\tau)}{\pi_i(0)} = \frac{\rho(\tau)^{\delta}}{\big(1 - \pi_i(0)\big) + \pi_i(0)\, \rho(\tau)^{\delta}}. \tag{15}$$

Using sample averages (same $\pi_i(0) = \pi(0)$ and $\Lambda_i = \bar{\Lambda}$), aggregates are N_w multiples; the scaling by $\bar{\Lambda}$ cancels in ratios.

6.1.3 International Environmental Organisation

Objective. An international environmental organisation chooses $\tau \in \{0,1\}$ (free trade versus ban) to protect biodiversity while internalising conflict externalities. Under symmetry across weak states,

the policymaker minimises the following loss function:

$$W(\tau) \;=\; \lambda\, N\, Q(\tau)^{\eta} \;+\; (1-\lambda)\, N_w\, \pi(\tau)\cdot \bar{\Lambda}, \qquad \lambda \in (0,1),\ \eta > 0, \tag{16}$$

$Q(\tau) = \sum_{i=1}^{N} h_i^*(\tau)$ is the total harvest of the scarce environmental resource, η captures biodiversity tipping points and irreversibility of ecological damage, and $\pi(\tau)$ is the per-weak-state average conflict probability.[25] The biodiversity loss is scaled by N, while conflict occurs in weak states only and therefore is scaled by N_w. A ban reduces the total harvest $Q(1) < Q(0)$ but raises conflict in weak states $\pi(1) > \pi(0)$.

Decision Rule. A ban is preferred if it minimises the international policymaker objective function $W(1) < W(0)$, which yields the following threshold rule:

$$\lambda \;>\; \frac{N_w\, \Delta V}{N\, \Delta Q^{\eta} + N_w\, \Delta V} \;\equiv\; \lambda^* \tag{17}$$

ΔV and ΔQ^{η} represent the changes in conflict and harvesting due to the ban. This is the policy threshold where a ban is optimal if λ, the planner's relative weight on environmental damage, is larger than λ^*.

Unit Free Rule. To avoid any misspecifications or scaling issues, such as measurements of stock, quantities, and price per unit, I normalise the expression inputs using their baseline levels, where $q_\tau \equiv \frac{Q(\tau)}{Q(0)}$, $v_\tau \equiv \frac{\pi(\tau)}{\pi(0)}$, and $q_0 = v_0 = 1$. To ensure that the baseline ecological and conflict losses are expressed in the same units, I set the conversion factor $\bar{\Lambda} \equiv Q(0)^{\eta}/\pi(0)$, so that $\bar{\Lambda}\pi(0) = Q(0)^{\eta}$. This normalisation makes the constants cancel and yields the compact unit-free rule below:

$$\lambda^* = \frac{N_w\,(v_1 - 1)}{N\left(1 - q_1^{\eta}\right) + N_w\,(v_1 - 1)} \tag{18}$$

Generalisability to Functional Forms. The policymaker decision rule depends only on the direction of the price and quantity responses to a supply contraction and on a monotone mapping from prices to conflict. Expressed in unit-free ratios (q_1, v_1), the policymaker threshold λ^* and its comparative statics are functional-form invariant under standard assumptions: (i) a downward-sloping demand curve, (ii) higher prices increasing lootable revenues, and (iii) higher revenues increasing conflict. The linear inverse demand and the conflict production function used in the baseline deliver closed-form magnitudes and facilitate parameter identification (a, b, δ); replacing them with constant-elasticity, CES, logistic, or threshold functions preserves all qualitative results, altering only calibration and curvature. Hence, the core comparative statics, that a trade ban raises prices, shifts production toward weak states, amplifies conflict, and that the optimality threshold λ^* rises with the magnitude of the conflict response, are robust to functional form.

[25] A higher η, which is associated with a more convex function, implies that ecological damage is less reversible. In practice, this could depend on wildlife reproduction rates.

6.2 Model Estimation

This section discusses the procedure used to recover the model's parameters and to conduct the welfare simulation under different policy scenario, for which I restrict the sample to Africa and focus on the case of rosewood as a source of data input to the model.

Observables. I take as given the sample structure, the number of strong and weak states, the average resource stocks for weak and strong states, the (normalised) two-regime prices (before and after the ban), and the loot share derived from the model. I also use the baseline conflict probability in weak states (Appendix Table A.6), and the estimated excess probability due to the ban on rosewood in Africa (Appendix Table E.4).

Recovering Model Parameters. Using this, I construct a system of equations for the pre- and post-ban periods, recovering the demand parameters (a and b) and the armed groups' revenue-violence elasticity δ. Appendix Section E provides the full derivation details, and Appendix Table E.1 summarises the recovered parameters together with the other model components required for estimation.

Recovering the Policymaker's Normative Weight λ^*. Using the threshold equation (equation (17)) and the data inputs from Appendix Table E.1, I recover the policy threshold, defined as the value of the normative parameter λ above which a ban becomes optimal.

$$\lambda^*(\eta) = \begin{cases} 0.69, & \eta = 0.5, \\ 0.54, & \eta = 1.0, \\ 0.46, & \eta = 1.5, \\ 0.40, & \eta = 2.0. \end{cases}$$

A higher λ^* suggests that a ban is less likely to be optimal. Hence, a larger η, the biodiversity tipping points parameter, which implies that current ecological destruction is less likely to be reversed, is associated with lower thresholds.

6.2.1 Comparative Statics

Figure 10 illustrates the model's main comparative statics following the implementation of a trade ban. Panel (a) shows that harvesting per weak state increases as the number of strong states increases—reflecting reduced competition among remaining active states. Panels (b) and (c) demonstrate how this increase in harvesting translates into higher revenues for both firms and armed groups. Panel (d) shows that, due to elevated looting revenues, an increase in the number of strong states leads to greater conflict likelihood in the remaining weak states. Together, this analysis underscores the model's core mechanism: a trade-off between biodiversity protection and armed conflict, consistent with the empirical patterns documented in the analysis.

Furthermore, this sheds light on counterfactual scenarios where either almost all states are strong or the spatial distribution of wild trees is more concentrated in strong states, both of which produce similar dynamics of higher conflict likelihood in the remaining weak states.

Figure 10: Comparative Statics Under a Ban: Harvesting, Profits, Looted Revenue, and Conflict

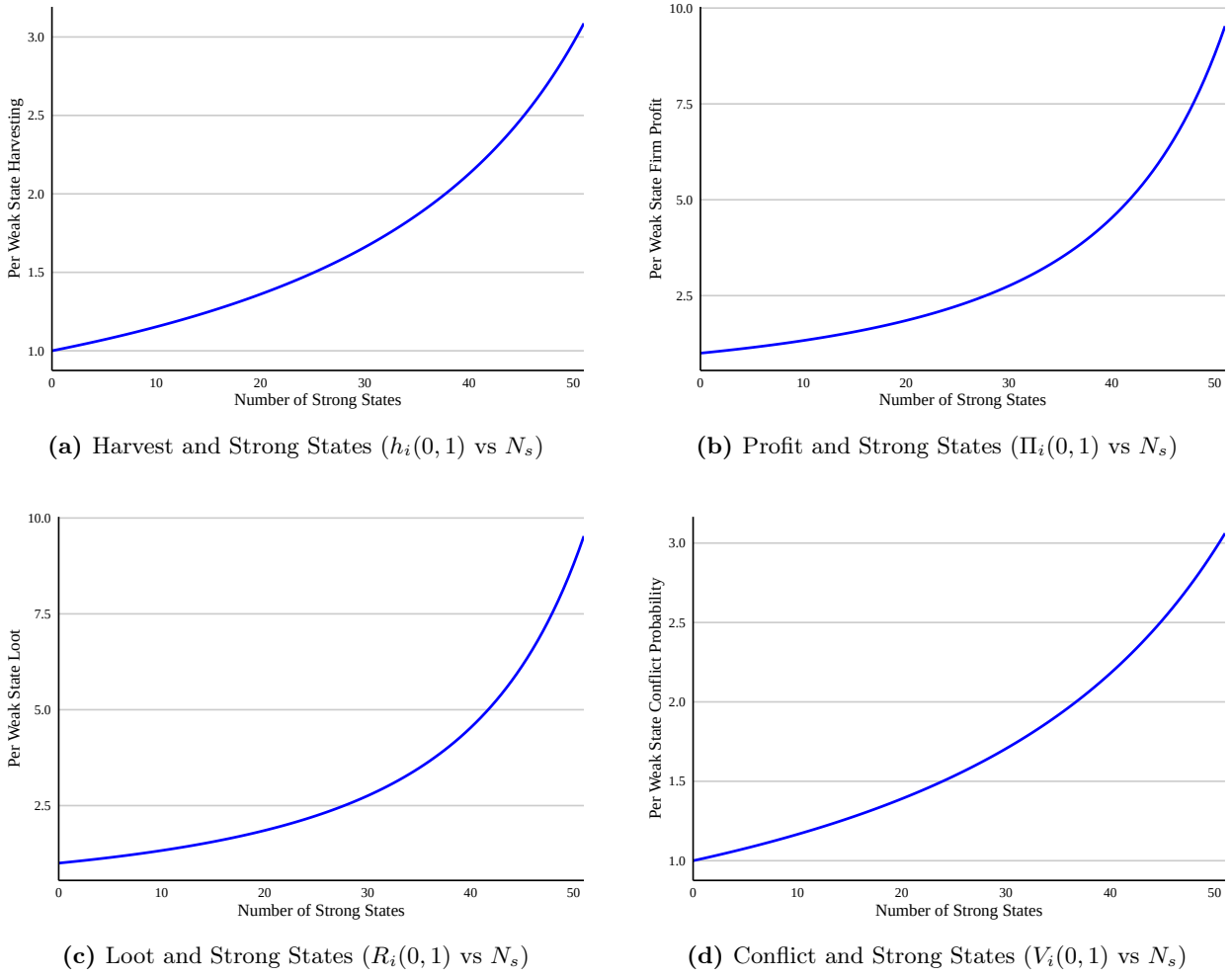

(a) Harvest and Strong States ($h_i(0,1)$ vs N_s)

(b) Profit and Strong States ($\Pi_i(0,1)$ vs N_s)

(c) Loot and Strong States ($R_i(0,1)$ vs N_s)

(d) Conflict and Strong States ($V_i(0,1)$ vs N_s)

Notes: The figure presents comparative statics showing how harvests, profits, looted revenues, and conflict likelihood in a given weak state change as the share of strong states (N_s) in the sample under a trade ban regime.

Policymaker Decision Rule. Using the values in Appendix Table E.1, Figure 11 shows the policymaker policy threshold rule as a function of the number of weak states (N_w). As N_w increases, the policymaker faces two opposing effects. On one hand, biodiversity gains from imposing a trade ban diminish, since harvesting in strong states is fully eliminated under the ban, and a larger N_w means more baseline harvesting already occurs in weak states where enforcement is absent. This reduces the marginal impact of the ban on total harvesting, and thus the biodiversity benefit. On the other hand, as N_w increases, conflict likelihood per weak state falls under the ban, as equilibrium prices are lower conditional on a ban (when weaker states remain active). However, at the extensive margin, a larger number of weak states may increase total violence ($N_w(v_1 - 1)$). Given the parameter values, the rise in aggregate conflict outweighs the ecological benefits of a ban, pushing the threshold λ^* upward and reducing the likelihood that a ban is optimal. When η is low, biodiversity losses are less convex, so the conflict term dominates more quickly.

Figure 11: Policymaker Decision Rule and Weak States (λ^* vs N_w (for different η))

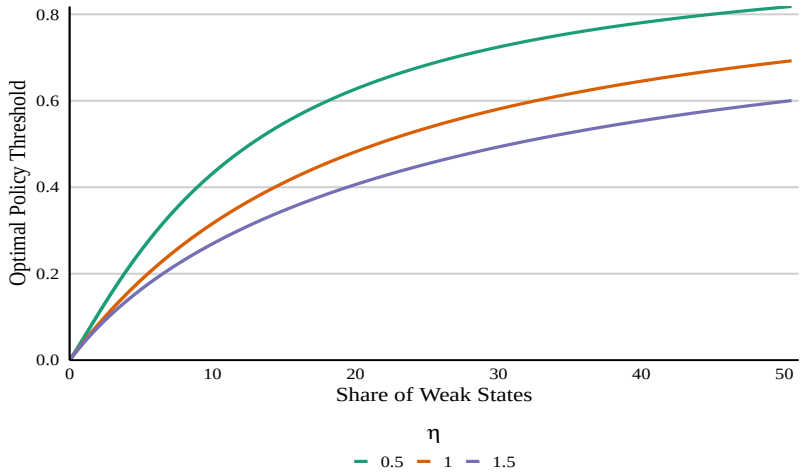

Notes: The figure shows how the optimal policymaker threshold value λ^*, above which a trade ban is optimal, varies with the number of weak states (N_w) (for fixed N) across different values of the ecological damage function η.

Demand Elasticity, Decision Rule and Conflict. When discussing the mechanism linking illicit actors' empowerment to trade restrictions, Becker et al. (2006) emphasises the role of the price elasticity of demand. They argue that trade restrictions on products with more inelastic demand are more likely to empower drug cartels and fuel violence, since a reduction in supply leads to a larger increase in prices, thereby attracting more resources to the illicit sector. Wildlife-related products are likely to differ in their degree of demand elasticity. For instance, ivory, rosewood, and ebony are considered to have relatively inelastic price elasticities of demand (Barbier and Swanson, 1990; Zhu, 2022; Ding and Yin, 2024). In contrast, hippo ivory and certain tree taxa used for industrial purposes are likely to have more elastic demand (Groves and Rutherford, 2023).

Figure 12 presents comparative statics of the conflict externality with respect to changes in demand elasticity. In the model, conflict is fuelled by looting revenues, which depend on the dispersion between pre- and post-ban prices. A more inelastic demand leads to a greater price dispersion, implying that trade bans on products with inelastic demand are more likely to increase conflicts.

Figure 12: Policymaker Decision Rule and Demand Elasticity (λ^* vs b (for different η))

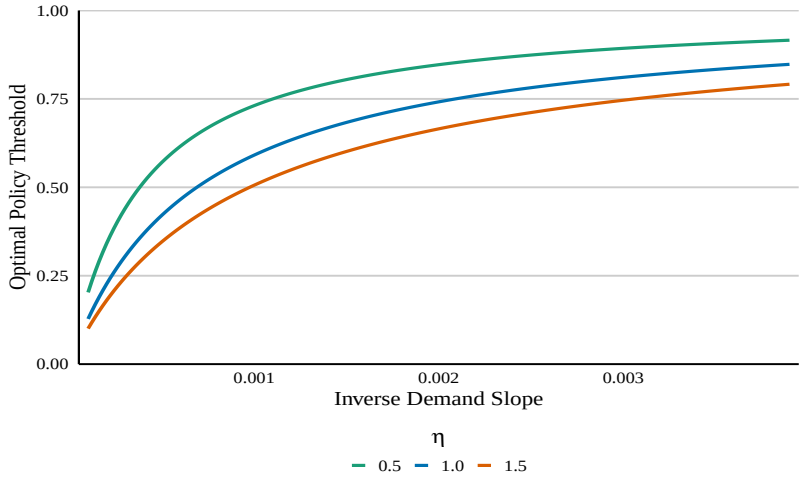

Notes: The figure shows how the optimal policymaker threshold value λ^*, above which a trade ban is optimal, varies with the inverse demand elasticity parameter (b) across different values of the ecological damage function η.

Revenue Decomposition. Furthermore, the revenue–conflict mechanism in the model is driven by two sources. Following the trade ban, the contraction in supply—due to enforcement in strong states—increases prices, but it also raises the quantities harvested by firms operating in those states. Appendix Section E.2.4 decomposes these two sources and shows that, given the values used in the calibration, the increase in price accounts for approximately 78 per cent of the rise in revenue—and hence of the loot available to armed groups—while the remaining 22 per cent is attributable to higher harvested quantities.

6.2.2 Simulations of Different Policies

Figure 13 displays loss simulations under different policies. Each panel corresponds to a different value of η, representing different dynamics for ecological damage. The x-axis represents the policymaker's relative preference for biodiversity (λ)—where higher values indicate greater weight on biodiversity protection. The y-axis shows the standardised policymaker's loss relative to the optimal targeted policy for a given λ and η, which is obtained through numerical optimisation that minimises the loss based on country-level state capacity and rosewood stock.

Beyond the optimal policy (the purple line), which serves as a benchmark but is assumed to be politically infeasible, I examine three alternative scenarios. First, I compute welfare under a uniform ban regime (red line), akin to the current policy. I then consider two targeted policies: one that restricts trade only in strong states with above-median rosewood stock (green line), and another that targets strong states with below-median stock (blue line). The rationale is that restricting trade in countries with small rosewood stock generates less conflict, since the resulting supply reduction—and thus the post-ban price increase—is smaller. This, in turn, lowers lootable revenue while still preserving rosewood from complete extinction.

Figure 13, Panel (a), shows that for $\eta = 0.5$, the current uniform ban results in the largest loss.

As the policymaker's weight on biodiversity (λ) increases, however, the loss under the uniform ban declines relative to the optimal policy. Panel (b) presents the linear case ($\eta = 1$), with a similar ranking. Importantly, the targeted policy that restricts trade only in strong states with low rosewood stock (blue line) performs nearly as good as the optimal policy (purple line). Panel (c) reports results for $\eta = 1.5$, reflecting stronger biodiversity tipping points. It shows that the targeted policy restricting trade only in strong states with above-median rosewood stock (green line) is consistently superior to the uniform ban and nearly as effective as the optimal policy.

The policymaker's loss simulations yield several policy insights. First, for a policymaker concerned with conflict and managing a resource with moderate biodiversity tipping points (e.g., high reproduction rate), a targeted policy that restricts trade in strong states with low stocks of the resource—where enforcement is effective and the price response muted—is nearly as effective as the optimal policy and clearly superior to the uniform ban.[26] Second, when biodiversity tipping points are stronger (i.e. $\eta > 1$), and ecological damage is less likely to be reversible, a targeted policy focusing on strong states with above-median forest stock performs nearly as good as the optimal policy, but may underperform relative to the uniform ban when ecological damage is extreme and λ—the normative weight—is high. Appendix Table E.3 summarises the policy rankings across scenarios.

Figure 13: Simulations of policymaker Losses under Alternative Policies

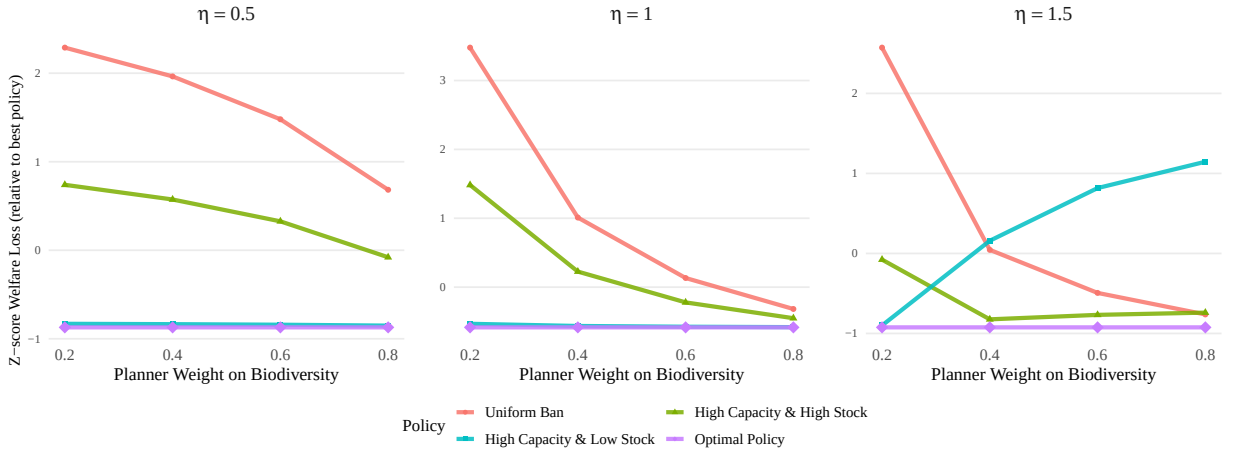

Notes: Each panel shows standardised welfare losses relative to the optimal benchmark (y-axis), computed as the percentage difference $(W^{\text{policy}} - W^{\text{opt}})/W^{\text{opt}} \times 100$, plotted against the planner's environmental preference parameter λ (x-axis). Four different policy scenarios are displayed in each panel: uniform ban (red), a targeted ban applied only to strong states with low rosewood stock (blue), a targeted ban applied to strong states with high rosewood stock (green), and the optimal policy obtained through numerical optimisation based on state capacity and rosewood stock (purple). The different panels correspond to simulations under varying biodiversity tipping point parameters (η).

7 Conclusion

In 1973, under the leadership of the United States and the United Kingdom, governments around the world came together to increase global cooperation in protecting biodiversity and established

[26] Different species are likely to exhibit different tipping points, as these depend on recovery capacity.

CITES, an international convention regulating wildlife trade. Since then, more and more countries have joined the Convention, which today has 184 signatories, and an increasing number of trade restrictions on wildlife have been imposed (Brondízio et al., 2019). Concurrently, mounting scientific evidence has shown that we are experiencing, for the first time, a human-induced mass extinction of species (Ceballos et al., 2015). While the urgency of protecting biodiversity continues to grow and restrictive conservation policies are being adopted widely (Waldron, 2020), little is known about the harmful externalities associated with many of these policies. For instance, they can alter market structures and incentives, potentially leading to unintended consequences.

This paper is the first to document the conflict effects—a negative and harmful externality—of a widely adopted global biodiversity protection mechanism. The paper shows that the policy fuels local conflict and violence, likely by making such activities financially feasible. Moreover, the study reveals several dimensions of heterogeneity that policymakers could exploit to mitigate these harmful externalities and suggests a concrete mitigation strategy using targeted bans.

The study's findings have several policy implications. First, they highlight a potential trade-off between conservation-motivated trade restrictions and armed conflict. Second, the analysis shows that variation in state capacity influences the conflict externality, a factor that policymakers can explicitly take into account when aiming to mitigate unintended costs. Third, the findings are important for peacebuilding efforts by uncovering a new source of variation—wildlife habitat—that explains armed conflict. Fourth, the quantitative model suggests that targeted bans in strong states with small stocks of wild trees can mitigate the policy's conflict externality and outperform the current uniform ban approach across a wide range of model parameters. In addition, the model also shows that policymakers should account for both demand elasticity and species reproduction rates when determining which species to ban from trade.

Importantly, this does not mean that CITES policies are inherently harmful; rather, it highlights the need to evaluate them through a cost-benefit lens, taking their externalities into account. The conflict externality documented in the paper is one example of the potential costs that need to be considered, particularly in light of growing evidence of environmental degradation and the urgent need to allocate resources effectively for conservation. Ultimately, any restriction-based conservation policy has the potential to generate some form of negative externalities, underscoring the importance of future research that assesses both the costs and benefits of environmental protection efforts.

References

D. Acemoglu, M. Golosov, A. Tsyvinski, and P. Yared. A dynamic theory of resource wars. *Quarterly Journal of Economics*, 127(1):283–331, 2012.

D. Acemoglu, C. García-Jimeno, and J. A. Robinson. State capacity and economic development: A network approach. *American economic review*, 105(8):2364–2409, 2015.

R. Adao, M. Kolesár, and E. Morales. Shift-share designs: Theory and inference. *Quarterly Journal of Economics*, 134(4):1949–2010, 2019.

M. Alsan. The effect of the tsetse fly on African development. *American Economic Review*, 105(1):382–410, 2015.

M. D. Alvarez. Forests in the time of violence: Conservation implications of the Colombian war. *Journal of Sustainable Forestry*, 16(3–4):47–68, 2003.

S. Anderson, P. Francois, D. Rohner, and R. Santarrosa. Hidden hostility: donor attention and political violence. 2022.

J. Angrist and G. Imbens. Identification and estimation of local average treatment effects. Working paper, National Bureau of Economic Research, 1994.

J. D. Angrist and A. D. Kugler. Rural windfall or a new resource curse? Coca, income, and civil conflict in Colombia. *Review of Economics and Statistics*, 90(2):191–215, 2008.

R. Arezki and M. Brückner. Food prices and political instability. Imf working paper, International Monetary Fund, 2011a.

R. Arezki and M. Brückner. Oil rents, corruption, and state stability: Evidence from panel data regressions. *European Economic Review*, 55(7):955–963, 2011b.

R. Arezki and M. Brückner. Rainfall, financial development, and remittances: Evidence from sub-saharan Africa. *Journal of International Economics*, 87(2):377–385, 2012.

J. Assunção and C. Gandour. Combating illegal deforestation: Strengthening command and control is fundamental. *Climate Policy Initiative*, 2019.

J. Assunção, C. Gandour, R. Rocha, and R. Rocha. The effect of rural credit on deforestation: Evidence from the Brazilian Amazon. *Economic Journal*, 130(626):290–330, 2020.

J. Assunção, C. Gandour, and R. Rocha. DETER-ing deforestation in the Amazon: Environmental monitoring and law enforcement. *American Economic Journal: Applied Economics*, 15(2):125–156, 2023.

C. Balboni, R. Burgess, A. Heil, J. Old, and B. A. Olken. Cycles of fire? politics and forest burning in Indonesia. In *AEA Papers and Proceedings*, volume 111, pages 415–419, 2021a.

C. Balboni, R. Burgess, and B. A. Olken. The origins and control of forest fires in the tropics. STICERD working paper, London School of Economics, 2021b.

E. Barbier and T. M. Swanson. *Elephants, economics and ivory*. Earthscan, 1990.

R. H. Bates. Ethnicity and development in Africa: A reappraisal. *American Economic Review*, 90(2): 131–134, 2000.

R. H. Bates. State failure. *Annual Review of Political Science*, 11:1–12, 2008.

G. Battiston, G. Daniele, M. Le Moglie, and P. Pinotti. Fueling organized crime: The mexican war on drugs and oil thefts. 2022.

S. Bazzi and C. Blattman. Economic shocks and conflict: Evidence from commodity prices. *American Economic Journal: Macroeconomics*, 6(4):1–38, 2014.

BBC. The illicit trade with China fuelling Mozambique's insurgency, 2024.

BBC News. Mozambique's hidden war over precious rosewood, 2023. URL https://www.bbc.co.uk/news/articles/c51nnzzkpkyo. Accessed 2025-06-03.

G. S. Becker, K. M. Murphy, and M. Grossman. The market for illegal goods: The case of drugs. *Journal of Political Economy*, 114(1):38–60, 2006.

M. F. Bellemare. Rising food prices, food price volatility, and social unrest. *American Journal of Agricultural Economics*, 97(1):1–21, 2015.

J. Bellows and E. Miguel. War and local collective action in Sierra Leone. *Journal of Public Economics*, 93 (11–12):1144–1157, 2009.

E. Ben-Michael, A. Feller, and J. Rothstein. The augmented synthetic control method. *Journal of the American Statistical Association*, 116(536):1789–1803, 2021.

N. Berman and M. Couttenier. External shocks, internal shots: The geography of civil conflicts. *Review of Economics and Statistics*, 97(4):758–776, 2015.

N. Berman, M. Couttenier, D. Rohner, and M. Thoenig. This mine is mine! how minerals fuel conflicts in africa. *American Economic Review*, 107(6):1564–1610, 2017.

N. Berman, M. Couttenier, A. Leblois, and R. Soubeyran. Crop prices and deforestation in the tropics. *Journal of Environmental Economics and Management*, 119:102819, 2023.

D. M. Bernhofen and J. C. Brown. A direct test of the theory of comparative advantage: The case of Japan. *Journal of Political Economy*, 112(1):48–67, 2004.

T. Besley and T. Persson. Wars and state capacity. *Journal of the European Economic Association*, 6(2–3): 522–530, 2008a.

T. Besley and T. Persson. Repression or civil war? *American Economic Review*, 99(2):292–297, 2009.

T. Besley and T. Persson. The logic of political violence. *The quarterly journal of economics*, 126(3): 1411–1445, 2011a.

T. Besley and T. Persson. Pillars of prosperity: The political economics of development clusters. In *Pillars of Prosperity*. Princeton University Press, 2011b.

T. J. Besley and T. Persson. The incidence of civil war: Theory and evidence. Working paper, National Bureau of Economic Research, 2008b.

J. Blanc et al. Loxodonta africana. The IUCN Red List of Threatened Species, 2008: T12392A3339343, 2008.

C. Blattman and E. Miguel. Civil war. *Journal of Economic Literature*, 48(1):3–57, 2010.

B. Bonadio, A. A. Levchenko, D. Rohner, and M. Thoenig. Feeding the tigers: Remittances and conflict in sri lanka. Technical report, National Bureau of Economic Research, 2024.

K. Borusyak, P. Hull, and X. Jaravel. Quasi-experimental shift-share research designs. Working paper, National Bureau of Economic Research, 2018.

K. Borusyak, X. Jaravel, and J. Spiess. Revisiting event-study designs: Robust and efficient estimation. *Review of Economic Studies*, 91(6):3253–3285, 2024.

E. S. Brondízio, J. Settele, S. Díaz, and H. T. Ngo, editors. *Global Assessment Report of the Intergovernmental Science-Policy Platform on Biodiversity and Ecosystem Services*. IPBES Secretariat, Bonn, Germany, 2019. ISBN 978-3-947851-20-1.

M. Brückner and A. Ciccone. Growth, democracy, and civil war. CEPR Discussion Paper DP6568, CEPR, 2007.

M. Brückner and A. Ciccone. International commodity prices, growth and the outbreak of civil war in sub-saharan Africa. *Economic Journal*, 120(544):519–534, 2010.

E. Bueno de Mesquita. Rebel tactics. *Journal of Political Economy*, 121(2):323–357, 2013.

R. Burgess, M. Hansen, B. A. Olken, P. Potapov, and S. Sieber. The political economy of deforestation in the tropics. *Quarterly Journal of Economics*, 127(4):1707–1754, 2012.

R. Burgess, E. Miguel, and C. Stanton. War and deforestation in Sierra Leone. *Environmental Research Letters*, 10(9):095014, 2015.

R. Burgess, O. Deschenes, D. Donaldson, and M. Greenstone. Weather, climate change and death in India. Unpublished manuscript, 2017.

R. Burgess, F. Costa, and B. A. Olken. The Brazilian Amazon's double reversal of fortune. SocArXiv preprint, 2019.

M. Burke, S. M. Hsiang, and E. Miguel. Climate and conflict. *Annu. Rev. Econ.*, 7(1):577–617, 2015a.

M. Burke, S. M. Hsiang, and E. Miguel. Global non-linear effect of temperature on economic production. *Nature*, 527(7577):235–239, 2015b.

R. W. Burn, F. M. Underwood, and J. Blanc. Global trends and factors associated with the illegal killing of elephants: A hierarchical Bayesian analysis of carcass encounter data. *PLoS ONE*, 6(9):e24165, 2011.

B. Callaway and P. H. C. Sant'Anna. Difference-in-differences with multiple time periods. *Journal of Econometrics*, 225(2):200–230, 2021.

J. C. Castillo and D. Kronick. The logic of violence in drug war. *American Political Science Review*, 114(3): 874–887, 2020.

J. C. Castillo, D. Mejía, and P. Restrepo. Scarcity without leviathan: The violent effects of cocaine supply shortages in the mexican drug war. *Review of Economics and Statistics*, 102(2):269–286, 2020.

G. Ceballos, P. R. Ehrlich, A. D. Barnosky, A. García, R. M. Pringle, and T. M. Palmer. Accelerated modern human–induced species losses: Entering the sixth mass extinction. *Science Advances*, 1(5):e1400253, 2015.

A. B. Chimeli and R. R. Soares. The use of violence in illegal markets: Evidence from mahogany trade in the brazilian amazon. *American Economic Journal: Applied Economics*, 9(4):30–57, 2017.

A. Ciccone. International commodity prices and civil war outbreak: New evidence for sub-saharan Africa and beyond. CEPR Discussion Paper DP12625, CEPR, 2018.

P. Collier and A. Hoeffler. Greed and grievance in civil war. *Oxford Economic Papers*, 56(4):563–595, 2004.

P. Collier and D. Rohner. Democracy, development, and conflict. *Journal of the European Economic Association*, 6(2–3):531–540, 2008.

P. Collier, A. Hoeffler, and D. Rohner. Beyond greed and grievance: feasibility and civil war. *oxford Economic papers*, 61(1):1–27, 2009.

A. M. Cotet and K. K. Tsui. Oil and conflict: What does the cross-country evidence really show? *American Economic Journal: Macroeconomics*, 5(1):49–80, 2013.

M. Couttenier, N. Monnet, and L. Piemontese. The economic costs of conflict: A production network approach. CEPR Discussion Paper DP16984, CEPR, 2022.

M. Couttenier, J. Marcoux, T. Mayer, and M. Thoenig. The gravity of violence. 2024.

D. Da Mata and M. Dotta. Commodity booms and the environment. *Available at SSRN 3900793*, 2021.

E. Dal Bó and P. Dal Bó. Workers, warriors, and criminals: Social conflict in general equilibrium. *Journal of the European Economic Association*, 9(4):646–677, 2011.

S. Dasgupta, K. Hamilton, S. Pagiola, and D. Wheeler. Environmental economics at the World Bank. *Review of Environmental Economics and Policy*, 2020.

C. De Chaisemartin and X. d'Haultfoeuille. Two-way fixed effects estimators with heterogeneous treatment effects. *American Economic Review*, 110(9):2964–2996, 2020.

A. Deaton. Commodity prices and growth in Africa. *Journal of Economic Perspectives*, 13(3):23–40, 1999.

M. Dell. Trafficking networks and the mexican drug war. *American Economic Review*, 105(6):1738–1779, 2015.

M. Dell, B. F. Jones, and B. A. Olken. What do we learn from the weather? the new climate-economy literature. *Journal of Economic Literature*, 52(3):740–798, 2014.

Y. Ding and Z. Yin. The study on the effect of restrictive rosewood trade policies on China's rosewood import prices. *Forestry Economics Review*, (ahead-of-print), 2024.

Q.-T. Do, A. A. Levchenko, L. Ma, J. Blanc, H. Dublin, and T. Milliken. The price elasticity of African elephant poaching. *World Bank Economic Review*, 35(3):545–562, 2021.

O. Dube and J. F. Vargas. Commodity price shocks and civil conflict: Evidence from Colombia. *Review of Economic Studies*, 80(4):1384–1421, 2013.

R. Durante and E. Zhuravskaya. Attack when the world is not watching? us news and the israeli-palestinian conflict. *Journal of Political Economy*, 126(3):1085–1133, 2018.

U. J. Eberle, D. Rohner, and M. Thoenig. Heat and hate: Climate security and farmer-herder conflicts in africa. 2020.

EIA. Vanishing point: Criminality, corruption and the devastation of Tanzania's elephants, 2014.

EIA. The rosewood racket: China's billion dollar illegal timber trade and the devastation of Nigeria's forests. Technical report, Environmental Investigation Agency, 2017.

EIA. Cashing-in on chaos: How traffickers, corrupt officials, and shipping lines in The Gambia have profited from Senegal's conflict timber, 2020.

Elephant Action League. Africa's white gold of jihad: Al-shabaab and conflict ivory. https://earthleagueinternational.org/project/africas-white-gold-of-jihad/, 2013. Accessed 2025-06-03.

Enough Project. Tusk wars: Inside the LRA and the bloody business of ivory, 2015. URL https://enoughproject.org/reports/tusk-wars. Accessed 2025-06-03.

J. Esteban, L. Mayoral, and D. Ray. Ethnicity and conflict: An empirical study. *American Economic Review*, 102(4):1310–1342, 2012.

FAO. Food and agriculture organization of the united nations, 2020.

N. Farah and J. R. Boyce. Elephants and mammoths: The effect of an imperfect legal substitute on illegal activity. *Environment and Development Economics*, 24(3):225–251, 2019.

N. Farah, J. R. Boyce, et al. Elephants and mammoths: Can ice ivory save blood ivory. In *Towards a Sustainable and Legal Wildlife Trade Symposium*, 2015.

J. D. Fearon. Why do some civil wars last so much longer than others? *Journal of peace research*, 41(3): 275–301, 2004.

J. D. Fearon. Primary commodity exports and civil war. *Journal of Conflict Resolution*, 49(4):483–507, 2005.

J. D. Fearon. Economic development, insurgency, and civil war. In *Institutions and Economic Performance*, pages 292–328. Harvard University Press, 2008.

J. D. Fearon and D. D. Laitin. Ethnicity, insurgency, and civil war. *American Political Science Review*, 97 (1):75–90, 2003.

R. Fisman and S.-J. Wei. The smuggling of art, and the art of smuggling: Uncovering the illicit trade in cultural property and antiques. *American Economic Journal: Applied Economics*, 1(3):82–96, 2009.

H. Fjelde. Farming or fighting? agricultural price shocks and civil war in Africa. *World Development*, 67: 525–534, 2015.

A. Flaaen, A. Hortaçsu, and F. Tintelnot. The production relocation and price effects of US trade policy: The case of washing machines. *American Economic Review*, 110(7):2103–2127, 2020.

E. Frank and K. Oremus. *Regulating biological resources: Lessons from marine fisheries in the United States*. SSRN, 2023.

E. Frank and A. Sudarshan. The social costs of keystone species collapse: Evidence from the decline of vultures in India. *American Economic Review*, 114(10):3007–3040, 2024.

E. G. Frank and D. S. Wilcove. Long delays in banning trade in threatened species. *Science*, 363(6428): 686–688, 2019.

R. Frank. Commodity prices, state capacity, and civil war: The interaction of economic diversification, price uncertainty, and violence. In *Annual Meeting of the Midwest Political Science Association*, 2006.

M. Funke, M. Schularick, and C. Trebesch. Populist leaders and the economy. *American Economic Review*, 113(12):3249–3288, 2023.

H. K. Gibbs and M. Herold. Tropical deforestation and greenhouse gas emissions. *Environmental Research Letters*, 2(4):045021, 2007.

V. Girard, T. Molina-Millán, G. Vic, et al. Artisanal mining in Africa, 2022. Working paper series, No. 2201.

R. Glennerster and S. Jayachandran. Think globally, act globally: Opportunities to mitigate greenhouse gas emissions in low- and middle-income countries. *Journal of Economic Perspectives*, 37(3):111–135, 2023.

Global Initiative Against Transnational Organized Crime. Poaching, wildlife trafficking and organized crime: Assessing the impact in central Africa. https://globalinitiative.net/analysis/wildlife-trafficking-central-africa/, 2017. Accessed 2025-06-03.

P. Goldsmith-Pinkham, I. Sorkin, and H. Swift. Bartik instruments: What, when, why, and how. *American Economic Review*, 110(8):2586–2624, 2020.

J. A. Goldstone, T. R. Gurr, B. Harff, M. A. Levy, M. G. Marshall, R. H. Bates, D. L. Epstein, C. H. Kahl, P. T. Surko, J. C. Ulfelder, et al. State failure task force report: Phase III findings, 2000.

M. Greenstone and B. K. Jack. Envirodevonomics: A research agenda for an emerging field. *Journal of Economic Literature*, 53(1):5–42, 2015.

H. I. Grossman. A general equilibrium model of insurrections. *American Economic Review*, 81(4):912–921, 1991.

C. Groves and C. Rutherford. CITES and timber: A guide to implementation, 2023.

M. C. Hansen, P. V. Potapov, R. Moore, M. Hancher, S. A. Turubanova, A. Tyukavina, D. Thau, S. V. Stehman, S. J. Goetz, T. R. Loveland, et al. High-resolution global maps of 21st-century forest cover change. *Science*, 342(6160):850–853, 2013.

M. Harari and E. La Ferrara. Conflict, climate, and cells: A disaggregated analysis. *Review of Economics and Statistics*, 100(4):594–608, 2018.

B. Harstad. The conservation multiplier. *Journal of Political Economy*, 131(7):1731–1771, 2023.

S. Hauenstein, M. Kshatriya, J. Blanc, C. F. Dormann, and C. M. Beale. African elephant poaching rates correlate with local poverty, national corruption and global ivory price. *Nature Communications*, 10(1): 2242, 2019.

B. Heid and L. Márquez-Ramos. International environmental agreements and imperfect enforcement: Evidence from cites. *Journal of Environmental Economics and Management*, 118:102784, 2023.

L. Heldring. The origins of violence in Rwanda. Unpublished manuscript, 2018.

C. Hendrix and H.-J. Brinkman. Food insecurity and conflict dynamics: Causal linkages and complex feedbacks. *Stability: International Journal of Security and Development*, 2(2), 2013.

C. S. Hendrix and I. Salehyan. Climate change, rainfall, and social conflict in Africa. *Journal of Peace Research*, 49(1):35–50, 2012.

T. Homer-Dixon. *States, scarcity, and civil strife in the developing world*. Princeton University Press, 2006.

T. F. Homer-Dixon. Environmental scarcity and global security. headline series no. 300. ERIC, 1993.

S. Hsiang and N. Sekar. Does legalization reduce black market activity? evidence from a global ivory experiment and elephant poaching data. Working Paper 22314, National Bureau of Economic Research, 2016.

A. Hsiao. Coordination and commitment in international climate action: Evidence from palm oil. Unpublished manuscript, Department of Economics, MIT, 2021.

J. R. Huber. Effect on prices of Japan's entry into world commerce after 1858. *Journal of Political Economy*, 79(3):614–628, 1971.

M. Humphreys. Natural resources, conflict, and conflict resolution: Uncovering the mechanisms. *Journal of Conflict Resolution*, 49(4):508–537, 2005.

INTERPOL. The environmental crime crisis: Threats to sustainable development from illegal exploitation and trade in wildlife and forest resources, 2014. URL https://wedocs.unep.org/handle/20.500.11822/9120. Accessed 2025-06-03.

D. A. Irwin. Tariff incidence: Evidence from US sugar duties, 1890–1930. Working paper, National Bureau of Economic Research, 2014.

IUCN. African elephants and rhinos, 1990.

D. Jaimovich and F. Toledo. The grievances of a failed reform: Chilean land reform and conflict with indigenous communities. Unpublished manuscript, 2021.

S. Jayachandran, J. De Laat, E. F. Lambin, C. Y. Stanton, R. Audy, and N. E. Thomas. Cash for carbon: A randomized trial of payments for ecosystem services to reduce deforestation. *Science*, 357(6348):267–273, 2017.

R. J. Keenan, G. A. Reams, F. Achard, J. V. de Freitas, A. Grainger, and E. Lindquist. Dynamics of global forest area: Results from the FAO global forest resources assessment 2015. *Forest Ecology and Management*, 352:9–20, 2015.

M. Köhl, R. Lasco, M. Cifuentes, Ö. Jonsson, K. T. Korhonen, P. Mundhenk, J. de Jesus Navar, and G. Stinson. Changes in forest production, biomass and carbon: Results from the 2015 UN FAO global forest resource assessment. *Forest Ecology and Management*, 352:21–34, 2015.

M. Kremer and C. Morcom. Elephants. *American Economic Review*, 90(1):212–234, 2000.

G. LaFree and L. Dugan. Introducing the global terrorism database. *Terrorism and Political Violence*, 19 (2):181–204, 2007.

F. Libois, J.-M. Baland, N. Delbart, and S. Pattanayak. Community forest management: The story behind a success story in Nepal. Working paper, 2022.

N. Limodio. Terrorism financing, recruitment and attacks: Evidence from a natural experiment. *Chicago Booth Research Paper*, (32), 2019.

S. A. Mainka and J. A. Mills. Wildlife and traditional chinese medicine: supply and demand for wildlife species. *Journal of zoo and wildlife medicine*, pages 193–200, 1995.

M. A. Malik, R. Ali Mirza, and F. U. Rehman. *Frontier governmentality*. Number 2023/42. WIDER Working Paper, 2023.

L. R. Martinez. Transnational insurgents: Evidence from colombia's farc at the border with chávez's venezuela. *Journal of Development Economics*, 126:138–153, 2017.

J.-F. Maystadt and O. Ecker. Extreme weather and civil war: Does drought fuel conflict in Somalia through livestock price shocks? *American Journal of Agricultural Economics*, 96(4):1157–1182, 2014.

J.-F. Maystadt, G. De Luca, P. G. Sekeris, and J. Ulimwengu. Mineral resources and conflicts in drc: a case of ecological fallacy? *Oxford Economic Papers*, 66(3):721–749, 2014.

M. McBride, G. Milante, and S. Skaperdas. Peace and war with endogenous state capacity. *Journal of Conflict Resolution*, 55(3):446–468, 2011.

E. McGuirk and M. Burke. The economic origins of conflict in Africa. *Journal of Political Economy*, 128 (10):3940–3997, 2020.

E. F. McGuirk and N. Nunn. Transhumant pastoralism, climate change, and conflict in Africa. Working paper, National Bureau of Economic Research, 2020.

E. F. McGuirk and N. Nunn. Development mismatch? evidence from agricultural projects in pastoral Africa. Working paper, National Bureau of Economic Research, 2024.

E. F. McGuirk and N. Nunn. Transhumant pastoralism, climate change, and conflict in africa. *Review of Economic Studies*, 92(1):404–441, 2025.

F. Merz. United nations office on drugs and crime: World drug report 2017. 2017. *SIRIUS–Zeitschrift für Strategische Analysen*, 2(1):85–86, 2018.

S. Michalopoulos and E. Papaioannou. Pre-colonial ethnic institutions and contemporary African development. *Econometrica*, 81(1):113–152, 2013.

S. Michalopoulos and E. Papaioannou. Historical legacies and African development. *Journal of Economic Literature*, 58(1):53–128, 2020.

E. Miguel, S. Satyanath, and E. Sergenti. Economic shocks and civil conflict: An instrumental variables approach. *Journal of Political Economy*, 112(4):725–753, 2004.

T. Milliken, R. W. Burn, and L. Sangalakula. An analysis of the trends of elephant product seizure data in ETIS: Report to the 12th meeting of the conference of the parties, 2000.

J. A. Miron. An economic analysis of alcohol prohibition. *Journal of Drug Issues*, 28(3):741–762, 1998.

G. P. Murdock. Ethnographic atlas: A summary. *Ethnology*, 6(2):109–236, 1967.

B. J. Ndulu, J.-P. Azam, S. A. O'Connell, R. H. Bates, A. K. Fosu, J. W. Gunning, and D. Nijinkeu. *The political economy of economic growth in Africa, 1960–2000*, volume 2. Cambridge University Press, 2008.

N. Nunn. The long-term effects of Africa's slave trades. *Quarterly Journal of Economics*, 123(1):139–176, 2008.

N. Nunn and N. Qian. US food aid and civil conflict. *American Economic Review*, 104(6):1630–1666, 2014.

N. Nunn and L. Wantchekon. The slave trade and the origins of mistrust in Africa. *American Economic Review*, 101(7):3221–3252, 2011.

S. J. Phillips, R. P. Anderson, and R. E. Schapire. Maximum entropy modeling of species geographic distributions. *Ecological Modelling*, 190(3–4):231–259, 2006.

P. Pinstrup-Andersen and S. Shimokawa. Do poverty and poor health and nutrition increase the risk of armed conflict onset? *Food Policy*, 33(6):513–520, 2008.

S. V. Price. War and tropical forests: Conservation in areas of armed conflict, 2003. Report.

C. Raleigh, A. Linke, H. Hegre, and J. Karlsen. Introducing ACLED: An armed conflict location and event dataset. *Journal of Peace Research*, 47(5):651–660, 2010.

M. L. Ross. A closer look at oil, diamonds, and civil war. *Annual Review of Political Science*, 9:265–300, 2006.

T. K. Rudel, O. T. Coomes, E. Moran, F. Achard, A. Angelsen, J. Xu, and E. Lambin. Forest transitions: Towards a global understanding of land use change. *Global Environmental Change*, 15(1):23–31, 2005.

RUSI. An illusion of complicity: Terrorism and the illegal ivory trade in east Africa. Technical report, Royal United Services Institute for Defence and Security Studies, 2015.

R. Sánchez De La Sierra. On the origins of the state: Stationary bandits and taxation in eastern Congo. *Journal of Political Economy*, 128(1):32–74, 2020.

J. Schipper, J. S. Chanson, F. Chiozza, N. A. Cox, M. Hoffmann, V. Katariya, J. Lamoreux, A. S. L. Rodrigues, S. N. Stuart, H. J. Temple, et al. The status of the world's land and marine mammals: Diversity, threat, and knowledge. *Science*, 322(5899):225–230, 2008.

D. M. Schwartz, T. Deligiannis, and T. F. Homer-Dixon. Commentary: Debating environment, population, and conflict. *Environmental Change and Security Project Report*, 6:77–94, 2000.

S. F. Senula, J. T. Scavetta, J. A. Banta, U. G. Mueller, J. N. Seal, and K. Kellner. Potential distribution of six North American higher-attine fungus-farming ant (hymenoptera: Formicidae) species. *Journal of Insect Science*, 19(6):24, 2019.

J. M. Shandra, E. Shircliff, and B. London. World Bank lending and deforestation: A cross-national analysis. *International Sociology*, 26(3):292–314, 2011.

J. N. Shapiro and D. A. Siegel. *Underfunding in terrorist organizations*. Springer, 2009.

S. Skaperdas. An economic approach to analyzing civil wars. *Economics of Governance*, 9(1):25–44, 2008.

M. C. Sosnowski and G. A. Petrossian. Luxury fashion wildlife contraband in the usa. *EcoHealth*, 17(1): 94–110, 2020.

M. C. Sosnowski, T. G. Knowles, T. Takahashi, and N. J. Rooney. Global ivory market prices since the 1989 CITES ban. *Biological Conservation*, 237:392–399, 2019.

E. Souza-Rodrigues. Deforestation in the Amazon: A unified framework for estimation and policy analysis. *Review of Economic Studies*, 86(6):2713–2744, 2019.

L. Sun and S. Abraham. Estimating dynamic treatment effects in event studies with heterogeneous treatment effects. *Journal of Econometrics*, 225(2):175–199, 2021.

R. Sundberg and E. Melander. Introducing the UCDP georeferenced event dataset. *Journal of Peace Research*, 50(4):523–532, 2013.

M. M. Sviatschi. Making a narco: Childhood exposure to illegal labor markets and criminal life paths. Working paper, Department of Economics, Princeton University. https://rpds.princeton.edu/sites/rpds/files/sviatschi_making-a-narco_march2018.pdf, 2018.

The Economist. The case for legalisation, July 2001. URL https://www.economist.com/leaders/2001/07/26/the-case-for-legalisation. Accessed: 2025-07-05.

C. Thouless, H. T. Dublin, J. Blanc, D. Skinner, T. Daniel, R. Taylor, F. Maisels, H. Frederick, and P. Bouché. African elephant status report 2016: An update from the african elephant database, 2016.

K. Titeca. Illegal ivory trade as transnational organized crime? an empirical study into ivory traders in Uganda. *British Journal of Criminology*, 59(1):24–44, 2019.

TRAFFIC. Ivory and terror: Fact or myth? Technical report, TRAFFIC, 2015.

F. M. Underwood, R. W. Burn, and T. Milliken. Dissecting the illegal ivory trade: An analysis of ivory seizures data. *PLoS ONE*, 8(10):e76539, 2013.

United Nations Security Council. Report of the secretary-general on the lord's resistance army-affected areas, 2013. URL https://digitallibrary.un.org/record/752291. Accessed 2025-06-03.

UNODC. Wildlife crime report. Policy report, United Nations Office on Drugs and Crime, 2016.

UNODC. Wildlife crime report. Policy report, United Nations Office on Drugs and Crime, 2020.

UNODC. Wildlife crime report. Policy report, United Nations Office on Drugs and Crime, 2024.

G. C. van Kooten. Protecting the African elephant: A dynamic bioeconomic model of ivory trade. *Biological Conservation*, 141(8):2012–2022, 2006.

A. Waldron. Protecting 30% of the planet for nature: Costs, benefits and economic implications (waldron report), 2020.

A. D. Walters, M. A. Brown, G. M. Cerbie, M. G. Williams, J. A. Banta, L. R. Williams, N. B. Ford, and D. J. Berg. Do hotspots fall within protected areas? a geographic approach to planning analysis of regional freshwater biodiversity. *Freshwater Biology*, 64(11):2046–2056, 2019.

S. K. Wasser, L. Brown, C. Mailand, S. Mondol, W. Clark, C. Laurie, and B. S. Weir. Genetic assignment of large seizures of elephant ivory reveals Africa's major poaching hotspots. *Science*, 349(6243):84–87, 2015.

J. Weinberg and R. Bakker. Let them eat cake: Food prices, domestic policy and social unrest. *Conflict Management and Peace Science*, 32(3):309–326, 2015.

M. Widiani. EUROPEAN UNION's environmental hegemony on palm oil issues. Unpublished manuscript.

WWF. Ivory, non-state armed groups and terrorism. Technical report, World Wide Fund for Nature, 2015.

A. L. Zhu. China's rosewood boom: A cultural fix to capital overaccumulation. *Annals of the American Association of Geographers*, 110(1):277–296, 2020.

A. L. Zhu. *Rosewood: Endangered species conservation and the rise of global China*. Harvard University Press, 2022.

Appendix

Wildlife and Conflict: The Cost of Protecting Biodiversity

Guy Pincus

This version: December 27, 2025

Table of Contents

A Descriptive Statistics

This section reports descriptive statistics related to the main estimates of the paper. Figures A.1 and A.2 show, respectively, the evolution of CITES membership over time and its current global coverage. Figure A.3 illustrates the supply chains of elephant ivory and rhino horn. Table A.2 presents policy dates and the level of imposed restrictions, and Tables A.5 and A.6 provide summary statistics. Figures A.4 and A.5 display the spatial distributions of conflict based on the UCDP and GTD datasets.

Figure A.6 presents event study estimates for animals (left) and trees (right). To estimate the statistical association between the policy and wildlife prices, I construct a wildlife-year panel and estimate an event study specification, using prices as the outcome and policy indicators as explanatory variables.[27] Wildlife consumption is often considered a luxury and therefore viewed as a substitute for other luxury goods (Kremer and Morcom, 2000; Hsiang and Sekar, 2016; Do et al., 2021; Zhu, 2020; Ding and Yin, 2024). Accordingly, I use precious metals as a control group for wildlife products. For endangered trees, I use the World Bank hardwood timber price indices for Cameroon and Indonesia as a control group, since these species share similar attributes and origins with rosewood and ebony. Given the staggered timing of the policy, I apply the imputation estimator proposed by Borusyak et al. (2024).[28]

I estimate the following specification:

$$\ln(p_{w,t}) = \sum_{z=\Gamma^-}^{-2} \beta_z D_{w,t+z} + \sum_{j=0}^{\Delta^+} \gamma_j D_{w,t+j} + \delta_w + \lambda_t + \epsilon_{w,t} \tag{19}$$

$\ln(p_{w,t})$ is the log-transformed and standardised price of wildlife/resource w in year t, $D_{w,t+z}$ and $D_{w,t+j}$ indicate the timing of the policy relative to treatment, and δ_w and λ_t represent wildlife/resource and year fixed effects, respectively. To mitigate concerns about serial correlation, standard errors are clustered at the category level.

Appendix Table C.2 reports the difference-in-differences estimates, showing that the effect of the policy on wildlife prices is positive, statistically significant, and is about 1.117 and 1.03 standard deviations for wild animals and wild trees, respectively.

[27] The six wildlife products included in the analysis are: elephant ivory, rhino horn, crocodile skin, *Dalbergia*, *Pterocarpus*, and *Diospyros*.

[28] The World Bank publishes price indices for Cameroon and Indonesia to serve as representative measures of tropical hardwood prices.

CITES Membership

Figure A.1: CITES Membership Over Time

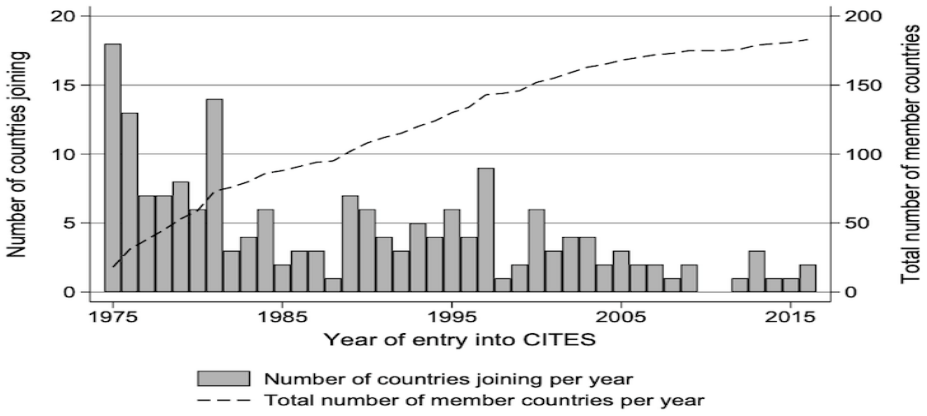

Notes: The figure shows the number of countries where CITES entered into force each year.

Figure A.2: Global Distribution of CITES Member States

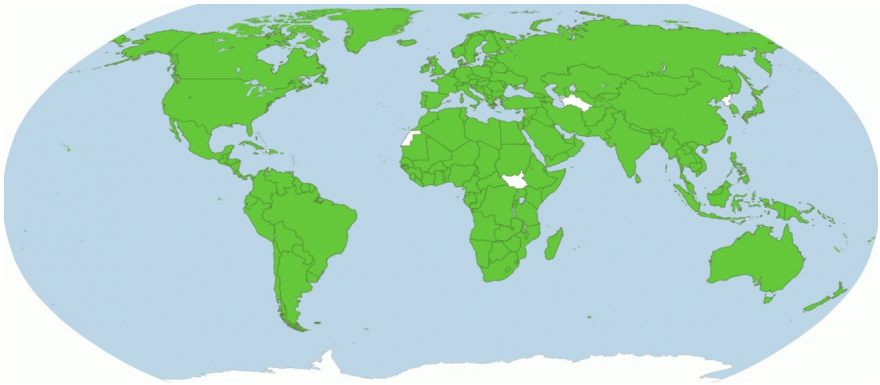

Notes: The figure shows the spatial distribution of CITES member states as of 2020.

Supply Chain of Elephant Ivory and Rhino Horn

Figure A.3: The Supply Chain of Ivory and Rhino Horn

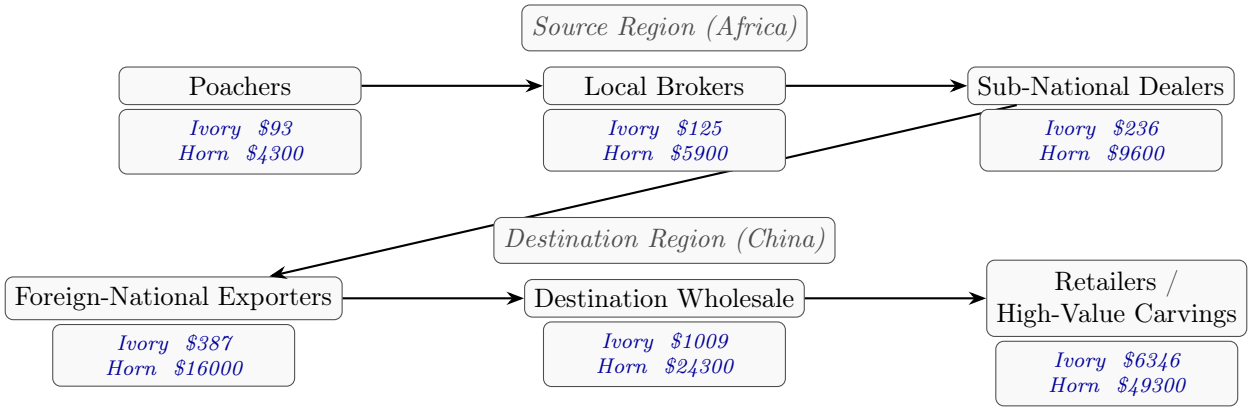

Notes: The figure illustrates the supply chains of elephant ivory and rhino horn, from poachers in source countries to final retailers in destination markets. Estimated prices are per kilogram, based on UNODC (2020).

Policy Timeline

Table A.1: Policy Timeline

	Date Announce	Date Enforce	Appendix
Wild Trees			
Luxury			
Swietenia Humilis	1975	1975	II
Pericopsis Elata	1991	1991	II
Dalbergia Nigra	1991	1991	I
Swietenia Mahagoni	1992	1992	II
Prunus	1994	1994	II
Swietenia Macro	1995	1995	II
Agarwood	2004	2004	II
Aniba	2009	2009	II
Diospyros	2013	2013	II
Pterocarpus	2016	2016	II
Dalbergia	2016	2016	II
Industrial			
Abies	1975	1975	II
Araucaria	1975	1975	II
Fitzroya	1975	1975	II
Pilgerodendron	1975	1975	II
Podocarpus P.	1975	1975	II
Podocarpus N.	1975	1975	II
Guaiacum	2002	2002	II
Gonystylus	2004	2004	II
Taxus	2004	2004	II
Gonopterodendron	2010	2010	II
Fraxinus	2014	2014	II
Cedrela	2019	2019	II
Handroanthus	2022	2022	II
Wild Animals			
Crocodile	1975	1975	I
Asian Elephants	1977	1977	I
African Elephants	1977	1977	II
Rhino	1977	1977	I
African Elephants	1989	1990	I
Hippo	1994	1994	II
African Elephants	1998	1999	Stock Release
Pangolin (Manis)	1999	1999	I
Abalone	2006	2006	III
African Elephants	2007	2008	Stock Release
African Elephants	2017	2018	China Ban

Notes: The table reports the dates and levels of trade restrictions imposed on species included in the sample.

Table A.2: Policy Timeline

	Date Announce	Date Enforce	Appendix
Wild Trees			
Luxury			
Swietenia Humilis	1975	1975	II
Pericopsis Elata	1991	1991	II
Dalbergia Nigra	1991	1991	I
Swietenia Mahagoni	1992	1992	II
Prunus	1994	1994	II
Swietenia Macro	1995	1995	II
Agarwood	2004	2004	II
Aniba	2009	2009	II
Diospyros	2013	2013	II
Pterocarpus	2016	2016	II
Dalbergia	2016	2016	II
Industrial			
Abies	1975	1975	II
Araucaria	1975	1975	II
Fitzroya	1975	1975	II
Pilgerodendron	1975	1975	II
Podocarpus P.	1975	1975	II
Podocarpus N.	1975	1975	II
Guaiacum	2002	2002	II
Gonystylus	2004	2004	II
Taxus	2004	2004	II
Gonopterodendron	2010	2010	II
Fraxinus	2014	2014	II
Cedrela	2019	2019	II
Handroanthus	2022	2022	II

Notes: The table reports the dates and levels of trade restrictions imposed on species included in the sample.

Table A.3: Policy Timeline (Chronologically Ordered)

	Date Announce	Date Enforce	Appendix
Luxury Trees			
Swietenia Humilis	1976	1976	II
Pericopsis Elata	1992	1992	II
Dalbergia Nigra	1992	1992	I
Swietenia Mahagoni	1992	1992	II
Prunus	1995	1995	II
Swietenia Macro	1995	1995	II
Agarwood	2004	2004	II
Aniba	2010	2010	II
Diospyros	2013	2013	II
Pterocarpus	2016	2016	II
Dalbergia	2016	2016	II
Industrial Trees			
Abies	1976	1976	II
Araucaria	1976	1976	II
Fitzroya	1976	1976	II
Pilgerodendron	1976	1976	II
Podocarpus P.	1976	1976	II
Podocarpus N.	1976	1976	II
Guaiacum	2001	2001	II
Gonystylus	2004	2004	II
Taxus	2004	2004	II
Gonopterodendron	2010	2010	II
Fraxinus	2013	2013	II
Cedrela	2019	2019	II
Handroanthus	2022	2022	II

Notes: Table sorted by Date Enforce. Luxury and Industrial groups preserved.

Summary Statistics

Table A.4: Conflict Correlogram

	ACLED	UCDP	GTD
ACLED	1	0.314***	0.259***
UCDP		1	0.421***
GTD			1

Notes: Entries show pairwise Pearson correlations between conflict datasets. * significant at 10%; ** significant at 5%; *** significant at 1%.

Table A.5: Descriptive Statistics: Global

	N	Mean	St. Dev.	Control − Treatment
Pr(Conflict > 0) ACLED				
All Cells	784,742	0.0557	0.2294	
If Wild Animals = 0	649,794	0.0457	0.2088	-0.0585^{***}
If Wild Animals > 0	134,948	0.1042	0.3055	(0.0010)
If Wild Trees = 0	627,126	0.0399	0.1957	-0.0788^{***}
If Wild Trees > 0	157,616	0.1188	0.3235	(0.0010)
If Industrial Mine = 0	248,250	0.0770	0.2666	-0.0838^{***}
If Industrial Mine > 0	4,875	0.1608	0.3674	(0.0040)
Pr(Conflict > 0) UCDP				
All Cells	3,375,400	0.0120	0.1088	
If Wild Animals = 0	3,189,060	0.0099	0.0991	-0.0374^{***}
If Wild Animals > 0	186,340	0.0474	0.2124	(0.0001)
If Wild Trees = 0	3,010,000	0.0090	0.0944	-0.0278^{***}
If Wild Trees > 0	365,400	0.0368	0.1882	(0.0001)
If Industrial Mine = 0	248,250	0.0378	0.1908	0.0101^{***}
If Industrial Mine > 0	4,875	0.0277	0.1641	(0.0030)
Pr(Conflict > 0) GTD				
All Cells	5,014,880	0.0082	0.0902	
If Wild Animals = 0	4,738,032	0.0074	0.0858	-0.0144^{***}
If Wild Animals > 0	276,848	0.0218	0.1461	(0.0001)
If Wild Trees = 0	4,472,000	0.0057	0.0752	-0.0233^{***}
If Wild Trees > 0	542,880	0.0290	0.1678	(0.0001)
If Industrial Mine = 0	248,250	0.0244	0.1541	0.0001
If Industrial Mine > 0	4,875	0.0242	0.1537	(0.0001)
Resources Distribution (Cross-Section)				
Wild Animals > 0	5,324	0.0552	0.2284	
Wild Trees > 0	10,440	0.1083	0.3107	
Industrial Mine > 0	195	0.0019	0.1374	

Notes: The table reports conditional and unconditional probabilities of conflict incidence based on the ACLED, UCDP, and GTD datasets, as well as resource distributions.

Table A.6: Descriptive Statistics: Africa

	N	Mean	St. Dev.	Control − Treatment
Pr(Conflict > 0) ACLED				
All Cells	343,952	0.0789	0.2696	
If Wild Animals = 0	269,724	0.0725	0.2593	−0.0297***
If Wild Animals > 0	74,228	0.1022	0.3029	(0.0012)
If Wild Trees = 0	269,612	0.0636	0.2440	−0.0709***
If Wild Trees > 0	74,340	0.1344	0.3411	(0.0013)
If Industrial Mine = 0	339,077	0.0777	0.2677	−0.0831***
If Industrial Mine > 0	4,875	0.1608	0.3674	(0.0053)
High State Capacity	98,980	0.0514	0.2209	−0.0397***
Low State Capacity	241,640	0.0911	0.2878	(0.0008)
Pr(Conflict > 0) UCDP				
All Cells	429,940	0.0338	0.1808	
If Wild Animals = 0	337,155	0.0328	0.1780	−0.0050***
If Wild Animals > 0	92,785	0.0378	0.1906	(0.0007)
If Wild Trees = 0	337,015	0.0306	0.1723	−0.0149***
If Wild Trees > 0	92,925	0.0456	0.2085	(0.0008)
If Industrial Mine = 0	425,065	0.0339	0.1810	0.0062***
If Industrial Mine > 0	4,875	0.0277	0.1641	(0.0024)
High State Capacity	123,725	0.0107	0.1032	−0.033***
Low State Capacity	302,050	0.0437	0.2044	(0.0004)
Pr(Conflict > 0) GTD				
All Cells	638,768	0.0133	0.1145	
If Wild Animals = 0	500,916	0.0131	0.1136	−0.0009***
If Wild Animals > 0	137,852	0.0140	0.1176	(0.0004)
If Wild Trees = 0	500,708	0.0111	0.1046	−0.0103***
If Wild Trees > 0	138,060	0.0213	0.1444	(0.0004)
If Industrial Mine = 0	633,893	0.0132	0.1141	−0.0110***
If Industrial Mine > 0	4,875	0.0242	0.1537	(0.0022)
High State Capacity	183,820	0.0078	0.0884	−0.0078***
Low State Capacity	448,760	0.0156	0.1241	(0.0002)
Resources Distribution (Cross-Section)				
Wild Animals > 0	2,651	0.2158	0.4114	
Wild Trees > 0	2,655	0.2161	0.4116	
Industrial Mine > 0	195	0.0159	0.1250	
State Capacity & Precious Trees				
Wild Trees Distribution| High=1	759,330	0.0587	0.2351	0.017***
Wild Trees Distribution| Low=0	1,346,026	0.0417	0.1999	(0.0003)

Notes: The table reports conditional and unconditional probabilities of conflict incidence based on the ACLED, UCDP, and GTD datasets, resource distributions across Africa, and the distribution of wild trees across high- and low-capacity states.

Conflicts Spatial Distributions

Figure A.4: Spatial Distributions of UCDP Conflict Events

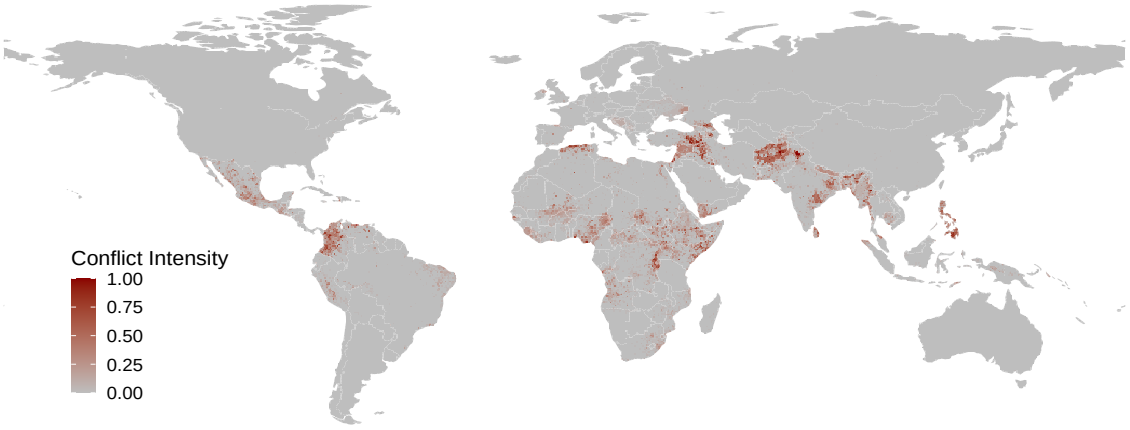

Figure A.5: Spatial Distributions of GTD Conflict Events

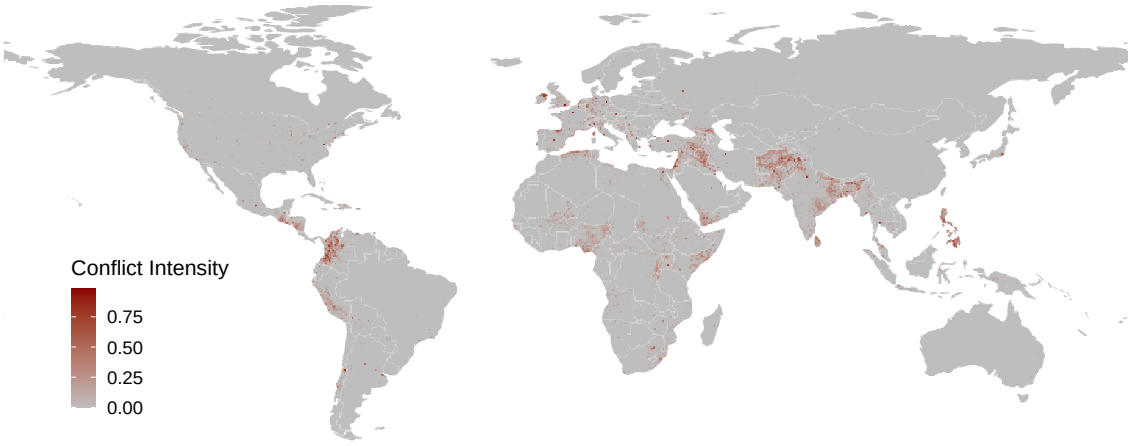

Notes: The maps present the spatial distribution of conflict for UCDP (1989–2023) and GTD (1970–2021). Darker shading indicates cells with a higher proportion of years featuring at least one conflict incident.

Wildlife Prices

Figure A.6: Trade Restrictions and Wildlife Prices

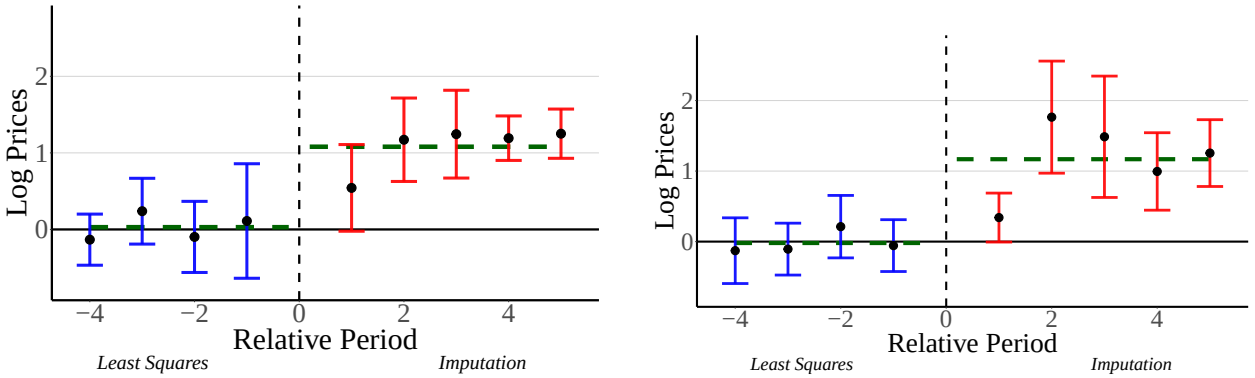

(a) Wild Animals **(b)** Wild Trees

Notes: The figure presents estimates using the staggered event study imputation estimator suggested by Borusyak et al. (2024). The pre-treatment coefficients are estimated using least squares, whereas the post-treatment coefficients are estimated with the imputation estimator. Each observation corresponds to a resource-year. The wild animal sample includes 386 observations, and the wild trees sample includes 549 observations. The estimates are based on equation (19), with the interaction term $Wildlife \times Policy$, an indicator explaining log standardised prices, and include category and year fixed effects. The omitted period is the year prior to the policy announcement. The control group for wild animals is precious metals (gold, silver, and platinum), and for wild precious trees it is the World Bank hard tropical timber index. The green horizontal lines indicate the average of the pre- or post-treatment coefficients. Error bars indicate 95% confidence intervals, with standard errors clustered to allow for arbitrary serial correlation.

Confiscations

Figure A.7: Wildlife Trade Restrictions and Confiscation Events

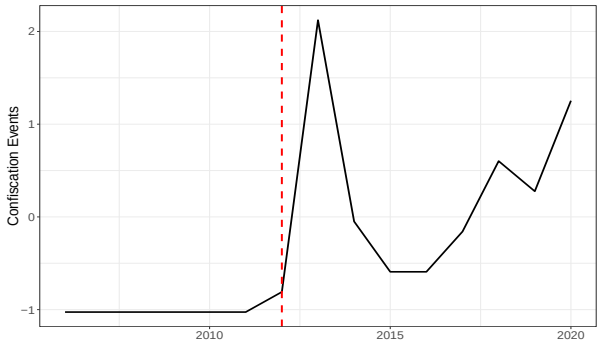

(a) Ebony (*Diospyros*)

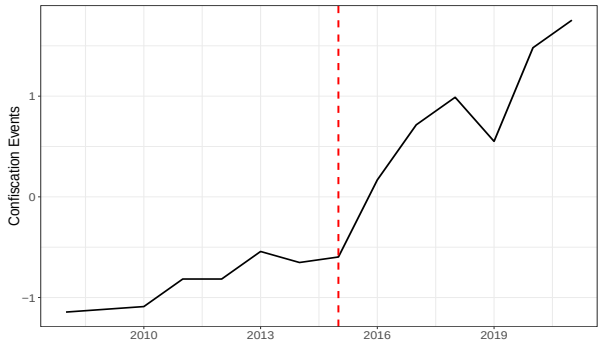

(b) Rosewood (*Dalbergia*)

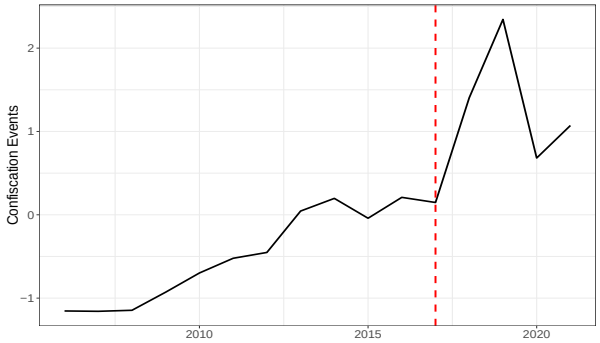

(c) Elephant Ivory

Notes: The figure depicts standardised sequences of wildlife confiscation events, alongside policy changes (in red) for blackwood (2013), rosewood (2016), and the Chinese ban on elephant ivory (2017).

B Further Results

This section reports additional results documented throughout the analysis, shedding more light on the conflict-wildlife nexus. Table B.1 follows the empirical approach of Berman et al. (2017), using wildlife prices as a source of time variation, while Table **??** reports a one-by-one price shock analysis. Table B.3 provides one-by-one long-difference estimates for individual wildlife species.

Table B.4 provides suggestive evidence that the demand for ivory is price-inelastic. I use two partially restrictive policy shocks (in 1977 and 1984) and import data from Hong Kong and Japan to estimate the price elasticity of demand using a 2SLS specification. Total traded volume increased following the shocks.

Figure B.1 provides evidence of substitution between elephant and hippo ivory, showing an increase in reported traded volumes of hippo teeth following restrictive policy in the elephant ivory market.

Table B.5 provides evidence of substitution between ivory-related and mineral-related conflicts. I interact the contractionary policy years in the ivory market with a distance measure between elephant habitat and the nearest industrial mineral site. The positive coefficient implies that in years of reduced conflict in elephant regions, there is an increase in conflict in nearby industrial mineral regions.

Finally, Figure B.2 provides suggestive evidence on the link between organised crime and the ivory trade, and how this nexus evolved over time. I plot the share of large confiscations out of total confiscations, showing a clear increase over time, which suggests that the involvement of criminal syndicates in the trade increased over time.[29]

[29]The analysis relies on the assumption that large-scale smuggling requires logistical capacity that small-scale smugglers do not possess.

Wildlife Price Shocks and Conflict Events

Table B.1: Wildlife Price Shocks and Conflict Likelihood

	Dep. Var.: Conflict (0/1)								
	ACLED			UCDP			GTD		
	(1)	(2)	(3)	(4)	(5)	(6)	(7)	(8)	(9)
Habitat × *Price*	0.0063***	0.0063***	0.0081***	0.0022***	0.0022***	0.0027***	0.0030***	0.0030***	0.0040***
	(0.0015)	(0.0015)	(0.0017)	(0.0007)	(0.0007)	(0.0009)	(0.0006)	(0.0006)	(0.0008)
	[0.0013]	[0.0013]	[0.0015]	[0.0007]	[0.0007]	[0.0008]	[0.0007]	[0.0007]	[0.0008]
Habitat Around × *Price*			0.0059***			0.0015**			0.0028***
			(0.0011)			(0.0007)			(0.0006)
			[0.0012]			[0.0006]			[0.0006]
Mineral × *Price*		0.0272***	0.0207***		0.0008	0.0004		0.0016	0.0006
		(0.0065)	(0.0060)		(0.0033)	(0.0033)		(0.0025)	(0.0026)
		[0.0059]	[0.0057]		[0.0032]	[0.0032]		[0.0025]	[0.0026]
Mineral Around × *Price*			0.0138***			0.0006			0.0018
			(0.0032)			(0.0032)			(0.0026)
			[0.0023]			[0.0019]			[0.0015]
Dep. Var. Mean	0.0531	0.0531	0.0531	0.0117	0.0117	0.0117	0.0081	0.0081	0.0081
Dep. Var. SD	0.2243	0.2243	0.2243	0.1075	0.1075	0.1075	0.0890	0.0890	0.0890
Cell FE	Y	Y	Y	Y	Y	Y	Y	Y	Y
Country-Year FE	Y	Y	Y	Y	Y	Y	Y	Y	Y
Observations	751,939	751,939	751,939	3,334,380	3,334,380	3,334,380	4,953,936	4,953,936	4,953,936

Notes: The table reports LPM estimates using OLS. Each observation corresponds to a cell-year. The variable *Habitat* is an indicator measuring the suitability of cell k for wildlife species w, and *price* denotes the log price of the corresponding wildlife species w in cell k at time t. The variable *Mineral* × *Price* captures the industrial mineral price shock (Berman et al., 2017). The *Around* variables indicate spatial lags. The dependent variable is a binary indicator for conflict incidence, equal to one if at least one conflict event occurs in a given cell and year, based on the conflict datasets referenced in the column titles. Standardised coefficients are reported with spatially clustered standard errors (in parentheses), which allow for spatial and temporal correlation within a 500 km radius of each cell's centroid. Standard errors in square brackets are clustered at the country-year and cell levels, allowing for spatial correlation within a country and infinite serial correlation within a cell. * significant at 10%; ** significant at 5%; *** significant at 1%.

Table B.2: Wildlife Price Shocks and Conflict Likelihood: Disaggregated Estimates

	Dep. Var.: GTD Conflict Indicator (0/1)							
	African Elephant	Asian Elephant	Hippo	Rhino	Crocodile	Dalbergia	Pterocarpus	Diospyros
	(1)	(2)	(3)	(4)	(5)	(6)	(7)	(8)
Habitat × *Price*	0.0060***	0.0168***	0.0074***	−0.0020***	0.0018***	0.0077***	0.0047***	0.0028***
	(0.0017)	(0.0032)	(0.0030)	(0.0006)	(0.0006)	(0.0011)	(0.0013)	(0.0005)
Around × *Price*	0.0061***	0.0017	0.0082***	−0.0010	0.0011**	0.0029***	0.0012	0.0010
	(0.0018)	(0.0017)	(0.0021)	(0.0011)	(0.0005)	(0.0008)	(0.0008)	(0.0005)
Composite Wildlife Index	0.0032***	0.0035***	0.0030***	0.0030***	0.0027***	0.0026***	0.0028***	0.0042***
	(0.0006)	(0.0006)	(0.0006)	(0.0006)	(0.0007)	(0.0008)	(0.0006)	(0.0016)
Dep. Var. Mean	0.0082	0.0082	0.0082	0.0082	0.0082	0.0082	0.0082	0.0082
Dep. Var. SD	0.0902	0.0902	0.0902	0.0902	0.0902	0.0902	0.0902	0.0902
Cell FE	Y	Y	Y	Y	Y	Y	Y	Y
Country-Year FE	Y	Y	Y	Y	Y	Y	Y	Y
Observations	2,507,440	2,507,440	2,507,440	964,400	4,822,000	964,400	964,400	2,411,000

Note: The table reports LPM estimates using OLS separately for the different wildlife species. Each observation corresponds to a cell-year. The variable *Habitat* is an indicator measuring the suitability of cell k for wildlife species w, and *price* denotes the log price of the corresponding wildlife species w in cell k at time t. The dependent variable is a binary indicator for conflict incidence, equal to one if at least one conflict event occurs in a given cell and year, based on the GTD dataset. In each column, the treatment group is restricted to the wildlife referenced in the title. Coefficients are reported with spatially clustered standard errors (in parentheses), which allow for spatial and temporal correlation within a 500 km radius of each cell's centroid. * significant at 10%; ** significant at 5%; *** significant at 1%.

Table B.3: Wildlife Trade Restrictions & Conflict: Difference-in-Differences One-by-One Estimates (GTD Conflict = 1 if any event)

	Dependent Variable: GTD Conflict (0/1)							
Panel A: Wild Animals								
	Crocodile	Asian Elephant	African Elephant	Rhino	Hippo	Pangolin	Abalone	
$Habitat \times Post_1$	0.0022***	−0.0006	0.0312***	−0.0011	0.0042*	0.0030	0.0120	
	(0.0010)	(0.0021)	(0.0071)	(0.0013)	(0.0024)	(0.0052)	(0.0254)	
$Habitat \times Post_2$	0.0095***	0.0371***	0.0219***	0.0106	0.0025	0.0322***	−0.0628	
	(0.0023)	(0.0098)	(0.0073)	(0.0090)	(0.0032)	(0.0111)	(0.0149)	
Cell FE	Y	Y	Y	Y	Y	Y	Y	
Country-Year FE	Y	Y	Y	Y	Y	Y	Y	
Observations	5,014,880	5,014,880	5,014,880	5,014,880	5,014,880	5,014,880	5,014,880	
Panel B: Wild Luxury Trees								
	S. Humilis	P. Elata	D. Nigra	Prunus	S. Mahagon	S. Macro	Agra	Aniba
$Habitat \times Post_1$	0.040***	0.0085	0.0032	0.0401***	0.0220	0.0156*	0.0166*	0.0010
	(0.0148)	(0.0097)	(0.0033)	(0.0113)	(0.0150)	(0.0091)	(0.0120)	(0.0027)
$Habitat \times Post_2$	0.0321***	0.0096	−0.0066	0.0209***	0.0098	0.0005	0.0417***	−0.0005
	(0.0121)	(0.0171)	(0.0042)	(0.0115)	(0.0137)	(0.0089)	(0.0140)	(0.0087)
Cell FE	Y	Y	Y	Y	Y	Y	Y	Y
Country-Year FE	Y	Y	Y	Y	Y	Y	Y	Y
Observations	5,014,880	5,014,880	5,014,880	5,014,880	5,014,880	5,014,880	5,014,880	5,014,880
Panel C: Wild Luxury & Industrial Trees								
	Diospyros	Pterocarpus	Dalbergia	Abies	Araucaria	Fitzr	Pilger	
$Habitat \times Post_1$	0.0017	0.0176***	0.0212***	0.0102	0.0248***	0.0013	−0.0127*	
	(0.0019)	(0.0046)	(0.0032)	(0.0104)	(0.0101)	(0.0106)	(0.0073)	
$Habitat \times Post_2$	0.0103***	0.0121***	0.0091***	0.0119	0.0201*	0.0054	−0.0178	
	(0.0021)	(0.0049)	(0.0030)	(0.0157)	(0.0118)	(0.0087)	(0.0118)	
Cell FE	Y	Y	Y	Y	Y	Y	Y	
Country-Year FE	Y	Y	Y	Y	Y	Y	Y	
Observations	5,014,880	5,014,880	5,014,880	5,014,880	5,014,880	5,014,880	5,014,880	
Panel D: Wild Industrial Trees								
	P. Parlatorei	Guaiacum	Gonystylus	Taxus	Gonopter	Fraxinus	Cedrela	
$Habitat \times Post_1$	−0.0105	−0.0016	0.0105	−0.009*	−0.0058	0.0024	−0.0163***	
	(0.0126)	(0.0055)	(0.0177)	(0.0049)	(0.0043)	(0.0029)	(0.0052)	
$Habitat \times Post_2$	−0.0447	0.0013	0.0168	−0.0017	−0.0082	0.0002	−0.0041	
	(0.0254)	(0.0058)	(0.0191)	(0.0025)	(0.0048)	(0.0018)	(0.0048)	
Cell FE	Y	Y	Y	Y	Y	Y	Y	
Country-Year FE	Y	Y	Y	Y	Y	Y	Y	
Observations	5,014,880	5,014,880	5,014,880	5,014,880	5,014,880	5,014,880	5,014,880	

Notes: The table reports LPM estimates using difference-in-differences. Each observation corresponds to a cell-year. The variable $Habitat$ is an indicator measuring the suitability of cell k for wildlife species w, and $Post_1$ indicates the three years following the imposition of CITES trade restrictions on wildlife species w. $Post_2$ indicates all subsequent periods, capturing the average long-term effect of the policy on conflicts. The dependent variable is a binary indicator for conflict incidence, equal to one if at least one conflict event occurs in a given cell and year, based on the GTD conflict dataset. Panel A reports estimates for wild animals, whereas the other panels report estimates for different tree species. Coefficients are reported with spatially clustered standard errors (in parentheses), which allow for spatial and temporal correlation within a 500 km radius of each cell's centroid. * significant at 10%; ** significant at 5%; *** significant at 1%.

Wildlife Trade Restrictions and Conflicts: One by One Long Difference Estimates

Suggestive Evidence on Ivory Demand Elasticity

Table B.4: Elephant Ivory Elasticity Analysis Based on Pre-Ban Imports to Japan and Hong Kong: 2SLS

	log(Ivory Revenue)	*log(Ivory Quantity)*
	(1)	(2)
Panel A: 2SLS		
Coefficient	1.3455***	0.3455
Panel B: First Stage		
Policy → Price	1.4556***	1.4556***
F-statistic	24.8	24.8
Panel C: Reduced Form		
Coefficient	1.9585***	0.5029
Panel D: OLS		
Coefficient	1.3246***	0.3246
Country Fixed Effects	Y	Y
Observations	70	70

Notes: The table provides empirical evidence suggesting that the demand for ivory is price-inelastic, based on pre-ban import data from Hong Kong and Japan. Panel A presents 2SLS estimates, using policy shocks as instruments, with the unit of observation being the log of total value and the log of total weight of imported ivory. Specifications include country fixed effects. Panel B shows the first-stage estimates and the F-statistic. Panel C reports the reduced-form estimates, and Panel D shows the OLS results. All standard errors are Newey-West to account for serial correlation. * significant at 10%; ** significant at 5%; *** significant at 1%.

Suggestive Evidence of Substitution between Elephant and Hippo Ivory

Figure B.1: Substitution of Elephant Ivory to Hippo Ivory

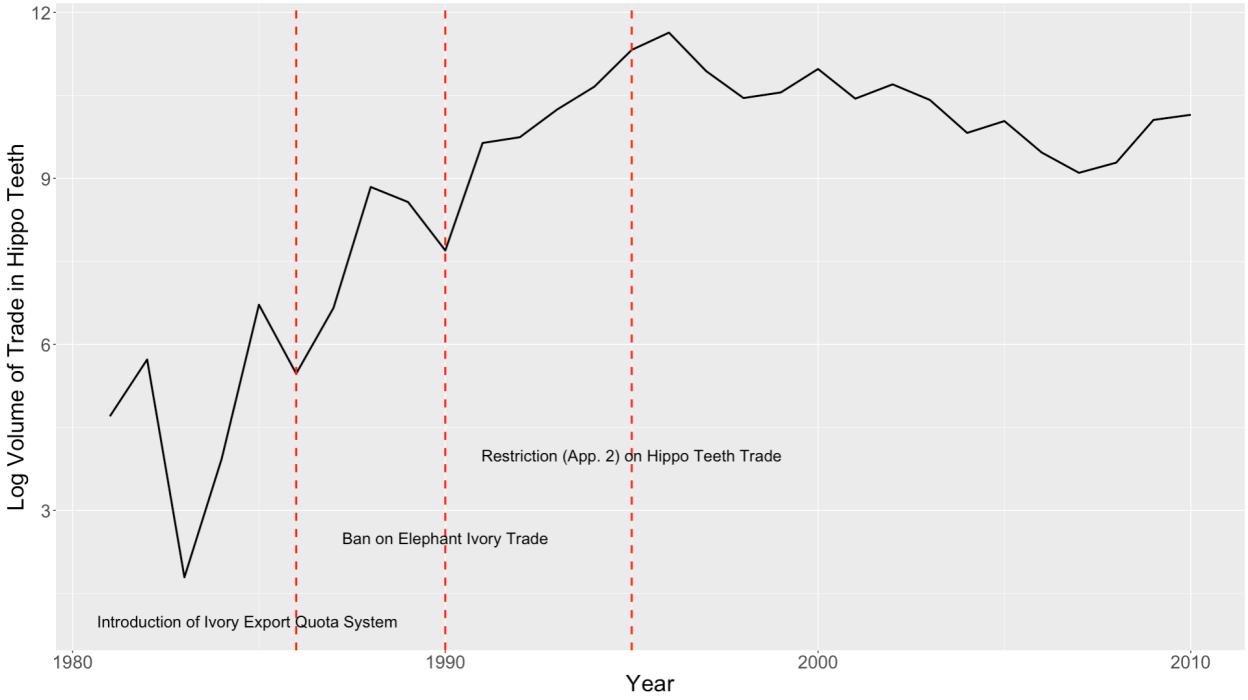

Notes: The figure shows the overall (log) export of hippo teeth from African countries to the rest of the world, measured in tonnes. The three vertical lines indicate different policy shocks. The first line marks the introduction of the ivory export quota system in 1984–1985. The second line marks the ban (Appendix I) on international trade in ivory in 1989. The third red line marks CITES's restriction on international trade in hippo teeth (Appendix II).

Suggestive Evidence of Conflict Substitution between Elephant Ivory and Industrial Minerals

Table B.5: Substitution between Ivory and Mineral Related Conflict Events in Africa

	ACLED Incident Indicator (1–3)			ACLED Onset Indicator (4–6)		
	(1)	(2)	(3)	(4)	(5)	(6)
Sales × Elephant Cell	−0.023***	−0.015***	−0.015***	−0.012***	−0.009***	−0.009***
	(0.009)	(0.006)	(0.006)	(0.006)	(0.005)	(0.005)
Sales × Distance Mine–Elephant	0.005***	0.003***	0.003***	0.002***	0.001***	0.001***
	(0.001)	(0.001)	(0.001)	(0.001)	(0.001)	(0.001)
p^{Ivory} × Elephant Cell		0.008***	0.016***		0.003	0.007
		(0.005)	(0.006)		(0.003)	(0.004)
p^{Ivory} × Elephant Around Cell			0.017***			0.008***
			(0.006)			(0.004)
p^{Mine} × Mine Cell		0.042***	0.037***		0.023***	0.020***
		(0.006)	(0.007)		(0.004)	(0.004)
p^{Mine} × Mine Around Cell			0.012***			0.007***
			(0.005)			(0.002)
Mean Dep. Var.	0.0788	0.0788	0.0788	0.0451	0.0451	0.0451
SD Dep. Var.	0.264	0.264	0.264	0.208	0.208	0.208
Cell FE	Y	Y	Y	Y	Y	Y
Country × Year FE	Y	Y	Y	Y	Y	Y
Observations	258,375	258,375	258,375	241,232	241,232	241,232

Notes: The table presents estimates showing substitution by armed groups between industrial minerals and ivory. Outcome variables measure conflict at the cell-year level. Columns 1–3 use an indicator for conflict incidents; columns 4–6 use an indicator for conflict onset. Columns 2 and 5 control for elephant ivory and industrial mineral price shocks (Berman et al., 2017); columns 3 and 6 additionally control for neighbouring areas of elephant habitat and industrial minerals. All specifications include interactions of supply shocks with elephant habitat and a negative distance measure between mining and elephant cells. All models include cell and country-year fixed effects. Standardised coefficients are reported with spatially clustered standard errors (in parentheses), which allow for spatial and temporal correlation within a 500 km radius of each cell's centroid. * significant at 10%; ** significant at 5%; *** significant at 1%.

Figure B.2: Share of Large Confiscations over Time

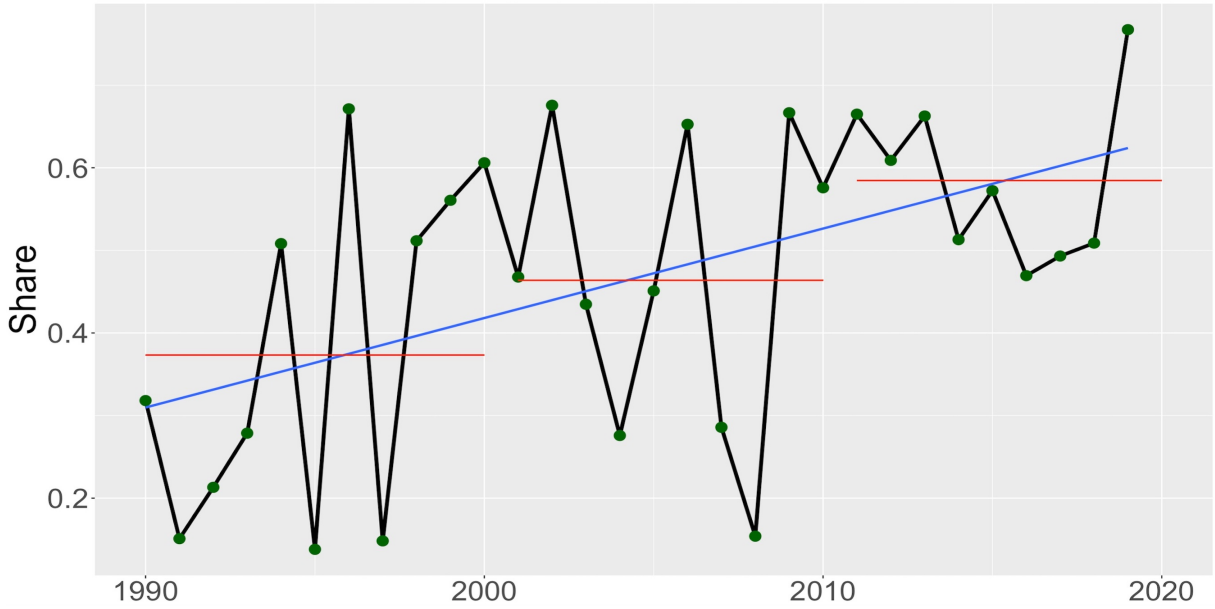

Notes: The figure depicts the share of large ivory confiscations (above 0.5 tonnes) from the total amount of confiscations at the annual level. The blue line indicates the relationship between the share and time, and the red horizontal lines indicate decade-level averages.

C Complementary Result Tables

This section presents supplementary tables that support the main results of the paper. Table C.1 reports difference-in-differences estimates for the confiscation analysis, Table C.2 shows difference-in-differences policy-price estimates, Table C.4 reports difference-in-differences policy-conflict estimates for high and low capacity states, and Table C.3 reports precious trees harvested quantities synthetic control estimates. Figure C.1 presents event-study estimates for the distance analysis, complementing Table 3.

Table C.1: Trade Restrictions and Wildlife Confiscations

	Dep. Var.: log(# Confiscation Events)		
	(1)	(2)	(3)
Habitat × *Policy*	1.6556***	0.7512**	0.6923***
	(0.2216)	(0.34752)	(0.21442)
Resource FE	Y	N	Y
Year FE	N	Y	Y
Observations	52	52	52

Note: The table reports difference-in-differences estimates for the effect of CITES trade restrictions on wildlife confiscations (*Diospyros* (ebonies), *Dalbergia* (rosewood), and elephant ivory). Standard errors are Newey-West, allowing for infinite-order serial correlation. * significant at 10%; ** significant at 5%; *** significant at 1%.

Table C.2: Trade Restrictions and Wildlife Prices: Difference-in-Differences

	Dep. Var.: Log Prices					
	Wild Animals			Wild Trees		
	(1)	(2)	(3)	(4)	(5)	(6)
$Wildlife \times Policy$	0.582***	1.806***	1.117***	0.125***	1.367***	1.030***
	(0.167)	(0.393)	(0.162)	(0.131)	(0.238)	(0.124)
Resource FE	N	Y	Y	N	Y	Y
Year FE	Y	N	Y	Y	N	Y
Observations	386	386	386	549	549	549

Notes: The table reports estimates using the Borusyak et al. (2024) imputation difference-in-differences estimator. Each observation corresponds to a resource-year (wildlife, and World Bank timber or precious metals prices as controls). $Wildlife \times Policy$ is an interaction of wildlife w with its corresponding policy indicator, indicating the timing of CITES trade restrictions imposed on wildlife w. The control group for wild animals is precious metals (gold, silver, and platinum), and for wild precious trees it is the World Bank hard tropical timber index. Standard errors are Newey-West, allowing for infinite serial correlation. * significant at 10%; ** significant at 5%; *** significant at 1%.

Table C.3: Trade Restrictions and the Harvesting of Precious Trees by State Capacity: A Synthetic Difference-in-Differences Analysis

	Dep. Var.: log(deforestation + 1)		
	Aggregate	High Capacity	Low Capacity
	(1)	(2)	(3)
$Habitat \times Policy$	−0.0058**	−0.097***	0.055**
	(0.008)	(0.031)	(0.025)
Cell FE	Y	Y	Y
Country-Year FE	Y	Y	Y
Observations	1,304,314	523,016	781,298
Dep. Var. Mean	2.13	1.762	2.31
Dep. Var. SD	1.899	1.852	1.896

Note: The table reports synthetic control difference-in-differences estimates using the Ben-Michael et al. (2021) estimator. Each observation corresponds to a cell-year. The variable $Habitat$ is an indicator measuring the suitability of cell k for wild tree species w, and $Policy$ indicates the timing of CITES trade restrictions imposed on wildlife species w at time t. The dependent variable is the annual log of deforested 30×30 cells within a larger $0.1° \times 0.1°$ cell. The sample is restricted to African countries, with column 1 showing aggregate quantities, column 2 showing estimates restricted to above-median-capacity states, and column 3 showing estimates restricted to below-median-capacity states. Coefficients are reported with standard errors which are computed using the wild bootstrap, following the procedure for synthetic control estimators in Ben-Michael et al. (2021).* significant at 10%; ** significant at 5%; *** significant at 1%.

Table C.4: Wild Trees, Trade Restrictions and Conflict Likelihood by State Capacity: Difference-in-Differences

	Dep. Var.: Conflict (0/1)					
	High Capacity			Low Capacity		
	ACLED	UCDP	GTD	ACLED	UCDP	GTD
	(1)	(2)	(3)	(4)	(5)	(6)
Habitat × *Policy*	0.0015	−0.0061	0.0054*	0.0331***	0.0163***	0.0264***
	(0.0036)	(0.0036)	(0.0030)	(0.0069)	(0.0063)	(0.0057)
Cell FE	Y	Y	Y	Y	Y	Y
Country-Year FE	Y	Y	Y	Y	Y	Y
Observations	131,663	166,342	250,741	191,137	242,541	367,459
Dep. Var. Mean	0.0199	0.0135	0.0075	0.0516	0.0337	0.0114
Dep. Var. SD	0.1398	0.1154	0.0862	0.2212	0.1805	0.1062

Notes: The table reports LPM estimates using the Borusyak et al. (2024) imputation difference-in-differences estimator. Each observation corresponds to a cell-year. The variable *Habitat* is an indicator measuring the suitability of cell k for wildlife species w, and *Policy* indicates the timing of CITES trade restrictions imposed on wildlife species w at time t. The dependent variable is a binary indicator for conflict incidence, equal to one if at least one conflict event occurs in a given cell and year, based on the conflict datasets referenced in the column title. The sample is restricted to African countries, where columns 1–3 are associated with above-median capacity states, and columns 4–6 are associated with below-median capacity states. Coefficients are reported with spatially clustered standard errors (in parentheses), which allow for spatial and temporal correlation within a 500 km radius of each cell's centroid. * significant at 10%; ** significant at 5%; *** significant at 1%.

Table C.5: Wild Trees, Trade Restrictions and Conflict Likelihood: Difference-in-Differences

	Dep. Var.: Conflict (0/1)		
	Wild Trees: Africa Sample		
	ACLED	UCDP	GTD
	(1)	(2)	(3)
$Habitat \times Policy$	0.053***	0.0091	0.0233***
	(0.0063)	(0.0054)	(0.00459)
Cell FE	Y	Y	Y
Country-Year FE	Y	Y	Y
Observations	343,952	429,940	638,768
Dep. Var. Mean	0.0789	0.0338	0.0133
Dep. Var. SD	0.26	0.1808	0.1145

Notes: The table reports linear probability model (LPM) estimates using the imputation-based difference-in-differences estimator of Borusyak et al. (2024), with treatment defined as the imposition of CITES trade restrictions on species, covering only wild trees in Africa. Each observation corresponds to a cell-year. The variable $Habitat$ is an indicator measuring the suitability of cell k for wildlife species w, and $Policy$ indicates the timing of CITES trade restrictions imposed on wildlife species w at time t. The dependent variable is a binary indicator for conflict incidence, equal to one if at least one conflict event occurs in a given cell and year, based on the conflict datasets referenced in the column title. Coefficients are reported with spatially clustered standard errors (in parentheses), which allow for spatial and temporal correlation within a 500 km radius of each cell's centroid. Standard errors reported in square brackets are clustered at the country-year and cell levels, allowing for within-country spatial correlation and infinite serial correlation within a cell. * significant at 10%; ** significant at 5%; *** significant at 1%.

Figure C.1: Distance Analysis Event Study for Rosewood 2016 Ban

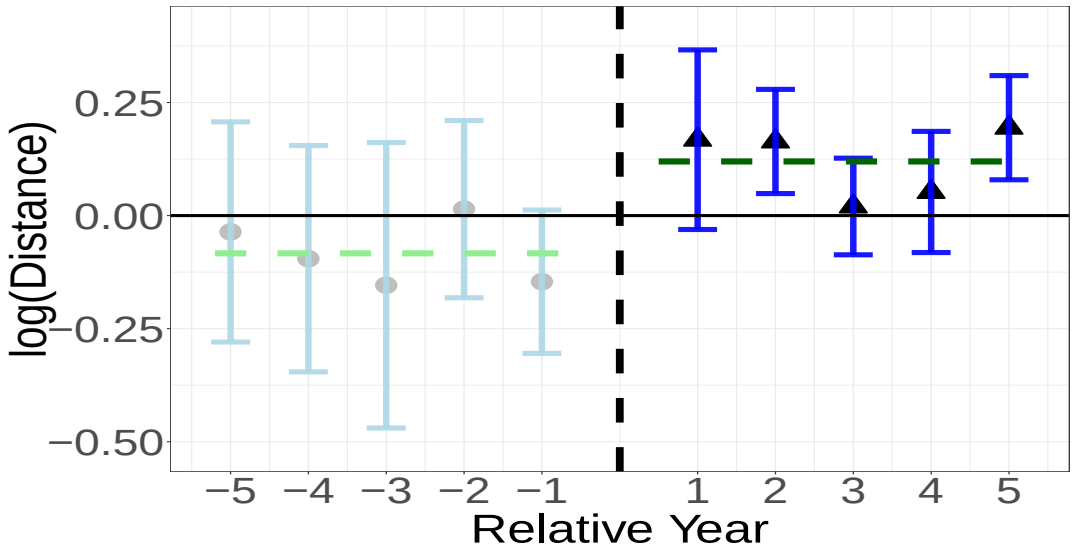

Notes: The figure reports a two-way fixed effects event study estimate with log distance as the outcome, presenting the estimates for rosewood. The omitted period is the year prior to the policy announcement (2015). The green horizontal lines indicate the average of the pre- or post-treatment coefficients. Error bars denote 95% confidence intervals, based on two-way clustered standard errors at the group and country-year levels.

D Sensitivity Checks

This section discusses alternative specifications and assesses the robustness of the paper's main estimates.

Predictive Power of Wildlife Habitat on Country-Level Stocks

One concern with the identification strategy based on wildlife habitat classification,

One concern with identification that relies on habitat data is whether these measures predict observed wildlife abundance. Unfortunately, granular data on wildlife stocks is unavailable. Table D.1 examines whether the country-level count of habitat-suitable grid cells predicts country-level wildlife stocks for the four species with available stock data. The estimates indicate that habitat suitability is a strong predictor of stock.

Table D.1: Wildlife Habitat and Country-Level Wildlife Stock

	Dep. Var.: Log (Country-Level Stocks + 1)			
	Diospyros	Dalbergia	Pterocarpus	Elephant
	(1)	(2)	(3)	(4)
log (# Diospyros cells + 1)	0.0134***			
	(0.0026)			
log (# Dalbergia cells + 1)		0.0297***		
		(0.0047)		
log (# Pterocarpus cells + 1)			0.0485[a]	
			(0.0038)	
log (# Elephant cells + 1)				0.0428***
				(0.0031)
Constant	1.9706***	1.8719***	1.0281***	0.8199***
	(0.2012)	(0.2160)	(0.1447)	(0.1922)
Observations	50	50	50	35
R^2	0.3563	0.4529	0.7748	0.5242
Adjusted R^2	0.3429	0.4415	0.7701	0.5215

Notes: The table reports OLS estimates showing the correlation of the log number of cells per country suitable for wildlife species w (based on a binary variable), with the country-level stock of that resource. * significant at 10%; ** significant at 5%; *** significant at 1%.

Exogeneity of Policy

Another identification concern is the exogeneity of the policy with respect to conflicts. Given the way it operates, it is unlikely that CITES intentionally targets conflict regions or specific conflict events in its policies. First, CITES decisions are largely political and require a 66% majority. Second, Frank and Wilcove (2019) documents an average delay of 10 years between species extinction and the imposition of CITES trade restrictions. Third, CITES meets every three years based on a pre-determined schedule. Fourth, a text analysis of CITES protocols reveals no explicit mention of armed conflict or armed groups in official meeting records. Taken together, these institutional features make the assumption of quasi-exogenous policy timing plausible. Furthermore, Figure D.1 shows an anticipation test, where shifting the policy six periods earlier yields insignificant

estimates. To further address concerns about policy endogeneity, Figures D.2 and D.3 confirm that the estimates remain robust when iteratively excluding different continental subregions, or random batches of 10% of the observations, reducing concerns that CITES systematically targets conflict-prone regions.

Figure D.1: Anticipation Test: Wildlife Trade Restrictions and Conflict Likelihood

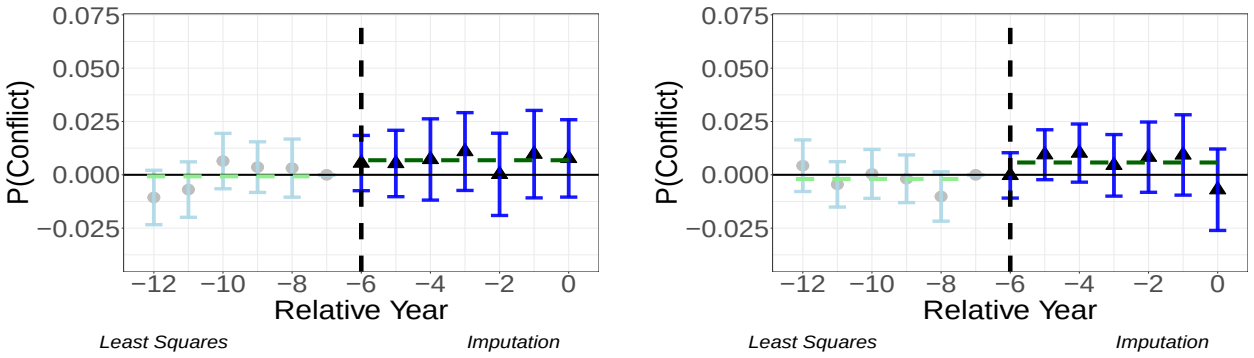

(a) High State Capacity **(b)** Low State Capacity

Notes: The figure reports a placebo anticipation test using the staggered event-study imputation estimator of Borusyak et al. (2024), where the actual treatment is artificially shifted six periods earlier. Pre-treatment coefficients are estimated using least squares, while post-treatment coefficients are obtained with the imputation estimator. Each observation corresponds to a cell-year (1,430,970 for wild animals and 1,435,230 for wild trees). The estimates follow equation (1), where the interaction term $Habitat \times Policy$ captures the effect of the policy on conflict probability. The dependent variable is a binary indicator equal to one if at least one conflict event occurs in a cell-year, based on ACLED data. The green horizontal lines indicate the average of the pre- or post-treatment coefficients. Error bars show 95% confidence intervals, with standard errors spatially clustered within a 500 km radius of each cell's centroid. A joint significance F-test yields p-values of 0.688 for animals (Panel a) and 0.284 for trees (Panel b).

Figure D.2: Wildlife Trade Restrictions and Conflict Likelihood: Sequential Exclusion of Subregions

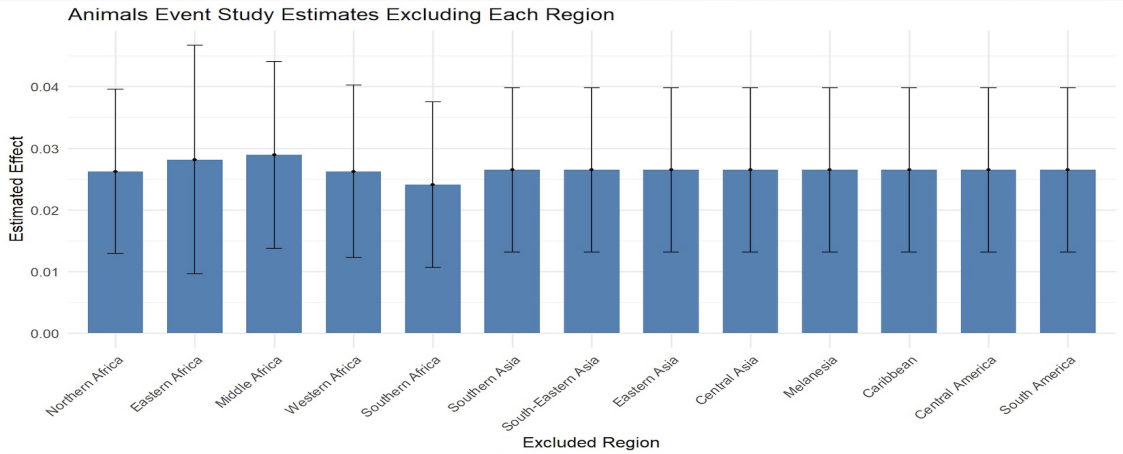

(a) Wild Animals

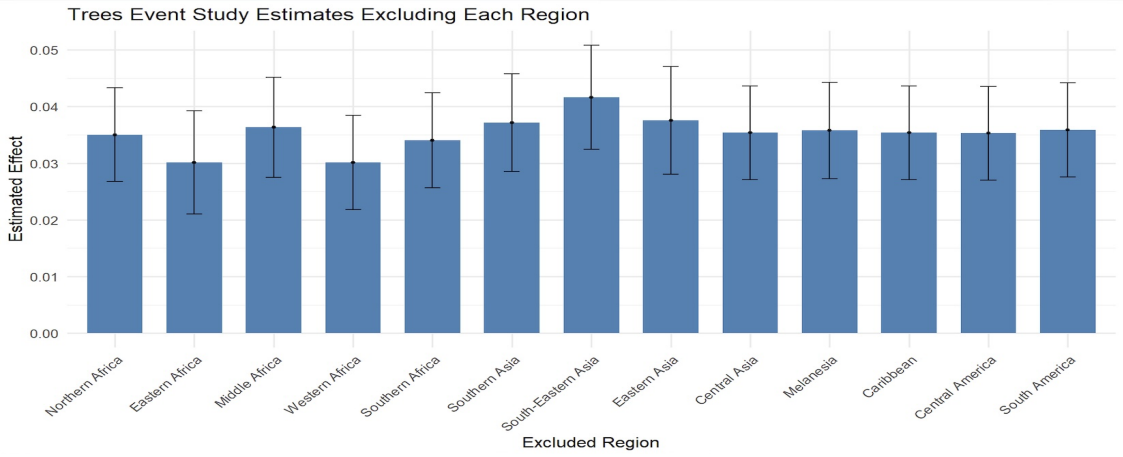

(b) Wild Precious Trees

Notes: The figure reports LPM estimates using the staggered event study imputation estimator (Borusyak et al., 2024). Each bar reports a point estimate, excluding one sub-continental region at a time. Each observation corresponds to a cell-year. The estimates are based on specification 1, with the interaction term $Habitat \times Policy$, an indicator explaining conflict probability. The omitted period is the year prior to the policy announcement. The dependent variable is a binary indicator for conflict incidence, equal to one if at least one conflict event occurs in a given cell and year, based on the ACLED dataset. Error bars indicate 95% confidence intervals, with standard errors that are spatially clustered to allow for spatial and temporal correlation within a 500 km radius of each cell's centroid.

Figure D.3: Wildlife Trade Restrictions and Conflict Likelihood: Excluding Random Batches of Pixels (10% at the time)

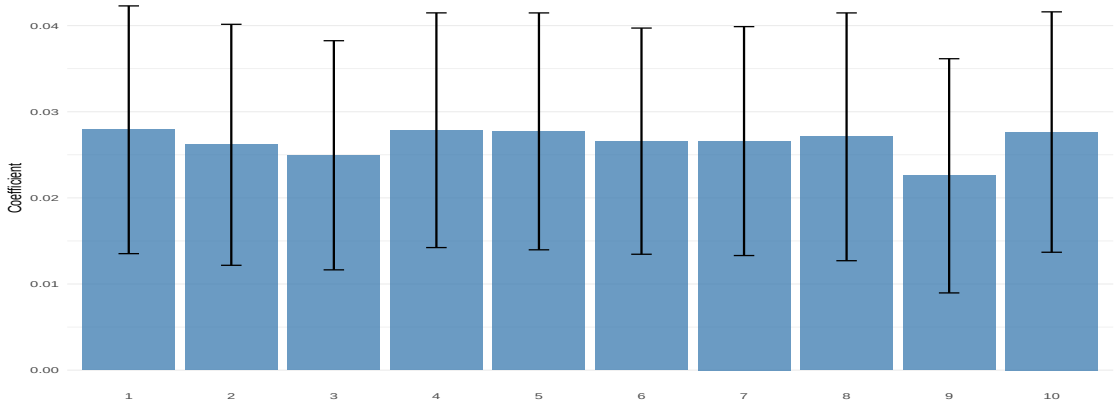

(a) Wild Animals

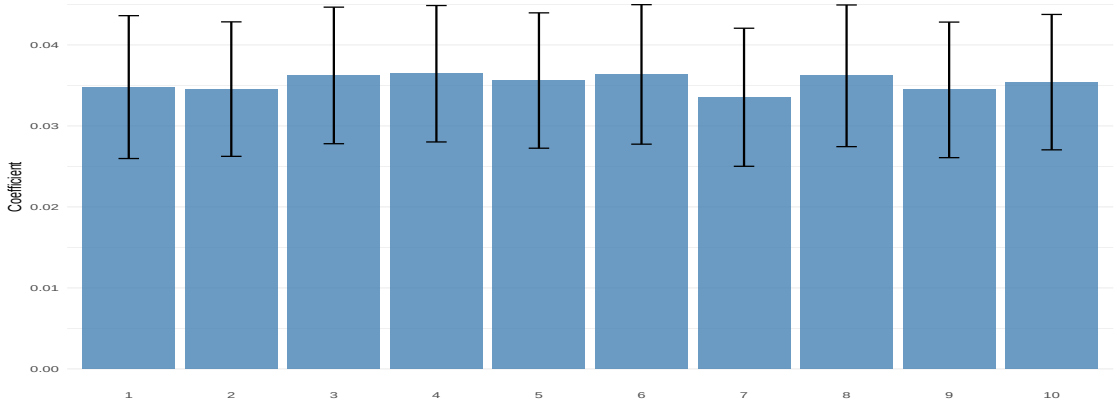

(b) Wild Precious Trees

Notes: The figure reports LPM estimates using the staggered event study imputation estimator (Borusyak et al., 2024). Each bar shows a point estimate based on the sample with 10% of the observations randomly excluded. Each observation corresponds to a cell-year. The estimates are based on specification 1, with the interaction term $Habitat \times Policy$, an indicator explaining conflict probability. The omitted period is the year prior to the policy announcement. The dependent variable is a binary indicator for conflict incidence, equal to one if at least one conflict event occurs in a given cell and year, based on the ACLED dataset. Error bars indicate 95% confidence intervals, with standard errors that are spatially clustered to allow for spatial and temporal correlation within a 500 km radius of each cell's centroid.

Measurement Error and Sensitivity to Cell-Size

Another concern when using wildlife habitat as a proxy for treatment exposure is the potential for measurement error. Table D.2 reports country-level shift-share style estimates. For each country I sum the total number of cells suitable for a given wildlife, and multiply it by the post-policy years for this wildlife. I then sum this variable across country-year to create a wildlife-weighted country-year level exposure to the policy, and due to the skewness of the distribution, take its log. The outcome variable is country-year log conflict events. Furthermore, to mitigate concerns regarding grid choice, I construct alternative grids, with $0.25° \times 0.25°$ and $1° \times 1°$ degree size. Tables D.3 and D.4 report

estimates, consistent with the paper's main results.

Table D.2: Wildlife Trade Restrictions and Conflict Events: Country-Level Estimates

	Dep. Var.: log (# Country-Year Conflict Events + 1)					
	Wild Animals			Wild Trees		
	ACLED	UCDP	GTD	ACLED	UCDP	GTD
log (*Policy Exposure* + 1)	0.4533**	0.2229*	0.16359***	0.4362***	0.5172**	0.4695**
	(0.0419)	(0.1285)	(0.0419)	(0.1228)	(0.2065)	(0.1790)
Country FE	Y	Y	Y	Y	Y	Y
Subcontinent Region Year FE	Y	Y	Y	Y	Y	Y
Mean Dep. Var.	1.9861	1.0345	0.7624	1.9861	1.0345	0.7624
SD Dep. Var.	1.5140	1.3993	1.1307	1.5140	1.3993	1.1307
Observations	2,024	3,710	5,512	2,024	3,710	5,512

Notes: The table reports LPM estimates using OLS. Each observation corresponds to a country-year. The variable *Policy Exposure* ranks countries by their total, wildlife-weighted annual exposure to the policy. The outcome is the log number of conflict events in a given country-year, based on the conflict dataset mentioned in the title. Coefficients are reported with two-way clustered standard errors (in parentheses), clustered at the levels of the fixed effects. * significant at 10%; ** significant at 5%; *** significant at 1%.

Table D.3: Wildlife Trade Restrictions and Conflict Likelihood at $0.25° \times 0.25°$ Resolution

	Dep. Var.: Conflict (0/1)					
	Wild Animals			Wild Trees		
	ACLED	UCDP	GTD	ACLED	UCDP	GTD
	(1)	(2)	(3)	(4)	(5)	(6)
Habitat × *Policy*	0.0204***	0.0099***	0.0116***	0.0272***	0.0063***	0.0107***
	(0.0053)	(0.0036)	(0.0031)	(0.0033)	(0.0022)	(0.0018)
Cell FE	Y	Y	Y	Y	Y	Y
Country-Year FE	Y	Y	Y	Y	Y	Y
Observations	5,723,880	13,355,720	19,842,784	5,740,920	13,395,480	19,901,856
Dep. Var. Mean	0.0583	0.0233	0.0134	0.0583	0.0233	0.0134
Dep. Var. SD	0.2037	0.1318	0.1005	0.2037	0.1318	0.1005

Notes: The table reports LPM estimates using the Borusyak et al. (2024) imputation difference-in-differences estimator. Each observation corresponds to a cell-year, with $0.25° \times 0.25°$ cell-size. The variable *Habitat* is an indicator measuring the suitability of cell k for wildlife species w, and *Policy* indicates the timing of CITES trade restrictions imposed on wildlife w at time t. The dependent variable is a binary indicator for conflict incidence, equal to one if at least one conflict event occurs in a given cell and year, based on the conflict datasets referenced in the column title. Coefficients are reported with spatially clustered standard errors (in parentheses), which allow for spatial and temporal correlation within a 500 km radius of each cell's centroid. * significant at 10%; ** significant at 5%; *** significant at 1%.

Table D.4: Wildlife Trade Restrictions and Conflict Likelihood at 1° × 1° Resolution

	Dep. Var.: Conflict (0/1)					
	Wild Animals			Wild Trees		
	ACLED	UCDP	GTD	ACLED	UCDP	GTD
	(1)	(2)	(3)	(4)	(5)	(6)
Habitat × *Policy*	0.0358***	0.0174***	0.0204***	0.0478***	0.0111***	0.0188***
	(0.0092)	(0.0063)	(0.0054)	(0.0057)	(0.0039)	(0.0031)
Cell FE	Y	Y	Y	Y	Y	Y
Country-Year FE	Y	Y	Y	Y	Y	Y
Observations	357,742	834,732	1,240,174	358,807	837,217	1,243,866
Dep. Var. Mean	0.1022	0.0408	0.0234	0.1022	0.0408	0.0234
Dep. Var. SD	0.3571	0.2311	0.1763	0.3571	0.2311	0.1763

Notes: The table reports LPM estimates using the Borusyak et al. (2024) imputation difference-in-differences estimator. Each observation corresponds to a cell-year, with 1° × 1° cell-size. The variable *Habitat* is an indicator measuring the suitability of cell k for wildlife species w, and *Policy* indicates the timing of CITES trade restrictions imposed on wildlife w at time t. The dependent variable is a binary indicator for conflict incidence, equal to one if at least one conflict event occurs in a given cell and year, based on the conflict datasets referenced in the column title. Coefficients are reported with spatially clustered standard errors (in parentheses), which allow for spatial and temporal correlation within a 500 km radius of each cell's centroid. * significant at 10%; ** significant at 5%; *** significant at 1%.

Potential Confounders

Given the broad spatial distribution of wildlife habitat, a potential concern is that it may overlap with other valuable resources—such as gold, minerals, or crops—thereby confounding the estimates. To address this, I exclude all cells geologically suitable for gold production (Girard et al., 2022), as well as those with precious mineral deposits and surrounding areas (Berman et al., 2017).[30] To further mitigate concerns about spatial confounders, I divide the sample into above- and below-median groups based on urban area coverage, crop production, human footprint, and population density, and replicate the difference in differences ACLED estimates within each subsample. Following Eberle et al. (2020), I also exclude all Sahel countries. Estimates are presented in Table D.5. While coefficient magnitudes vary—likely due to reduced sample sizes—the results remain robust across all specifications.

[30] Although the geological suitability map from Girard et al. (2022) is specific to gold, it covers approximately 43% of African grid cells and likely captures other artisanal mining zones as well.

Table D.5: Wildlife Trade Restrictions and Conflict Likelihood: Excluding Potential Confounders

	Dep. Var.: ACLED Conflict (0/1)									
	Built		Crop		Human Footprint		Pop		Gold & Sahel	
	High	Low	High	Low	High	Low	High	Low	Gold	Sahel
	(1)	(2)	(3)	(4)	(5)	(6)	(7)	(8)	(9)	(10)
Panel A: Wild Animals										
Habitat × *Policy*	0.0282***	0.0222***	0.0213***	0.0212**	0.0195**	0.0273***	0.0330***	0.0230***	0.0281***	0.0211***
	(0.0096)	(0.0088)	(0.0077)	(0.0112)	(0.0083)	(0.0095)	(0.0160)	(0.0072)	(0.0088)	(0.0072)
Panel B: Wild Trees										
Habitat × *Policy*	0.0204***	0.0398***	0.0305***	0.0297***	0.0205***	0.0299***	0.0267***	0.0466***	0.0312***	0.0271***
	(0.0049)	(0.0057)	(0.0048)	(0.0058)	(0.0080)	(0.0092)	(0.0047)	(0.0075)	(0.0043)	(0.0042)
Cell FE	Y	Y	Y	Y	Y	Y	Y	Y	Y	Y
Country-Year FE	Y	Y	Y	Y	Y	Y	Y	Y	Y	Y
Observations	261,397	309,042	276,535	299,357	284,670	291,222	241,265	320,450	451,572	436,984
Dep. Var. Mean	0.1142	0.0440	0.1100	0.0441	0.1130	0.0393	0.0936	0.0602	0.0663	0.0792
Dep. Var. SD	0.3180	0.2051	0.3129	0.2052	0.3166	0.1943	0.2912	0.0602	0.2488	0.2701

Note: The table reports LPM estimates using OLS. Each observation corresponds to a cell-year. Each column splits the sample into above- or below-median groups based on the variable indicated in the title. The variable *Habitat* is an indicator measuring the suitability of cell k for wildlife w, and *Policy* denotes the timing of CITES trade restrictions imposed on species w. The dependent variable is an ACLED binary indicator for conflict incidence, equal to one if at least one conflict event occurs in a given cell and year. Coefficients are reported with spatially clustered standard errors (in parentheses), which allow for spatial and infinite temporal correlation within a 500 km radius of each cell's centroid. * significant at 10%; ** significant at 5%; *** significant at 1%.

Different Control Groups

The global approach—essential for external validity and for capturing a broad range of resources and policy shocks—raises concerns about the adequacy of the control group. To address this, I estimate a staggered event study model using the augmented synthetic control estimator from Ben-Michael et al. (2021), which constructs control groups that exactly match the pre-treatment outcome trends of treated units (Figure D.4 and Table D.6). In Table D.7, I pool wild animals and wild trees, defining treatment as CITES restrictions on either category.

Figure D.4: Wildlife Trade Restrictions and Conflict Likelihood: A Synthetic Control Analysis

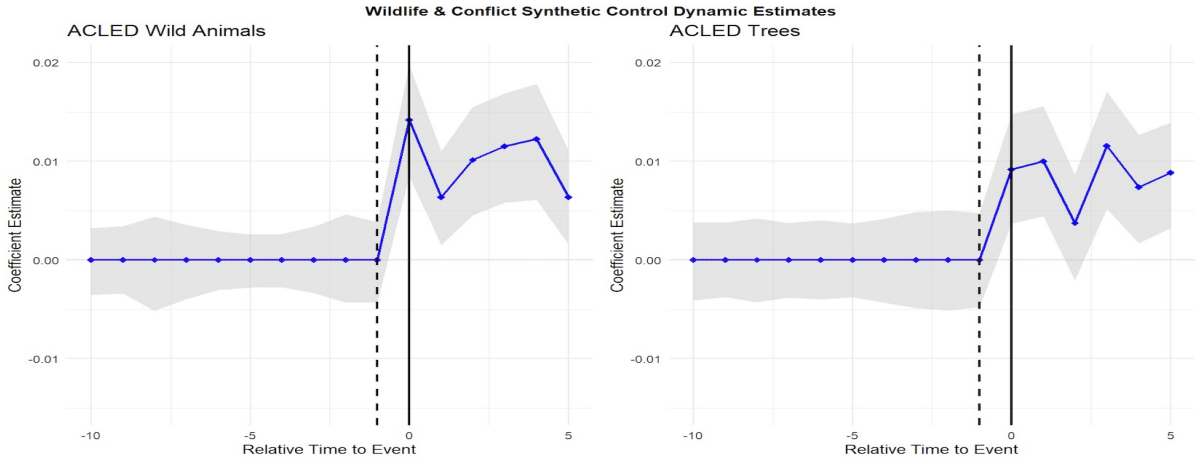

Notes: The figure depicts LPM estimates using the staggered event study synthetic control estimator from Ben-Michael et al. (2021). Each observation corresponds to a cell-year. The sample includes 1,430,970 observations for animals and 1,430,970 observations for trees. The estimates are based on specification 1, with the interaction term *Habitat* × *Policy*, an indicator explaining conflict probability. The dependent variable is a binary indicator for conflict incidence, equal to one if at least one conflict event occurs in a given cell and year, based on the ACLED dataset. Coefficients are reported with standard errors which are computed using the wild bootstrap, following the procedure for synthetic control estimators in Ben-Michael et al. (2021).

Table D.6: Wildlife Trade Restrictions and Conflict Likelihood: A Synthetic Difference in-Differences Analysis

	Dep. Var.: ACLED Conflict (0/1)	
	Wild Animals	Wild Trees
	(1)	(2)
Habitat × *Policy*	0.005***	0.008***
	(0.001)	(0.002)
Cell FE	Y	Y
Country-Year FE	Y	Y
Observations	1,430,970	1,430,970
Dep. Var. Mean	0.075	0.075
Dep. Var. SD	0.264	0.264

Notes: The figure reports LPM estimates using the staggered event study synthetic control estimator from Ben-Michael et al. (2021). Each observation corresponds to a cell-year. The estimates are based on specification 1, with the interaction term *Habitat* × *Policy* an indicator explaining conflict probability. The dependent variable is a binary indicator for conflict incidence, equal to one if at least one conflict event occurs in a given cell and year, based on the ACLED dataset. Coefficients are reported with standard errors which are computed using the wild bootstrap, following the procedure for synthetic control estimators in Ben-Michael et al. (2021). * significant at 10%; ** significant at 5%; *** significant at 1%.

Table D.7: Wildlife Trade Restrictions and Conflict Likelihood: Difference-in-Differences

	Dep. Var.: Conflict (0/1)		
	Wild Animals and Trees		
	ACLED	UCDP	GTD
	(1)	(2)	(3)
Habitat × *Policy*	0.0391***	0.01***	0.0137***
	(0.0040)	(0.0027)	(0.0028)
Cell FE	Y	Y	Y
Country-Year FE	Y	Y	Y
Observations	1,430,970	3,338,930	4,960,696
Dep. Var. Mean	0.0757	0.0302	0.0173
Dep. Var. SD	0.2645	0.1712	0.1306

Notes: The table reports linear probability model (LPM) estimates using the imputation-based difference-in-differences estimator of Borusyak et al. (2024), with treatment defined as the imposition of CITES trade restrictions on species, covering both wild animals and wild trees. Each observation corresponds to a cell-year. The variable *Habitat* is an indicator measuring the suitability of cell k for wildlife species w, and *Policy* indicates the timing of CITES trade restrictions imposed on wildlife species w at time t. The dependent variable is a binary indicator for conflict incidence, equal to one if at least one conflict event occurs in a given cell and year, based on the conflict datasets referenced in the column title. Coefficients are reported with spatially clustered standard errors (in parentheses), which allow for spatial and temporal correlation within a 500 km radius of each cell's centroid. Standard errors reported in square brackets are clustered at the country-year and cell levels, allowing for within-country spatial correlation and infinite serial correlation within a cell. * significant at 10%; ** significant at 5%; *** significant at 1%.

Sensitivity to Standard Errors Spatial Clustering

Figure D.5 plots the baseline estimates using different levels of spatial clustering, from $1° \times 1°$ to $10° \times 10°$ (110×110 km to $1{,}100 \times 1{,}100$ km at the equator), showing that the estimates are insensitive to the choice of spatial cluster size.

Figure D.5: Sensitivity of Estimates to Spatial Clustering

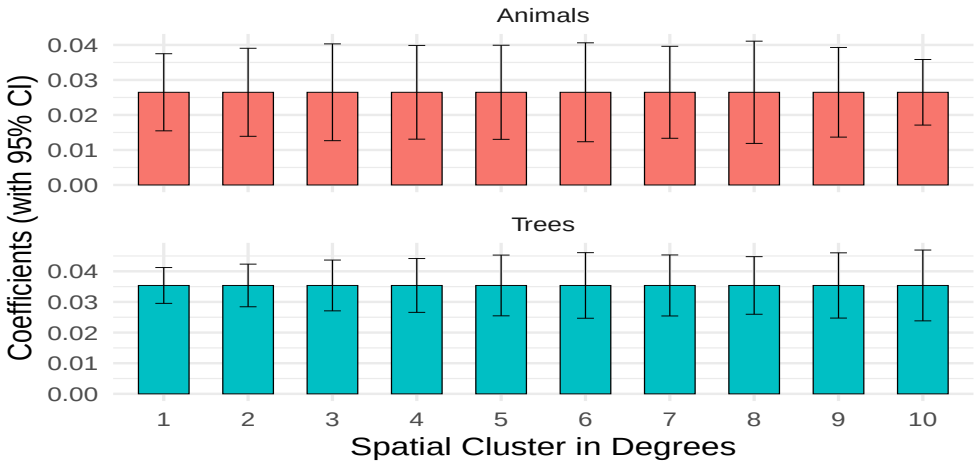

Notes: The figure shows estimated coefficients from equation (1) for spatial clusters at various degrees (1–10). The top panel reports estimates for animals, and the bottom panel reports estimates for trees. The main dependent variable is an ACLED conflict indicator, while the key explanatory variable is the interaction between the policy indicator and wildlife habitat suitability. The sample in all analyses is global.

Alternative Conflict Outcomes

Conflict measurement is complex and likely to suffer from measurement error. As such, the literature commonly uses a binary conflict indicator variable (Bazzi and Blattman, 2014; Berman et al., 2017; Ciccone, 2018). The UCDP and GTD conflict outcomes—owing to their narrower definitions—are likely to suffer less from measurement error and yield estimates consistent with those based on ACLED data. Tables D.8 and D.9 report estimates using alternative conflict outcomes, including the number of conflict events or deaths per cell-year, as well as conflict onset, defined as transitions from peace to war. These estimates remain consistent with the paper's main findings. Table D.10 reports estimates based on a binary indicator for conflict events with a number of deaths above the sample median for each dataset, showing results consistent with the baseline analysis.

Table D.8: Wildlife Trade Restrictions and the Number of Conflict Events

	Dep. Var.: log (# Conflict Events+1)					
	Wild Animals			Wild Precious Trees		
	ACLED	UCDP	GTD	ACLED	UCDP	GTD
	(1)	(2)	(3)	(4)	(5)	(6)
Habitat × *Policy*	0.0486***	0.0046***	0.0177***	0.0691***	0.0162***	0.0198***
	(0.0149)	(0.0105)	(0.0060)	(0.0084)	(0.0056)	(0.0043)
Cell FE	Y	Y	Y	Y	Y	Y
Country-Year FE	Y	Y	Y	Y	Y	Y
Observations	1,430,970	3,338,930	4,960,696	1,435,230	3,348,870	4,975,464
Dep. Var. Mean	0.0707	0.0406	0.0212	0.0707	0.0406	0.0212
Dep. Var. SD	0.385	0.273	0.1887	0.385	0.273	0.1887

Notes: The table reports LPM estimates using the Borusyak et al. (2024) imputation difference-in-differences estimator. Each observation corresponds to a cell-year. The variable *Habitat* is an indicator measuring the suitability of cell k for wildlife species w, and *Policy* indicates the timing of CITES trade restrictions imposed on wildlife w at time t. The dependent variable is log number of conflict events in a given cell-year, based on the conflict datasets referenced in the column title. Coefficients are reported with spatially clustered standard errors (in parentheses), which allow for spatial and temporal correlation within a 500 km radius of each cell's centroid. * significant at 10%; ** significant at 5%; *** significant at 1%.

Table D.9: Wildlife Trade Restrictions and the Onset of Conflict Events

	Dep. Var.: Conflict Onset (0/1)					
	Wild Animals			Wild Precious Trees		
	ACLED	UCDP	GTD	ACLED	UCDP	GTD
	(1)	(2)	(3)	(4)	(5)	(6)
Habitat × *Policy*	0.0112***	0.0065***	0.0056***	0.0206***	0.0025**	0.0070***
	(0.0041)	(0.0026)	(0.0016)	(0.0026)	(0.0013)	(0.0010)
Cell FE	Y	Y	Y	Y	Y	Y
Country-Year FE	Y	Y	Y	Y	Y	Y
Observations	1,430,970	3,338,930	4,960,696	1,435,230	3,348,870	4,975,464
Dep. Var. Mean	0.0453	0.0143	0.0088	0.0453	0.0143	0.0088
Dep. Var. SD	0.2081	0.1188	0.0935	0.2081	0.1188	0.0935

Notes: The table reports LPM estimates using the Borusyak et al. (2024) imputation difference-in-differences estimator. Each observation corresponds to a cell-year. The variable *Habitat* is an indicator measuring the suitability of cell k for wildlife species w, and *Policy* indicates the timing of CITES trade restrictions imposed on wildlife w at time t. The dependent variable is the onset of conflict events in a given cell and year, based on the conflict datasets referenced in the column title. Coefficients are reported with spatially clustered standard errors (in parentheses), which allow for spatial and temporal correlation within a 500 km radius of each cell's centroid. * significant at 10%; ** significant at 5%; *** significant at 1%.

Table D.10: Wildlife Trade Restrictions and Conflict Likelihood: Above Median Events

	Dep. Var.: Large Conflict Events (0/1)					
	Animals			Trees		
	ACLED	UCDP	GTD	ACLED	UCDP	GTD
	(1)	(2)	(3)	(4)	(5)	(6)
Habitat × *Policy*	0.02**	0.011**	0.015	0.024***	0.006	0.009***
	(0.007)	(0.05)	(0.009)	(0.08)	(0.004)	(0.003)
Cell FE	Y	Y	Y	Y	Y	Y
Country-Year FE	Y	Y	Y	Y	Y	Y
Observations	1,430,970	3,338,930	4,960,696	1,435,230	3,348,870	4,975,464
Dep. Var. Mean	0.036	0.02	0.01	0.036	0.02	0.01
Dep. Var. SD	0.21	0.16	0.13	0.21	0.16	0.13

Notes: The table reports LPM estimates using the Borusyak et al. (2024) imputation difference-in-differences estimator. Each observation corresponds to a cell-year. The variable *Habitat* is an indicator measuring the suitability of cell k for wildlife taxon w, and *Policy* indicates the timing of CITES trade restrictions imposed on wildlife taxon w at time t. The dependent variable is a binary indicator for conflict incidence, equal to one for events with above median death in a given cell and year, based on the conflict datasets referenced in the column title. Coefficients are reported with spatially clustered standard errors (in parentheses), which allow for spatial and temporal correlation within a 500 km radius of each cell's centroid. Standard errors reported in square brackets are clustered at the country-year and cell levels, allowing for within-country spatial correlation and infinite serial correlation within a cell. * significant at 10%; ** significant at 5%; *** significant at 1%.

Alternative Event-Study Estimators

Recent innovations in the literature on panel data econometrics highlight the potential for bias in estimating heterogeneous treatment effects. While the main estimates rely on the Borusyak et al. (2024) estimator, which accounts for such bias, Table D.11 reports estimates based on alternative heterogeneous treatment effect estimators (Callaway and Sant'Anna, 2021; Sun and Abraham, 2021). The estimates are consistent with the main estimates presented in Table 1 and Figure 5.

Table D.11: Wildlife Trade Restrictions and Conflict Likelihood: Alternative Estimators

	Dep. Var.: Conflict (0/1)					
	Wild Animals			Wild Trees		
	ACLED	UCDP	GTD	ACLED	UCDP	GTD
Panel A: Callaway and Sant'Anna (2021)						
Habitat × *Policy*	0.0315***	0.0067	0.0226***	0.0612***	0.0153***	0.0126***
	(0.0077)	(0.0048)	(0.002)	(0.0064)	(0.0022)	(0.0019)
Panel B: Sun and Abraham (2021)						
Habitat × *Policy*	0.0294***	0.008**	0.0203***	0.0733***	0.013***	0.0126***
	(0.0097)	(0.0038)	(0.0052)	(0.0091)	(0.0041)	(0.004)
Cell FE	Y	Y	Y	Y	Y	Y
Country-Year FE	Y	Y	Y	Y	Y	Y
Observations	575,892	1,126,720	1,673,984	575,892	1,126,720	1,673,984
Dep. Var. Mean	0.0757	0.0302	0.0173	0.0757	0.0302	0.0173
Dep. Var. SD	0.2645	0.1712	0.1306	0.2645	0.1712	0.1306

Notes: The table reports LPM estimates using the Callaway and Sant'Anna (2021) and Sun and Abraham (2021) difference-in-differences estimators. Each observation corresponds to a cell-year. The variable *Habitat* is an indicator measuring the suitability of cell k for wildlife species w, and *Policy* indicates the timing of CITES trade restrictions imposed on wildlife w at time t. The dependent variable is a binary indicator for conflict incidence, equal to one if at least one conflict event occurs in a given cell and year, based on the conflict datasets referenced in the column title. Coefficients are reported with bootstrapped standard errors (in parentheses). * significant at 10%; ** significant at 5%; *** significant at 1%.

Sensitivity Checks Related to the 2SLS Ivory Market Analysis

This sub-section provides three different sensitivity analyses addressing concerns regarding the exogeneity of policies in the ivory market and other potential confounders. Table D.12 shows regression estimates of the policy shocks on the log detrended price series of ivory and other minerals. As can be seen, the shocks have predictive power only for the ivory price series. Table D.13 reports placebo estimates for the 2SLS ivory market analysis shown in Table 2, where I intentionally code the policy shocks two years earlier. Reassuringly, all conflict coefficients are statistically insignificant. Finally, Table D.14 replicates the ACLED estimates from Table 2, excluding different continental sub-regions sequentially. This shows that the effect is not driven by a particular location, alleviating concerns that CITES targeted the policy based on specific regional conditions.

In estimating the effect of the ivory shock on conflict, I use the price of mammoth ivory. This is considered a close substitute for elephant ivory (Farah et al., 2015; Hauenstein et al., 2019), and

because mammoth ivory is traded legally, its price series is both the longest (1992-2024) available and likely the most reliable. However, Table D.15 reports estimates based on alternative ivory price sequences. Columns 1–2 and 4–5 use the price series constructed by Sosnowski et al. (2019) for 1990–2016 and Do et al. (2021) for 1985–2013, both derived from confiscation data, whereas columns 3 and 6 use prices obtained from art and antique auction websites for 2012–2021. All coefficients are positive and statistically significant, consistent with the main estimates in Table 2. Table D.16 presents a sufficient-statistics test in which both the policy vector and the price series are used to explain conflict incidence, showing that the policy vector has no effect on conflicts once prices are controlled for.

Table D.12: Placebo Estimates for Elephant Ivory Policy Shocks and Mineral Prices

	Dep. Var.: Detrended Log Price										
	(1)	(2)	(3)	(4)	(5)	(6)	(7)	(8)	(9)	(10)	(11)
	Ivory	Gold	Silver	Copper	Platinum	Iron	Lead	Nickel	Tin	Zinc	Aluminum
Ivory Policy Shocks	0.7702**	0.1398	0.0900	0.1299	−0.1358	−0.2189	0.1113	−0.2588	0.2805	0.0275	−0.2041
	(0.3500)	(0.3652)	(0.3926)	(0.4582)	(0.4189)	(0.4443)	(0.4579)	(0.4064)	(0.4018)	(0.3819)	(0.3268)
Observations	26	54	54	54	54	54	54	54	54	54	54

Note: The table reports placebo OLS estimates for the effect of supply-side policies in the ivory market on ivory prices and on the prices of other minerals. Each observation corresponds to a year. *Ivory Policy Shocks* is an indicator variable for the two supply-increasing policies (1998, 1999, 2007, 2008) and the supply-decreasing shocks (2017 and 2018), with signs applied accordingly. The outcome variable is the detrended log price of the resource mentioned in the title. Coefficients are reported with standard errors (in parentheses), which allow for infinite temporal correlation. * significant at 10%; ** significant at 5%; *** significant at 1%.

Table D.13: Placebo Estimates for Elephant Ivory Policy Shocks and Conflict Likelihood

	Dep. Var.: Conflict (0/1)		
	ACLED	UCDP	GTD
	(1)	(2)	(3)
Panel A: IV Estimates			
$\widehat{Habitat \times Price}$	−0.0012	0.0031	0.0041
	(0.0078)	(0.0055)	(0.0042)
Panel B: First Stage			
Habitat × Expansionary Policy	−0.4974***	−0.6478***	−0.6478***
	(0.0914)	(0.0882)	(0.0882)
Habitat × Contractionary Policy	0.7964***	0.7964***	0.7964***
	(0.0639)	(0.0639)	(0.0639)
F-stat	12,054	17,945	17,945
Cell FE	Y	Y	Y
Country-Year FE	Y	Y	Y
Industrial Mineral	Y	Y	Y
Dep. Var. Mean	0.0811	0.0370	0.0137
Dep. Var. SD	0.2730	0.1887	0.1163
Observations	272,600	283,504	283,504

Note: The table reports placebo 2SLS estimates for African elephants, where policy shocks are intentionally coded two years before the actual policy dates (1996, 1997, 2005, 2006, 2015, 2016). Each observation corresponds to a cell-year, and the sample is restricted to Africa. Panel A reports the main 2SLS estimates, where the variable *Habitat* is an indicator measuring the suitability of cell k for African elephants, and *Price* denotes the log price of ivory at time t. The estimates are based on first-stage predicted values based on equation (3). The dependent variable is a binary indicator for conflict incidence, equal to one if at least one conflict event occurs in a given cell-year, based on the conflict datasets referenced in the column titles. Panel B reports the first-stage estimates, in which policies explain the price shocks. *Expansionary Shock* is an indicator for policy-driven increases in ivory supply, while *Contractionary Shock* reflects policy-induced supply reductions. Coefficients are reported with spatially clustered standard errors (in parentheses), which allow for spatial and temporal correlation within a 500 km radius of each cell's centroid. * significant at 10%; ** significant at 5%; *** significant at 1%.

Table D.14: Policies, Price Shocks, and Conflict Likelihood in the Elephant Ivory Market: 2SLS with Sequential Exclusion of Subregions

	Dep. Var.: ACLED Conflict (0/1)				
	Excluded African Region				
	South	East	Centre	West	North
	(1)	(2)	(3)	(4)	(5)
Panel A: IV Estimates					
$\widehat{Habitat \times Price}$	0.0196***	0.0203**	0.0219***	0.0192***	0.0188***
	(0.0063)	(0.0083)	(0.0083)	(0.0067)	(0.0063)
Panel B: First Stage					
Habitat × Expansionary Policy	−0.8291***	−0.8291***	−0.8291***	−0.8291***	−0.8291***
	(0.0947)	(0.1251)	(0.1078)	(0.1084)	(0.0953)
Habitat × Contractionary Policy	0.7663***	0.7663***	0.7663***	0.7663***	0.7663***
	(0.1644)	(0.2172)	(0.1872)	(0.1883)	(0.1655)
F-stat	24,786	18,889	18,971	19,024	17,520
Cell FE	Y	Y	Y	Y	Y
Country-Year FE	Y	Y	Y	Y	Y
Dep. Var. Mean	0.0811	0.0667	0.0841	0.0759	0.0990
Dep. Var. SD	0.2729	0.2495	0.2775	0.2649	0.2987
Observations	272,475	207,650	208,550	209,125	192,600

Note: The table reports 2SLS estimates for African elephants, where I iteratively exclude the region mentioned in the title. Each observation corresponds to a cell-year, and the sample is restricted to Africa. Panel A reports the main 2SLS estimates, where the variable *Habitat* is an indicator measuring the suitability of cell k for African elephants, and *Price* denotes the log price of ivory at time t. The estimates are based on first-stage predicted values based on equation (3). The dependent variable is a binary indicator for conflict incidence, equal to one if at least one conflict event occurs in a given cell-year, based on the ACLED conflict dataset. Panel B reports the first-stage estimates, in which policies explain the price shocks. *Expansionary Shock* is an indicator for policy-driven increases in ivory supply, while *Contractionary Shock* reflects policy-induced supply reductions. Coefficients are reported with spatially clustered standard errors (in parentheses), which allow for spatial and temporal correlation within a 500 km radius of each cell's centroid. * significant at 10%; ** significant at 5%; *** significant at 1%.

Table D.15: Conflict and Ivory Price Shocks: Alternative Price Sequences

	Dep. Var.: Conflict (0/1)					
	ACLED			UCDP		
	Sosnowski et al. (2019)	Do et al. (2021)	Art and Antique Markets	Sosnowski et al. (2019)	Do et al. (2021)	Art and Antique Markets
	(1)	(2)	(3)	(4)	(5)	(6)
Elephant Habita × Ivory Price	0.0065***	0.0063***	0.0093***	0.0057***	0.0085***	0.005*
	(0.0017)	(0.0025)	(0.004)	(0.0022)	(0.003)	(0.003)
Cell FE	Y	Y	Y	Y	Y	Y
Country-Year FE	Y	Y	Y	Y	Y	Y
Observations	294,816	182,250	110,556	393,088	182,250	110,556
Dep. Var. Mean	0.06	0.049	0.112	0.028	0.026	0.0472
Dep. Var. SD	0.237	0.217	0.316	0.166	0.026	0.212

Notes: The table reports OLS estimates for African elephants, using alternative price sequences. Each observation corresponds to a cell-year, and the sample is restricted to Africa. The variable *Elephant Habitat* is an indicator for the suitability of cell k for African elephants, and *Ivory Price* denotes the log price of ivory at time t, based on the source indicated in the table title. The dependent variable is a binary indicator for conflict incidence, equal to one if at least one conflict event occurs in a given cell-year, as defined by the conflict datasets referenced in the column titles. Coefficients are reported with spatially clustered standard errors (in parentheses), which allow for spatial and temporal correlation within a 500 km radius of each cell's centroid. * significant at 10%; ** significant at 5%; *** significant at 1%.

Table D.16: Conflict and Ivory Price Shocks: A Sufficient Statistics Test

	Dep. Var.: Conflict (0/1)		
	ACLED	UCDP	GTD
	(1)	(2)	(3)
Elephant Habitat × Price	0.013***	0.006***	0.004**
	(0.003)	(0.002)	(0.002)
Elephant Habitat × Contractionary	−0.004	−0.006	−0.001
	(0.004)	(0.005)	(0.002)
Elephant Habitat × Expansionary	0.009	0.009	0.007
	(0.007)	(0.007)	(0.005)
Minerals	0.022**	0.001	0.004
	(0.008)	(0.005)	(0.004)
Cell FE	Yes	Yes	Yes
Country–Year FE	Yes	Yes	Yes
Observations	272,600	283,504	283,504
Dep. Var. Mean	0.081	0.037	0.014
Dep. Var. SD	0.272	0.188	0.116

Notes: OLS estimates for African elephants testing the sufficient-statistics relationship between ivory price shocks and conflict incidence. The regression interacts both the ivory price series and policy shock indicators with Elephant Habitat, measuring cell-level suitability for elephants. Expansionary indicates years of policy-driven supply increases (1998–1999, 2007–2008), while Contractionary marks supply reductions (2017–2018). Each observation is a cell–year; the sample is restricted to Africa. Standard errors (in parentheses) are spatially clustered within a 500 km radius around each cell centroid. * $p < 0.10$, ** $p < 0.05$, *** $p < 0.01$.

E Model

This section provides the complete set of derivations necessary to solve the model presented in section 6.

E.1 Model Setup

E.1.1 Harvesting Sector and Equilibrium Aggregation

There are N countries indexed by i, of which N_w are weak ($s_i = 0$) and N_s are strong ($s_i = 1$). Each country has local stock F_i. Firms in weak states face a loot rate $t_i \in [0, 1]$ set by the armed sector; in strong states I assume no looting, $t_i \equiv 0$. A representative firm chooses $h_i \geq 0$ to maximise:

$$\Pi_i \;=\; p(\tau)\, h_i(1 - t_i) \;-\; \frac{h_i^2}{2F_i} \;-\; \tau\, s_i\, \theta\, h_i. \tag{1}$$

The FOC implies:

$$h_i^* \;=\; F_i\big[\, p(\tau)(1 - t_i) \;-\; \tau\, s_i\, \theta \,\big]. \tag{2}$$

With $h_i^* = 0$ if the bracket is negative. Under high enforcement in strong states ($\theta > p(\tau)$) and an interior solution in weak states:

$$h_i^*(s_i, \tau) = \begin{cases} F_i\, p(0)(1 - t_i), & \text{if } \tau = 0,\ s_i = 0, \\ F_i\, p(0), & \text{if } \tau = 0,\ s_i = 1 \text{ (since } t_i = 0), \\ F_i\, p(1)(1 - t_i), & \text{if } \tau = 1,\ s_i = 0, \\ 0, & \text{if } \tau = 1,\ s_i = 1 \ (\theta > p(1)). \end{cases} \tag{3}$$

Profits at the optimum are:

$$\Pi_i^*(s_i, \tau) = \begin{cases} \tfrac{1}{2}\, F_i\, p(0)^2(1 - t)^2, & \text{if } \tau = 0,\ s_i = 0, \\ \tfrac{1}{2}\, F_i\, p(0)^2, & \text{if } \tau = 0,\ s_i = 1, \\ \tfrac{1}{2}\, F_i\, p(1)^2(1 - t)^2, & \text{if } \tau = 1,\ s_i = 0, \\ 0, & \text{if } \tau = 1,\ s_i = 1. \end{cases} \tag{4}$$

Later, I derive the revenue-maximising loot share from the armed section: $t = \frac{1}{2}$ for weak states, independent of local stock, and $t = 0$ for strong states.

Aggregation. Let $\bar{F}_w$ and $\bar{F}_s$ denote sample average stocks in weak and strong states, and set $t_i = t$ for weak states. The effective supply coefficients for before and after the ban are:

$$S_0 \;=\; (1 - t)\, N_w\, \bar{F}_w \;+\; N_s\, \bar{F}_s, \qquad S_1 \;=\; (1 - t)\, N_w\, \bar{F}_w. \tag{5}$$

With linear inverse demand $p(Q) = a - bQ$ and $Q = S_\tau p$, market clearing yields regime-specific prices and quantities:

$$p(\tau) \;=\; \frac{a}{1+bS_\tau}, \qquad Q(\tau) \;=\; \frac{a\,S_\tau}{1+bS_\tau}, \qquad S_\tau \in \{S_0, S_1\}. \tag{6}$$

Combining (3) with (6) gives country-level harvest under each regime:

$$h_i^*(s_i,\tau) = \begin{cases} F_i \cdot \dfrac{a(1-t)}{1+bS_0}, & \text{if } s_i = 0,\ \tau = 0, \\ F_i \cdot \dfrac{a}{1+bS_0}, & \text{if } s_i = 1,\ \tau = 0, \\ F_i \cdot \dfrac{a(1-t)}{1+bS_1}, & \text{if } s_i = 0,\ \tau = 1, \\ 0, & \text{if } s_i = 1,\ \tau = 1. \end{cases} \tag{7}$$

Profits follow analogously from (4) with $p(\tau) = a/(1+bS_\tau)$.

Constructing unit-free indices (for welfare). Define:

$$r_S \equiv \frac{S_1}{S_0}, \qquad \phi \equiv bS_0. \tag{8}$$

Then the price and quantity ratios used in the planner's rule are:

$$\frac{p(1)}{p(0)} = \frac{1+\phi}{1+\phi r_S}, \qquad \frac{Q(1)}{Q(0)} = r_S \cdot \frac{1+\phi}{1+\phi r_S}. \tag{9}$$

These objects are invariant to common rescalings of stocks and plug directly into the violence and welfare expression.

E.1.2 Armed Sector

Environment and timing. In each weak state ($s_i = 0$) an armed group extracts a share $t_i \in [0,1]$ of the representative firm's revenue. Taking the world price p as given, the firm's optimal harvest in a weak state solves the harvesting FOC (from the production block), yielding:

$$h_i^*(t_i) \;=\; F_i\, p(\tau)\,(1-t_i). \tag{10}$$

Thus looting acts like a revenue tax that scales down supply.

Looted revenue and the optimal loot share. Given (10), the group's looted revenue is:

$$R_{ji}(t_i) \;=\; t_i\, p(\tau)\, h_i^*(t_i) \;=\; F_i\, p(\tau)^2\, t_i(1-t_i). \tag{11}$$

Maximising (11) over $t_i \in [0,1]$ gives:

$$\frac{\mathrm{d}R_{ji}}{\mathrm{d}t_i} = F_i p(\tau)^2(1-2t_i) = 0 \implies t_i^* = \tfrac{1}{2}, \qquad \frac{\mathrm{d}^2 R_{ji}}{\mathrm{d}t_i^2} = -2F_i p(\tau)^2 < 0,$$

So the optimum is interior and unique, and independent of local stock. Substituting t_i^* back into (11):

$$R_{ji}^* \;=\; \frac{F_i\, p(\tau)^2}{4}. \tag{12}$$

Armed group contest. Let $\pi_i(\tau) \in [0,1]$ denote the conflict probability in weak state i under regime $\tau \in \{0,1\}$. I model group j competing against a rival group $-j$, whose baseline resources are fixed at R_{-ji} but whose realised effectiveness is subject to a multiplicative lognormal shock, capturing uncertainty about the rival's true strength:

$$\widetilde{R}_{-ji} \;=\; R_{-ji}\, Z_{-ji}, \qquad \ln Z_{-ji} \sim \mathcal{N}(0, \sigma^2),$$

The contest function with exponent $\delta > 0$ delivers, for any realised Z_{-ji}:

$$\pi_i(\tau) = \frac{\big(R_{ji}^*(\tau)\big)^{\delta}}{\big(R_{ji}^*(\tau)\big)^{\delta} + \big(R_{-ji} Z_{-ji}\big)^{\delta}}.$$

Under the lognormal distribution, the expectation is $\mathbb{E}[Z_{-ji}^{\delta}] = \exp(\frac{1}{2}\delta^2\sigma^2)$. I represent the *ex-ante* success probability by evaluating the rival term at its mean under the lognormal shock, which yields a convenient constant:

$$\kappa_i \;\equiv\; R_{-ji}^{\delta}\, \mathbb{E}[Z_{-ji}^{\delta}] \;=\; R_{-ji}^{\delta}\, \exp\!\Big(\tfrac{1}{2}\delta^2\sigma^2\Big), \tag{13}$$

and hence the maintained contest specification:

$$\pi_i(\tau) \;\approx\; \frac{\big(R_{ji}^*(\tau)\big)^{\delta}}{\big(R_{ji}^*(\tau)\big)^{\delta} + \kappa_i} \;=\; \frac{\Big(\frac{F_i\, p(\tau)^2}{4}\Big)^{\delta}}{\Big(\frac{F_i\, p(\tau)^2}{4}\Big)^{\delta} + \kappa_i}. \tag{14}$$

The constant κ_i represents rival baseline resources and uncertainty dispersion; it is policy-invariant and will drop out under baseline normalisation.

Unit-free normalisation. Let $p(0)$ be the baseline price and $\pi_{i0} \equiv \pi_i(0)$. Evaluating (14) at $\tau = 0$ yields

$$\pi_{i0} \approx \frac{\Big(\frac{F_i\, p(0)^2}{4}\Big)^{\delta}}{\Big(\frac{F_i\, p(0)^2}{4}\Big)^{\delta} + \kappa_i} \;\Longrightarrow\; \frac{\kappa_i}{\Big(\frac{F_i\, p(0)^2}{4}\Big)^{\delta}} = \frac{1-\pi_{i0}}{\pi_{i0}}.$$

Let $\rho(\tau) \equiv \big(\frac{p(\tau)}{p(0)}\big)^2$. Since $R_{ji}^*(\tau)/R_{ji}^*(0) = \rho(\tau)$, substitution gives the unit-free probability map:

$$\boxed{\pi_i(\tau) = \frac{\pi_{i0}\, \rho(\tau)^{\delta}}{(1-\pi_{i0}) + \pi_{i0}\, \rho(\tau)^{\delta}}}, \qquad \rho(\tau) = \left(\frac{p(\tau)}{p(0)}\right)^2. \tag{15}$$

All dimensional objects (F_i, R_{-ji}, σ) cancel; comparative statics depend only on the price ratio

and δ.

Intensities and aggregation. Let $\bar{V}_i(\tau)$ denote observed intensity (e.g., affected resource cells), with a scaling factor $\Lambda_i > 0$:

$$\bar{V}_i(\tau) \;=\; \Lambda_i\, \pi_i(\tau), \qquad \frac{\bar{V}_i(\tau)}{\bar{V}_{i0}} = \frac{\pi_i(\tau)}{\pi_{i0}} = \frac{\rho(\tau)^\delta}{\big(1-\pi_{i0}\big) + \pi_{i0}\,\rho(\tau)^\delta}. \tag{16}$$

Under symmetry across weak states (same $\pi_{i0} = \pi_0$ and, if using sample average intensity, so $\Lambda_i = \bar{\Lambda}$), aggregates are N_w multiples; the scaling by $\bar{\Lambda}$ cancels in ratios.

Summary. (i) The group's FOC yields $t_i^* = \frac{1}{2}$ and $R_{ji}^* = \frac{F_i p(\tau)^2}{4}$. (ii) A contest function with lognormal rival uncertainty implies the tractable contest form (14) with a policy-invariant constant κ_i in (13). (iii) Normalising at the baseline produces the unit-free law (15); all dimensional constants drop out. (iv) Intensities inherit the same unit-free scaling via (16).

E.1.3 Social Planner

Objective. An international planner chooses $\tau \in \{0, 1\}$ (free trade vs. ban), internalising biodiversity and conflict externalities. Under symmetry across weak states, welfare loss is:

$$W(\tau) \;=\; \lambda\, N\, Q(\tau)^\eta \;+\; (1-\lambda)\, N_w\, \pi(\tau)\bar{\Lambda}, \qquad \lambda \in (0,1),\ \eta > 0. \tag{17}$$

Where $Q(\tau) = \sum_{i=1}^{N} h_i^*(\tau)$ is total harvest and $\pi(\tau)$ is the per-weak-state average conflict probability (under symmetry, this equals the common per-weak-state probability).[31] Where:

$$Q(1) < Q(0), \qquad \pi(1) > \pi(0). \tag{18}$$

A ban reduces total harvest but raises conflict in weak states.

Planner Decision rule. A ban is preferred iff $W(1) < W(0)$:

$$W(1) - W(0) = \lambda\, N\big(Q(1)^\eta - Q(0)^\eta\big) + (1-\lambda)\, N_w\big(\pi(1) - \pi(0)\big)\bar{\Lambda} < 0. \tag{19}$$

Define strictly positive changes under (18):

$$\Delta Q^\eta \equiv Q(0)^\eta - Q(1)^\eta > 0, \qquad \Delta V \equiv \bar{\Lambda}(\pi(1) - \pi(0)) > 0. \tag{20}$$

Then $Q(1)^\eta - Q(0)^\eta = -\Delta Q^\eta$, so (19) becomes:

$$\begin{aligned} 0 &> \lambda\, N(-\Delta Q^\eta) + (1-\lambda)\, N_w\, \Delta V = -\lambda\, N\, \Delta Q^\eta + N_w\, \Delta V - \lambda\, N_w\, \Delta V \\ &= \lambda\big(-N\, \Delta Q^\eta - N_w\, \Delta V\big) + N_w\, \Delta V. \end{aligned} \tag{21}$$

Rearrange:

[31] The biodiversity loss is scaled by N, while conflict occurs in weak states only (scaled by N_w).

$$\lambda\big(-N\,\Delta Q^{\eta}-N_w\,\Delta V\big)<-N_w\,\Delta V. \tag{22}$$

The bracket is strictly negative, so dividing flips the inequality:

$$\lambda\;>\;\frac{N_w\,\Delta V}{N\,\Delta Q^{\eta}+N_w\,\Delta V}\;\equiv\;\lambda^{*}. \tag{23}$$

This is the policy threshold: a ban is optimal if $\lambda > \lambda^{*}$.

Unit-free normalisation. Define the unit-free indices:

$$q_\tau \equiv \frac{Q(\tau)}{Q(0)}, \qquad v_\tau \equiv \frac{\pi(\tau)}{\pi(0)}, \qquad q_0 = v_0 = 1, \tag{24}$$

and let $\rho(\tau) \equiv \left(\frac{p(\tau)}{p(0)}\right)^2$. From the contest function normalisation:

$$v_\tau = \frac{\pi(\tau)}{\pi(0)} = \frac{\rho(\tau)^{\delta}}{(1-\pi_0)+\pi_0\,\rho(\tau)^{\delta}}, \qquad \rho(0) = 1. \tag{25}$$

Since $V(\tau) \equiv \bar{\Lambda}\,\pi(\tau)$, then:

$$\frac{\Delta Q^{\eta}}{Q(0)^{\eta}} = 1 - q_1^{\eta}, \qquad \frac{\Delta V}{V(0)} = \frac{V(1)-V(0)}{V(0)} = \frac{\pi(1)-\pi(0)}{\pi(0)} = v_1 - 1.$$

I obtain the unit-free threshold:

$$\lambda^{*} = \frac{N_w\,(v_1-1)}{N\left(1-q_1^{\eta}\right)+N_w\,(v_1-1)}, \qquad v_1 = \frac{\rho_1^{\delta}}{(1-\pi_0)+\pi_0\,\rho_1^{\delta}}, \quad \rho_1 = \left(\frac{p_1}{p_0}\right)^2. \tag{26}$$

Explicit unit-free terms. With linear inverse demand $p(Q) = a - bQ$ and regime-specific linear supply coefficients:

$$S_0 = (1-t)N_w\bar{F}_w + N_s\bar{F}_s, \qquad S_1 = (1-t)N_w\bar{F}_w,$$

market clearing implies $Q = S_\tau p$ and therefore:

$$p(0) = \frac{a}{1+bS_0}, \qquad p(1) = \frac{a}{1+bS_1}.$$

Hence the price ratio and quantity ratio are:

$$\frac{p(1)}{p(0)} = \frac{1+bS_0}{1+bS_1}, \qquad q_1 \equiv \frac{Q(1)}{Q(0)} = \frac{S_1}{S_0}\cdot\frac{1+bS_0}{1+bS_1}. \tag{27}$$

Under the contest function, the violence ratio becomes:

$$v_1 = \frac{\left(\frac{1+bS_0}{1+bS_1}\right)^{2\delta}}{(1-\pi_0)+\pi_0\left(\frac{1+bS_0}{1+bS_1}\right)^{2\delta}}. \tag{28}$$

Substituting (27)–(28) into (26) yields a fully explicit λ^* in primitives $(N, N_w, N_s, \bar{F}_w, \bar{F}_s, t, b, \pi_0, \delta, \eta)$.

Equivalent compact form. Define:

$$r_S \equiv \frac{S_1}{S_0} = \frac{(1-t)N_w\bar{F}_w}{(1-t)N_w\bar{F}_w + N_s\bar{F}_s}, \qquad \phi \equiv b\,S_0 = b\big[(1-t)N_w\bar{F}_w + N_s\bar{F}_s\big].$$

Then:

$$\frac{p(1)}{p(0)} = \frac{1+\phi}{1+\phi r_S}, \qquad q_1 = r_S \cdot \frac{1+\phi}{1+\phi r_S}, \qquad v_1 = \frac{\left(\frac{1+\phi}{1+\phi r_S}\right)^{2\delta}}{(1-\pi_0)+\pi_0\left(\frac{1+\phi}{1+\phi r_S}\right)^{2\delta}},$$

and (26) follows.

E.2 Model Estimation

This section discusses the procedure used to recover the model's parameters and to conduct the welfare simulation, for which I restrict the sample to Africa and focus on the case of rosewood.

E.2.1 Recovery of Model Parameters

This subsection shows how all parameters used in the simulations are recovered from observables and model-implied relationships. I proceed in four steps: (i) fix the primitives observed in the data; (ii) compute the effective supply coefficients that summarise composition; (iii) use the two observed regime prices to recover the demand parameters (a, b) and the key unit-free ratios; and (iv) pin down the violence elasticity δ from the observed probability change under the contest function. Throughout, units cancel in the ratios that feed the welfare analysis.

Step 1: Inputs (observables). I take as given the sample structure, stocks, the two regime prices and use the loot share derived from the model:

$$N_w = 26, \quad N_s = 25, \quad \bar{F}_w = 98.27, \quad \bar{F}_s = 54.76, \quad t = \tfrac{1}{2}, \quad p_0 = 92.33, \quad p_1 = 143.33,$$

and the conflict-probability moments from Appendix Table A.6 and Appendix Table E.4:

$$\pi(0) = 0.0911, \qquad \Delta\,\Pr = 0.054.$$

Step 2: Effective supply (composition). Given the revenue-maximising loot share in weak

states ($t^* = \frac{1}{2}$), the regime-specific linear supply coefficients are:

$$S_1 = (1-t)N_w\bar{F}_w = 1277.51, \qquad S_0 = S_1 + N_s\bar{F}_s = 2646.51, \qquad r_S = \frac{S_1}{S_0} = 0.4827.$$

Step 3: Demand recovery and unit-free ratios. With linear inverse demand $p(Q) = a - bQ$ and $Q = S_\tau p$, market clearing implies $p(\tau) = \dfrac{a}{1 + bS_\tau}$ for $\tau \in \{0, 1\}$. Using the two observed prices $(p(0), p(1))$ and the two S's, I obtain:

$$b = \frac{p(1) - p(0)}{p(0)S_0 - p(1)S_1} = 0.0008, \qquad a = p(0)\big(1 + bS_0\big) = 295.8014.$$

The price, quantity, and tightness ratios used later are:

$$\frac{p(1)}{p(0)} = \frac{1 + bS_0}{1 + bS_1} = 1.5524, \qquad \frac{Q(1)}{Q(0)} = r_S \cdot \frac{1 + bS_0}{1 + bS_1} = 0.7494, \qquad \phi = bS_0 = 2.2037.$$

Interpretation: $\frac{p(1)}{p(0)}$ is the endogenous price change across regimes; $\frac{Q(1)}{Q(0)} \equiv q_1$ is the proportional fall in total harvest under the ban; ϕ is a convenient unit-free summary of demand tightness at the free-trade composition.

Step 4: Violence elasticity δ. Under the baseline-normalised Tullock contest in the armed sector, the unit-free probability ratio satisfies:

$$v_1 \;\equiv\; \frac{\pi(\tau)}{\pi(0)} \;=\; \frac{\rho^\delta}{(1 - \pi(0)) + \pi(0)\,\rho^\delta}, \qquad \rho \;\equiv\; \left(\frac{p(\tau)}{p(0)}\right)^2.$$

From the event study, I obtain $v_1 = 1 + \Delta \Pr / \pi(0)$. Solving the contest function expression for δ gives:

$$\rho^\delta \;=\; \frac{v_1(1 - \pi(0))}{1 - v_1\pi(0)} \quad \Longrightarrow \quad \delta = \frac{\ln\!\left(\dfrac{v_1(1 - \pi(0))}{1 - v_1\pi(0)}\right)}{\ln \rho}\,.$$

Numerically, with:

$$\frac{p(1)}{p(0)} = 1.5524, \quad \rho = (1.5524)^2 = 2.4098, \quad v_1 = 1 + \frac{0.054}{0.0911} = 1.59,$$

I obtain:

$$\delta \approx 0.599\,.$$

Summary of Model Parameter Recovery. Table E.1 reports the parameters used in the model. N_w and N_s are the numbers of weak and strong states in the sample (below/above median state capacity). $\bar{F}_w$ and $\bar{F}_s$ are sample-average stocks; in all welfare objects they enter only through ratios, so common rescalings of units do not affect the results.

Looting. The armed group's revenue-maximising choice yields $t^* = \frac{1}{2}$, implying the weak-state

supply wedge $(1 - t^*)$. These deliver the effective supply coefficients

$$S_0 = (1 - t^*)N_w\bar{F}_w + N_s\bar{F}_s, \qquad S_1 = (1 - t^*)N_w\bar{F}_w,$$

and the unit–free composition/compression terms

$$r_S \equiv \frac{S_1}{S_0}, \qquad \phi \equiv b\, S_0.$$

Demand. With linear inverse demand $p(Q) = a - bQ$ and $Q = S_\tau p$, the two observed regime prices p_0 (free trade) and p_1 (ban) identify:

$$b = \frac{p(1) - p(0)}{p(0)S_0 - p(1)S_1}, \qquad a = p(0)\big(1 + bS_0\big) = p(1)\big(1 + bS_1\big).$$

The corresponding unit-free ratios used in welfare are

$$\frac{p(1)}{p(0)} = \frac{1 + bS_0}{1 + bS_1} = \frac{1 + \phi}{1 + \phi r_S}, \qquad \frac{Q(1)}{Q(0)} \equiv q_1 = r_S \cdot \frac{1 + \phi}{1 + \phi r_S}.$$

Violence elasticity. Conflict probability in weak states follows the unit-free contest mapping:

$$\frac{\pi(\tau)}{\pi(0)} = \frac{\left(\frac{p(\tau)}{p(0)}\right)^{2\delta}}{(1 - \pi(0)) + \pi(0)\left(\frac{p(\tau)}{p(0)}\right)^{2\delta}},$$

so that with $v_1 = 1 + \Delta \Pr / \pi(0)$ and $\rho = (p(1)/p(0))^2$,

$$\delta = \frac{\ln\left(\dfrac{v_1(1 - \pi(0))}{1 - v_1\pi(0)}\right)}{\ln \rho}.$$

Planner's rule. The unit-free objects entering the policy rule are:

$$q_1 = \frac{Q(1)}{Q(0)}, \qquad v_1 = \frac{\left(\frac{p(1)}{p(0)}\right)^{2\delta}}{(1 - \pi(0)) + \pi(0)\left(\frac{p(1)}{p(0)}\right)^{2\delta}}, \qquad \lambda^* = \frac{N_w\,(v_1 - 1)}{N\left(1 - q_1^{\eta}\right) + N_w\,(v_1 - 1)},$$

where $N = N_w + N_s = 51$ in my sample.

Model Parameters.

Table E.1: Model Parameters

Symbol	Description	Value	Source / Notes
	Sample Structure		
N_w	Number of weak states	26	Below median state capacity
N_s	Number of strong states	25	Above median state capacity
	Forest Stocks and Prices		
$\bar{F}_w$	Forest in weak states	98.27	Sample average (units cancel in ratios)
$\bar{F}_s$	Forest in strong states	54.76	Sample average (units cancel in ratios)
t	Looting share in weak states	0.5	Revenue-maximising ($t = 1/2$)
$p(0)$	Price under free trade	92.33	Observed
$p(1)$	Price under ban	143.33	Observed
	Supply		
S_0	Effective supply coeff. (FT)	2646.51	$(1-t)N_w\bar{F}_w + N_s\bar{F}_s$
S_1	Effective supply coeff. (Ban)	1277.51	$(1-t)N_w\bar{F}_w$
r_S	Supply composition ratio	0.4827	S_1/S_0
	Demand		
a	Inverse demand intercept	295.8014	From $(p(0)), p(1), S_0, S_1)$ via $p(\tau) = \frac{a}{1+bS_\tau}$
b	Slope of inverse demand	0.0008	$\dfrac{p(1)-p(0)}{p(0)S_0 - p(1)S_1}$
ϕ	Unit-free demand tightness	2.2037	bS_0
Q_0	Quantity under FT	244,352.27	$S_0\, p(0)$
Q_1	Quantity under Ban	183,105.51	$S_1\, p(1)$
	Violence / Conflict Parameters		
$\pi(0)$	Baseline weak-state conflict probability	0.0911	From data
$\Delta\,\Pr$	Ban-induced change in probability	0.054	From event study
v_1	Probability ratio	1.59	$1 + \Delta\,\Pr\,/\pi(0)$
δ	Elasticity (violence wrt loot revenue)	0.599	$\delta = \dfrac{\ln\left(\frac{v_1(1-\pi(0))}{1-v_1\pi(0)}\right)}{\ln\left((p(1)/p(0))^2\right)}$
$\bar{\Lambda}$	Cells per weak state (intensity scale)	29.04	Resource cells
	Planner Preferences		
λ	Weight on biodiversity	$[0, 1]$	Scenario variable
η	Convexity of biodiversity loss	$(0, 2)$	Scenario variable

E.2.2 Price Elasticity of Demand

For the linear inverse demand:

$$p(Q) = a - bQ,$$

the (Marshallian) point price elasticity of demand at a given equilibrium $(p(\tau), Q_\tau)$ ($\tau = 0$ free trade, $\tau = 1$ ban) is:

$$\varepsilon_\tau \;\equiv\; \frac{dQ}{dp}\cdot\frac{p(\tau)}{Q_\tau}.$$

Since $Q = (a - p(\tau))/b$, so $dQ/dp = -1/b$. In the model the market clears against a linear supply schedule $Q = S_\tau\, p(\tau)$, so at the equilibrium $Q_\tau = S_\tau p(\tau)$. Therefore:

$$\varepsilon_\tau = \Big(-\frac{1}{b}\Big)\cdot\frac{p(\tau)}{Q_\tau} = -\frac{1}{b\,S_\tau}\,.$$

Numerical evaluation. Using the recovered values $S_0 = 2646.51$, $S_1 = 1277.51$, and $b = 0.0008326971$,

$$\varepsilon_0 = -\frac{1}{bS_0} = -0.4538 \quad \text{(free trade)}, \qquad \varepsilon_1 = -\frac{1}{bS_1} = -0.9400 \quad \text{(ban)}.$$

Interpretation. Demand is inelastic in both regimes, and becomes more elastic under the ban.

Elasticity across regimes. The midpoint elasticity between the two equilibria:

$$\varepsilon_{01} = \frac{(Q_1 - Q_0)/\big((Q_0 + Q_1)/2\big)}{(p(1) - p(0))/\big((p(0) + p(1))/2\big)} = -0.6621.$$

E.2.3 Recovering λ^*

Given the unit-free threshold:

$$\lambda^* = \frac{N_w\,(v_1 - 1)}{N\,(1 - q_1^\eta) + N_w\,(v_1 - 1)}, \qquad q_1 \equiv \frac{Q(1)}{Q(0)}, \quad v_1 \equiv \frac{\pi(1)}{\pi(0)},$$

evaluating λ^* at the calibrated point:

$$N_w = 26, \quad N = 51, \quad q_1 = 0.7494, \quad v_1 = 1.59.$$

Under the normalised contest function:

$$v_1 = \frac{\left(\frac{p(1)}{p(0)}\right)^{2\delta}}{(1 - \pi_0) + \pi_0\left(\frac{p(1)}{p(0)}\right)^{2\delta}} = 1 + \frac{\Delta\,\mathrm{Pr}}{\pi(0)}.$$

Where the equality holds by construction of δ in the parameter recovery.

The conflict term is

$$N_w(v_1 - 1) = 26 \times (1.59 - 1) = 15.41.$$

For each η, I compute the biodiversity term $N(1 - q_1^\eta)$ and then λ^*.

Intermediate quantities.

η	q_1^η	$1-q_1^\eta$	$N(1-q_1^\eta)$
0.5	0.8657	0.1343	6.8504
1.0	0.7494	0.2506	12.7806
1.5	0.6487	0.3513	17.9143
2.0	0.5616	0.4384	22.3584

Policy threshold λ^*.

$$\lambda^*(\eta) = \frac{15.4116}{N(1-q_1^\eta)+15.4116} = \begin{cases} 0.6923, & \eta = 0.5, \\ 0.5467, & \eta = 1.0, \\ 0.4625, & \eta = 1.5, \\ 0.4080, & \eta = 2.0. \end{cases}$$

Interpretation. As η rises (more convex biodiversity damages), $N(1-q_1^\eta)$ increases, so λ^* falls: bans are optimal for a wider range of planner weights λ and is more likely to happen.

Kitagawa–Oaxaca–Blinder (KOB) decomposition (price–then–quantity)

The change in profits between the free-trade and ban equilibria can be expressed as a two-step decomposition:

$$\Delta\Pi = \underbrace{\big[\Pi(p(1),h(0)) - \Pi(p(0),h(0))\big]}_{\text{price effect}} + \underbrace{\big[\Pi(p(1),h(1)) - \Pi(p(1),h(0))\big]}_{\text{quantity effect}}.$$

Compute each term in closed form:

$$\Delta\Pi_{\text{price}} = F(1-t)^2\, p(0)\big[p(1)-p(0)\big] = F(1-t)^2\, p(0)^2\,[\chi-1],$$

$$\Delta\Pi_{\text{qty}} = \tfrac{1}{2}\, F(1-t)^2\,[p(1)-p(0)]^2 = \tfrac{1}{2}\, F(1-t)^2\, p(0)^2\,[\chi-1]^2,$$

$$\Delta\Pi = \tfrac{1}{2}\, F(1-t)^2\,[p(1)^2 - p(0)^2] = \tfrac{1}{2}\, F(1-t)^2\, p(0)^2\,[\chi^2-1].$$

Shares of the total profit change follow directly:

$$\text{Price share} = \frac{\Delta\Pi_{\text{price}}}{\Delta\Pi} = \frac{2}{1+\chi}, \qquad \text{Quantity share} = \frac{\Delta\Pi_{\text{qty}}}{\Delta\Pi} = \frac{\chi-1}{1+\chi}.$$

Normalizing by baseline profits $\Pi(0) = \frac{1}{2}F(1-t)^2p(0)^2$ gives

$$\frac{\Delta\Pi}{\Pi(0)} = \chi^2 - 1, \qquad \frac{\Delta\Pi_{\text{price}}}{\Pi(0)} = 2(\chi-1), \qquad \frac{\Delta\Pi_{\text{qty}}}{\Pi(0)} = (\chi-1)^2.$$

Numerical illustration (calibration)

Using the calibrated parameters from Table E.1:

$$N_w = 26, \qquad \bar{F}_w = 98.27 \;\Rightarrow\; F = N_w \bar{F}_w = 2555.02, \qquad t = 0.5, \qquad p(0) = 92.33, \qquad p(1) = 143.33,$$

which implies $\chi = p(1)/p(0) \approx 1.5524$. Substituting these values yields

$$\Pi(0) = \tfrac{1}{2} F (1-t)^2 p(0)^2 \approx 2{,}722{,}638.54.$$

The decomposition components are

$$\Delta\Pi_{\text{price}} = F(1-t)^2 p(0)^2 (\chi - 1) \approx 3{,}007{,}788.71, \qquad \Delta\Pi_{\text{qty}} = \tfrac{1}{2} F (1-t)^2 p(0)^2 (\chi-1)^2 \approx 830{,}700.88,$$

and the total change

$$\Delta\Pi = \tfrac{1}{2} F (1-t)^2 p(0)^2 (\chi^2 - 1) \approx 3{,}838{,}489.58.$$

Hence, the price component accounts for

$$\text{Price share} = \frac{2}{1+\chi} \approx 0.7836, \quad \text{and} \quad \text{Quantity share} = \frac{\chi - 1}{1+\chi} \approx 0.2164.$$

Normalizing by $\Pi(0)$ gives

$$\frac{\Delta\Pi}{\Pi(0)} \approx 1.4098, \qquad \frac{\Delta\Pi_{\text{price}}}{\Pi(0)} \approx 1.1047, \qquad \frac{\Delta\Pi_{\text{qty}}}{\Pi(0)} \approx 0.3051.$$

In this calibration, approximately 78% of the increase in weak-state profits after the ban arises from the rise in price, while the remaining 22% is attributable to higher quantities produced in weak states.

E.2.5 Derivation of the Optimal Continuous Conservation Tax

This section details the mathematical steps taken to derive the optimal continuous tax rate (τ^*) in the scenario where the tax revenue is not redistributed but vanishes from the economy, providing the τ that minimises the policymaker's aggregate loss.[32]

Reformulation of the Harvesting Firm's Problem. To introduce the continuous percentage tax τ into the market structure, I first reformulate the representative harvesting firm's profit maximisation problem. For a strong state ($s_i = 1$), the loot share (t_i) is zero. The parameter θ is omitted as the continuous tax rate τ now functions as the restriction cost levied as a percentage of revenue. The firm in country i chooses its harvest quantity $h_i \geq 0$ to maximise profit:

[32] The policymaker does not redistribute the revenues in order to experiment with a tax-based policy that is as close as possible to the actual trade-ban policy.

$$\Pi_i(\tau) = p(\tau)h_i(1-t_i) - \mathbf{1}_{s_i=1} \cdot \tau \cdot p(\tau)h_i - \frac{h_i^2}{2F_i}$$

For weak states ($s_i = 0$), the tax term vanishes, leaving the firm's optimal harvest $h_w^*(\tau)$ reliant on the loot rate $t^* = 1/2$. For strong states ($s_i = 1$), where $t_i = 0$, the optimal harvest $h_s^*(\tau)$ is derived from the first-order condition $\frac{\partial \Pi_i}{\partial h_i} = 0$:

$$h_s^*(\tau) = F_i p(\tau)(1-\tau)$$

This continuous function of τ allows the derivation to proceed. The total supply $S(\tau)$ is then defined as the sum of optimal harvesting across all weak and strong states, which determines the equilibrium price $p(\tau)$ and the total harvest $Q(\tau)$.

The Reformulated Loss Function. The necessary condition for a local minimum τ^* is established by setting the marginal loss with respect to τ to zero. Since the tax revenue vanishes, the Loss Function (W_{new}) is defined solely by the two social costs: Environmental Loss and the Conflict Externality.

$$W_{\text{new}}(\tau) = \lambda N Q(\tau)^\eta + (1-\lambda) N_w \pi(\tau) \bar{\Lambda}$$

Solving the First-Order Condition. The necessary condition for a local minimum τ^* is established by setting the marginal loss with respect to τ to zero:

$$\frac{dW_{\text{new}}(\tau)}{d\tau}|_{\tau=\tau^*} = 0$$

I differentiate $W_{\text{new}}(\tau)$ with respect to τ using the chain rule:

$$\frac{dW_{\text{new}}(\tau)}{d\tau} = \lambda N \frac{dQ(\tau)^\eta}{d\tau} + (1-\lambda) N_w \bar{\Lambda} \frac{d\pi(\tau)}{d\tau}$$

The marginal conservation gain is $-\lambda N \frac{dQ^\eta}{d\tau}$, and setting the sum to zero and rearranging yields:

$$-\lambda N \frac{dQ(\tau)^\eta}{d\tau} = (1-\lambda) N_w \bar{\Lambda} \frac{d\pi(\tau)}{d\tau}$$

Final Condition. Expanding the marginal environmental loss term and isolating the ratio of the planner's weights, I obtain the final condition that τ^* must satisfy:

$$\frac{\lambda}{1-\lambda} = \frac{N_w \bar{\Lambda} \frac{d\pi(\tau)}{d\tau}}{N \cdot \eta Q(\tau)^{\eta-1} \left(-\frac{dQ(\tau)}{d\tau}\right)}$$

The optimal tax rate τ^* is the numerical solution to this condition, balancing the marginal conflict cost against the marginal environmental benefit at the point of optimal policy intervention.

Table E.2: Optimal Continuous Conservation Tax Rate (τ^*)

Planner's Preference (λ) (Env. Weight)	$\eta = 0.5$	$\eta = 1.0$	$\eta = 1.5$	$\eta = 2.0$
0.2	18.2%	23.5%	27.8%	31.1%
0.4	31.1%	35.7%	39.5%	42.6%
0.6	45.4%	48.3%	51.0%	53.6%
0.8	60.8%	61.8%	63.3%	64.9%

Notes: The table reports the optimal tax rate (τ^*) required to minimise the policymaker's loss function, expressed as a percentage of tax on the revenues of harvesting firms in strong states. Calculations are based on calibrated parameters for the African rosewood market (λ = policymaker's environmental weight, η = convexity of ecological damage).

E.2.6 Policy Rankings

Table E.3: Ranking of Feasible Policies by Planner Preferences (λ) and Biodiversity Tipping Point (η)

η	λ	Free Trade	Uniform Ban	Targeted Ban 1	Targeted Ban 2	Optimal Policy
0.5	0.2	3rd	4th	2nd	**1st**	Benchmark
0.5	0.4	3rd	4th	2nd	**1st**	Benchmark
0.5	0.6	3rd	4th	2nd	**1st**	Benchmark
0.5	0.8	3rd	4th	2nd	**1st**	Benchmark
1.0	0.2	3rd	4th	2nd	**1st**	Benchmark
1.0	0.4	3rd	4th	2nd	**1st**	Benchmark
1.0	0.6	3rd	4th	2nd	**1st**	Benchmark
1.0	0.8	3rd	4th	2nd	**1st**	Benchmark
1.5	0.2	3rd	4th	2nd	**1st**	Benchmark
1.5	0.4	4th	2nd	**1st**	3rd	Benchmark
1.5	0.6	4th	2nd	**1st**	3rd	Benchmark
1.5	0.8	4th	**1st**	2nd	3rd	Benchmark
2.0	0.2	4th	**1st**	2nd	3rd	Benchmark
2.0	0.4	4th	**1st**	2nd	3rd	Benchmark
2.0	0.6	4th	**1st**	2nd	3rd	Benchmark
2.0	0.8	4th	**1st**	2nd	3rd	Benchmark

Notes: Policies are ranked from 1st (lowest welfare loss) to 4th (highest) among the feasible options. The Optimal Policy is shown for reference as a benchmark but is assumed to be politically infeasible. Rankings vary with the planner's biodiversity preference (λ) and the ecological damage parameter (η).

Rosewood in Africa: Difference-in-Differences Estimates

Table E.4: Trade Restrictions and Rosewood Conflict in Africa: Difference in Differences Estimates

	Dep. Var.: Conflict (0/1)		
	(1)	(2)	(3)
$Habitat \times Policy$	0.127**	0.1477***	0.054***
	(0.01)	(0.0127)	(0.0085)
Cell FE	Y	N	Y
Country-Year FE	N	Y	Y
Observations	343,952	343,952	343,952
Dep. Var. Mean	0.0788	0.0788	0.0788
Dep. Var. SD	0.269	0.269	0.269

Note: The table reports LPM estimates using a difference-in-differences estimator of the effect of CITES trade restrictions on rosewood on conflict in Africa. Each observation corresponds to a cell-year. The variable $Habitat$ is an indicator measuring the suitability of cell k for wildlife species w, and $Policy$ indicates the timing of CITES trade restrictions imposed on wildlife species w at time t. The dependent variable is a binary indicator for conflict incidence, equal to one if at least one conflict event occurs in a given cell and year, based on the conflict datasets referenced in the column title. Coefficients are reported with spatially clustered standard errors (in parentheses), which allow for spatial and temporal correlation within a 500 km radius of each cell's centroid. Standard errors reported in square brackets are clustered at the country-year and cell levels, allowing for within-country spatial correlation and infinite serial correlation within a cell. * significant at 10%; ** significant at 5%; *** significant at 1%.

F Trees Distribution Modelling

Occurrence records for the focal tree taxa were obtained from the Global Biodiversity Information Facility (GBIF). The raw presence-only data were filtered to remove duplicate records, entries with georeferencing errors (e.g., invalid or imprecise coordinates), and spatial outliers, so that the retained observations more accurately represented each species' realised distribution. These occurrences were then linked to pixel-level environmental covariates that characterise the ecological conditions at each location.

To estimate potential distributions, I employed the Maximum Entropy (MaxEnt) algorithm. MaxEnt contrasts the environmental conditions observed at presence locations with those sampled at background points across the study region and estimates a probability distribution of maximum entropy subject to constraints defined by the average values of the predictor variables at occurrence sites. The predictors used in the analysis comprised climatic, topographic, edaphic, vegetation, and accessibility variables, selected for their ecological relevance to tree growth and persistence and after checking for multicollinearity among candidate predictors. The complete set of variables is reported in Table F.1. Predictor variables were internally transformed into multiple feature classes (linear, quadratic, hinge, product, and threshold), with a regularisation penalty applied to avoid overfitting. The output is a continuous, unitless suitability surface ranging from 0 (unsuitable) to 1 (highly suitable) for each pixel.

For integration into subsequent analyses, the continuous suitability surfaces were converted into binary presence–absence maps. Thresholding followed the *minimum training presence* rule: I first computed

$$T^* \;=\; \min_{x \in \mathcal{D}^{\text{pres}}_{\text{train}}} s(x),$$

the lowest predicted suitability among all in-sample occurrence locations, where $s(x)$ denotes the MaxEnt suitability at pixel x and $\mathcal{D}^{\text{pres}}_{\text{train}}$ is the set of training presences. Out-of-sample pixels were then classified as:

$$\text{presence}(x) \;=\; \begin{cases} 1 & \text{if } s(x) \;\geq\; T^* \\ 0 & \text{if } s(x) \;<\; T^*. \end{cases}$$

This rule guarantees zero omission for the training occurrences and yields inclusive maps of potential habitat suited for downstream ecological and economic integration. As robustness checks, I also considered (i) the threshold that maximises sensitivity + specificity (Youden's J) on held-out data (with specificity computed against background points), and (ii) the 10th percentile of training presences. Results in the main text use the minimum training presence rule as the primary specification; conclusions are qualitatively similar under the alternative thresholds.

Table F.1: Environmental variables used in MaxEnt modelling

Category	**Variable**	**Source**	**Resolution**
Climate	Mean annual temperature	WorldClim v2	1 km
Climate	Temperature seasonality (standard deviation)	WorldClim v2	1 km
Climate	Maximum temperature of the warmest month	WorldClim v2	1 km
Climate	Minimum temperature of the coldest month	WorldClim v2	1 km
Climate	Annual precipitation	WorldClim v2	1 km
Climate	Precipitation seasonality (coefficient of variation)	WorldClim v2	1 km
Topography	Elevation	Geodata	90 m
Topography	Slope	Geodata	90 m
Topography	Aspect	Geodata	90 m
Topography	Terrain ruggedness index	Geodata	90 m
Soils	Soil type	Geodata	250 m
Soils	Soil texture (sand, silt, clay fractions)	Geodata	250 m
Soils	Soil pH	Geodata	250 m
Soils	Soil organic carbon	Geodata	250 m
Land cover	Land cover class (forest, cropland, grassland, etc.)	MODIS	500 m
Vegetation	Normalised Difference Vegetation Index (NDVI)	MODIS	250 m
Vegetation	Enhanced Vegetation Index (EVI)	MODIS	250 m
Accessibility	Distance to rivers	Geodata	500 m
Accessibility	Distance to roads and settlements	Geodata	500 m

Table F.2: Wildlife Trade Restrictions and Conflict Likelihood: Constant Sample Size

	Dep. Var.: Conflict (0/1)					
	Animals			Trees		
	ACLED	UCDP	GTD	ACLED	UCDP	GTD
	(1)	(2)	(3)	(4)	(5)	(6)
Habitat × *Policy*	0.021***	0.01**	0.01**	0.044***	0.011***	0.023***
	(0.006)	(0.005)	(0.004)	(0.006)	(0.003)	(0.004)
Cell FE	Y	Y	Y	Y	Y	Y
Country-Year FE	Y	Y	Y	Y	Y	Y
Observations	294,816	294,816	294,816	294,816	294,816	294,816
Dep. Var. Mean	0.069	0.033	0.022	0.069	0.033	0.022
Dep. Var. SD	0.253	0.179	0.146	0.253	0.179	0.146

Notes: The table reports LPM estimates using the imputation difference-in-differences estimator of Borusyak et al. (2024), where I hold the sample size constant across datasets over the period 1997–2020, restricted to Africa. Each observation corresponds to a cell-year. The variable *Habitat* is an indicator measuring the suitability of cell k for wildlife taxon w, and *Policy* indicates the timing of CITES trade restrictions imposed on wildlife taxon w at time t. The dependent variable is a binary indicator for conflict incidence, equal to one if at least one conflict event occurs in a given cell and year, based on the conflict datasets referenced in the column title. Coefficients are reported with spatially clustered standard errors (in parentheses), which allow for spatial and temporal correlation within a 500 km radius of each cell's centroid. Standard errors reported in square brackets are clustered at the country-year and cell levels, allowing for within-country spatial correlation and infinite serial correlation within a cell. * significant at 10%; ** significant at 5%; *** significant at 1%.

Table F.3: Wild Trees Trade Restrictions and Conflict Likelihood: In and Out of Sample Analysis

	Dep. Var.: Conflict (0/1)					
	In Sample (32%)			Out of Sample (68%)		
	ACLED	UCDP	GTD	ACLED	UCDP	GTD
	(1)	(2)	(3)	(4)	(5)	(6)
Habitat × *Policy*	0.047***	0.01**	0.016***	0.029**	0.005**	0.012**
	(0.01)	(0.004)	(0.006)	(0.013)	(0.002)	(0.05)
Cell FE	Y	Y	Y	Y	Y	Y
Country-Year FE	Y	Y	Y	Y	Y	Y
Observations	1,316,442	3,105,204	4,613,447	1,191,240	2,779,562	4,129,635
Dep. Var. Mean	0.076	0.030	0.017	0.076	0.030	0.017
Dep. Var. SD	0.265	0.171	0.131	0.265	0.171	0.131

Notes: The table reports LPM estimates using the imputation difference-in-differences estimator of Borusyak et al. (2024). Each observation corresponds to a cell–year. The variable *Habitat* is an indicator measuring the suitability of cell k for wildlife species w, and *Policy* indicates the timing of CITES trade restrictions imposed on species w at time t. The dependent variable is a binary indicator for conflict incidence, equal to one if at least one conflict event occurs in a given cell–year, based on the conflict datasets referenced in the column titles. The treatment group in columns 1–3 is defined using in-sample observations of trees from GBIF surveys, whereas the treatment group in columns 4–6 is defined using out-of-sample predictions of tree presence from the MaxEnt machine-learning algorithm described in Section F. Coefficients are reported with spatially clustered standard errors (in parentheses), allowing for spatial and temporal correlation within a 500-km radius of each cell's centroid. * significant at 10%; ** significant at 5%; *** significant at 1%.